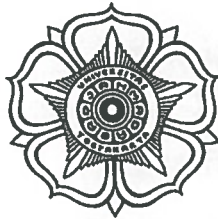


ANALYZING RUNOFF DYNAMICS THROUGH PARAMETERIZING A HYDROLOGICAL MODEL IN A WATERSHED

A Case Study in Upper Part of Serayu Watershed, Central Java Province, Indonesia

Thesis submitted to the Double Degree M.Sc. Programme, Gadjah Mada University
and Faculty of Geo-Information Science and Earth Observation, University of Twente
in partial fulfillment of the requirement for the degree of Master of Science in Geo-
Information for Spatial Planning and Risk Management



UGM



By:

Adhi Nurul Hadi

UGM : 09/292236/PMU/06156

ITC : 24609



SUPERVISORS:

Prof. Dr. H. A. Sudibyakto, M.S. (UGM)

Dr. Dhruba Shrestha (ITC)

**DOUBLE DEGREE M.Sc. PROGRAMME
GADJAH MADA UNIVERSITY
FACULTY OF GEO-INFORMATION AND EARTH OBSERVATION
UNIVERSITY OF TWENTE
2011**

THESIS

**Analyzing Runoff Dynamics Through Parameterizing
a Hydrological Model in a Watershed**
A Case Study in Upper Part of Serayu Watershed, Central Java Province, Indonesia

By :

ADHI NURUL HADI
UGM : 09/292236/PMU/06156
ITC : 24609

Has been approved in Yogyakarta
On 15 February 2011

By Thesis Assessment Board:

Supervisor 1:



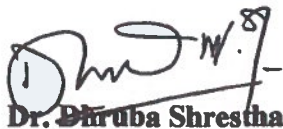
Prof. Dr. H. A. Sudibyakto, M.S.

ITC Examiner 1:



Prof. Dr. Victor Jetten

Supervisor 2:



Dr. Dhruva Shrestha

ITC Examiner 2:



Drs. Tom Loran

This thesis has been accepted as one of the requirements
To obtain a Master's degree
Date:

**Program Director of
Geo-Information for Spatial
Planning and Risk Management**



Prof. Dr. H.A. Sudibyakto, M.S.

**On behalf of Director
Vice Director for Academic Affairs,
Development and Cooperation**

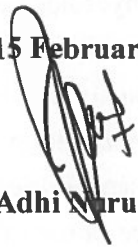


Prof. Dr. Suryo Purwono, MA.Sc., Ph.D.

DISCLAIMER

This document describes work undertaken as part of a program of study at The Double Degree International Program of Geo-information for Spatial Planning and Risk Management, a Joint Educational Program of Faculty of Geo-Information and Earth Observation, University of Twente, The Netherlands, and Gadjah Mada University, Indonesia. All views and opinions expressed therein remain the sole responsibility of the author, and do not necessarily represent those of the institute.

Yogyakarta, 15 Februari 2011



Adhi Nurul Hadi

ABSTRACT

A hydrological model can represent processes of precipitation, interception, evapotranspiration, and infiltration, as hydrological components, in an upper part of a watershed. The hydrological components determine runoff dynamic on the upper part of watershed itself and on the low land area. Upper part of Serayu Hulu Watershed, as the study area, contributed to the occurrences of flooding on next lower area, Banjarnegara District. This research constructed a hydrological model by means of available data, hydrological equations, and GIS program to find out the runoff dynamic on the study area. The runoff dynamic was analyzed by describing runoff on different landcover types, figuring the correlation between hydrological component and runoff, calculating the sensitivities of the hydrological components to runoff, and identifying the response of runoff to possible landcover change.

The model resulted that during research period, the highest runoff occurred on built up area and the lowest occurred on cultivation area. The strongest correlation coefficient was shown by infiltration-runoff positive correlations. It shows that infiltration and runoff have the strongest linear relationship and have the same responses to rainfall, the factor mostly determining values of hydrological components. Infiltration was also the hydrological component that mostly influenced runoff. When infiltration was added by half of its original value, runoff decreased more than 20 %, and the decreasing raised up to 35 % as infiltration was increased two times of its original value. Replacing forest, shrub, and plantation by cultivation greatly reduced runoff up to 49 %. Changing cultivation, forest, and shrub to plantation gave different effects to two Sub Watersheds. It increased runoff on integrated Serayu Hulu Sub Watershed about 16 %, meanwhile it decreased runoff on Merawu Sub Watershed about 24 %. Enlarging forest area increased runoff on the study area about 12 %. Based on those findings, the hydrological component having the strongest correlation with runoff gave the most influence to runoff change, and enlarging forest area does not always decrease runoff.

Key Words: Flood, hydrological model, runoff, Serayu Hulu, Merawu

INTISARI

Model hidrologi dapat menggambarkan proses komponen hidrologi (presipitasi, intersepsi, evapotranspirasi dan infiltrasi) pada wilayah hulu suatu daerah aliran sungai. Komponen hidrologi menentukan dinamika limpasan air permukaan pada wilayah hulu itu sendiri dan daerah yang berada di bawahnya. Hulu daerah aliran sungai Serayu sebagai lokasi penelitian berkontribusi terhadap banjir yang terjadi di daerah bawahnya, diantaranya Kabupaten Banjarnegara. Penelitian ini membangun model hidrologi dengan menggunakan data yang tersedia, persamaan hidrologi dan program SIG untuk mengetahui dinamika limpasan air. Dinamika limpasan air dianalisa dengan cara mengetahui perbedaan limpasan air pada setiap jenis tutupan lahan, menggambarkan hubungan korelasi antara komponen hidrologi dengan limpasan air, menghitung sensitivitas komponen hidrologi terhadap limpasan air dan mengidentifikasi respon limpasan air terhadap kemungkinan bentuk perubahan tutupan lahan.

Model hidrologi menunjukkan bahwa selama periode penelitian, limpasan air tertinggi terjadi pada areal terbangun dan yang terendah terjadi pada ladang. Koefisien korelasi menunjukkan infiltrasi dan limpasan air memiliki hubungan linear yang kuat dan memiliki respon yang sama terhadap hujan. Penelitian ini juga menunjukkan bahwa infiltrasi sangat berpengaruh terhadap limpasan air. Ketika infiltrasi ditambah setengah dari nilai semula, limpasan air turun lebih dari 20 % dari nilai semula dan pada saat infiltrasi dikalikan dua, limpasan air menurun sampai 35 %. Merubah hutan, semak dan perkebunan menjadi ladang menurunkan limpasan air sampai dengan 49 %, kemudian merubah ladang, hutan dan semak menjadi perkebunan meningkatkan limpasan air pada sub daerah aliran sungai Serayu Hulu sampai dengan 16 %, sementara di sisi,lain perubahan tersebut menurunkan limpasan air pada sub daerah aliran sungai Merawu sampai 24 %, dan terakhir memperluas hutan dengan cara merubah perkebunan, ladang dan semak menjadi hutan meningkatkan limpasan air sekitar 12 %. Berdasarkan temuan-temuan tersebut, disimpulkan bahwa infiltrasi memiliki hubungan korelasi paling kuat dengan limpasan air dan memberikan pengaruh yang kuat terhadap limpasan air, dan memperluas areal hutan tidak selalu menurunkan limpasan air.

Kata kunci : Banjir, model hidrologi, limpasan air, Serayu Hulu, Merawu

ACKNOWLEDGEMENT

Alhamdulillahirabbil'aalamiin, praises to the Almighty, Allah SWT, for His endless Grace and Blessing on my life, and for giving me opportunity, strengths, and directions to finish my M.Sc. study and my thesis.

I would give my grateful thanks to Gadjah Mada University, Faculty of Geo-Information and Earth Observation-University of Twente, Pusbindiklatren-BAPPENAS, Netherlands Education Support Office, and Ministry of Forestry for their great supports during my study.

I deeply appreciate to my supervisors, Prof. Dr. H. A. Sudibyakto, M.S. for giving me continuous supports, guidance, encouragements, and advices, and Dr. Dhruva Shresta, for giving me supervisions, great ideas, constructive remarks, and improvements during writing research proposal until the final thesis.

Many thanks to all lecturers and staff members in GMU and ITC for sharing knowledge and experiences, especially to Prof. Dr. Junun Sartohadi, M.Sc., Prof. Dr. V. G. Jetten, Dr. D. G. Rossiter, Dr. M. Pramono Hadi, M.Sc., Dr. Djarot Sadharto W., M.Sc., Dr. Muh. Aris Marfai, M.Sc., Dr. C. J. van Westen, Dr. D. Alkema, Ms. Drs. N. C. Kingma Ir. B. G. C. M Krol, Mba Indri, Mba Tutik, Mas Wawan, and Mas Didit.

My appreciations to my classmates in Geo-information for Spatial Planning and Risk Management, Ali, Mas Bagus, Ulil, Bayu, Inus, Inul, Mas Koes, Beng2, Roni, Shinta, and Tipuk. My Special appreciation goes to my struggling fieldworks partners, Nana and Mba Elna. Thanks to Mas Pongky and Mas Andry Rustanto for valuable data and discussions. Thanks to all Indonesian students in ITC 2010 for the warm friendship during my study in Enschede. Special thanks to Kang Ogi and Rahmayanti for the unforgettable traveling in Europe.

I thank to Pa Nashrudin, Pa Rudi, Pa Aris, Pa Supri, and Ipur for shelters and guidance during my fieldwork.

The last is special heartfelt thanks to the most important people, my late parents, Abdul Matin Rozaq and Siti Asyiah (your wish has been granted), my beloved wife, Yulita Anggraini, my cheerful son, Akhtar Nurfadhillah Hadi (lets welcome a new member of our family), my parents in law, H. Cek Ulan and Hj. Maisaroh, my brother A Ali, my sisters, Neng Leli and De Yumi, my sister in law, Yovita, and my brothers in law, Budi and Apri.

TABLE OF CONTENTS

DISCLAIMER.....	I
ABSTRACT.....	II
INTISARI	III
ACKNOWLEDGEMENT.....	IV
TABLE OF CONTENTS.....	V
LIST OF TABLES	VI
LIST OF FIGURES	VII
LIST OF GRAPHS	VII
LIST OF APPENDIX	VIII
1. INTRODUCTION	1
1.1. BACKGROUND	1
1.2. PROBLEM STATEMENT.....	2
1.3. OBJECTIVES.....	4
1.4. RESEARCH QUESTIONS	4
1.5. HYPOTHESES	5
1.6. BENEFIT OF THE RESEARCH.....	5
2. LITERATURE REVIEW	6
2.1. HYDROLOGIC CYCLE	7
2.2. THE EFFECT OF LANDCOVER CHANGE IN FLOODING	13
2.3. REMOTE SENSING IN MODELING.....	16
2.4. DYNAMIC HYDROLOGICAL MODEL	18
3. STUDY AREA.....	21
4. MATERIALS, TOOLS, AND METHOD.....	25
4.1. MATERIALS	25
4.2. TOOLS	25
4.3. METHOD.....	26
5. DATA PROCESSING	39
5.1. CONSTRUCTING A DYNAMIC HYDROLOGICAL MODEL	39
5.2. ANALYZING RUNOFF DYNAMICS.....	57

6. RESULT AND DISCUSSION	64
6.1. CHARACTERISTICS OF HYDROLOGICAL COMPONENTS ON EACH LANDCOVER TYPE	64
6.2. COMPARING MODELED RUNOFF AND MEASURED RUNOFF	66
6.3. CORRELATION BETWEEN EACH HYDROLOGICAL COMPONENT AND MODELED RUNOFF	68
6.4. SENSITIVITIES OF HYDROLOGICAL COMPONENTS TO MODELED RUNOFF	71
6.5. RESPONSES OF MODELED RUNOFF TO POSSIBLE MODIFIED LANDCOVER	72
7. CONCLUSIONS AND RECOMMENDATIONS	74
7.1. CONCLUSIONS	74
7.2. RECOMMENDATIONS	77
8. REFERENCES.....	78
APPENDIXS.....	83

LIST OF TABLES

Table 1.1. Research objectives and questions.....	4
Table 3.1. Products and area of agriculture in Wonosobo districts	24
Table 3.2. Commodities in Banjarnegara District.....	24
Table 4.1. Square of correlation coefficient between each monthly rainfall and altitude for the period 2008 – 2009	29
Table 5.1. List of rainfall stations on the study area	40
Table 5.2. List of MOD13Q1 imageries used in the research.....	41
Table 5.3. Growth stages and crop factor for dry land cultivation	44
Table 5.4. Growth stage and crop factor of each landcover type.....	45
Table 5.5. Mean daylight hours for latitude of the study area	47
Table 5.6. Numbers of sample points on each landcover type.....	48
Table 5.7. Soil moisture content at field capacity on the study area.....	49
Table 5.8. Porosity of soil texture on the study area	53
Table 5.9. calculating EHD of shrub area	53
Table 5.10. Effective Hydrological Depths of shrub area.....	54
Table 5.11. Times from the peak to the end for two hydrograph stations	57
Table 5.12. Total of Measured Daily Runoffs From Two Stations	58
Table 5.13. Codes and cell numbers of all landcover types.....	63
Table 6.1. Total of hydrological component in each landcover type.....	64
Table 6.2. Modeled runoffs compared to measured runoffs	68
Table 6.3. Correlation coefficient between hydrological component and modeled runoff.....	69
Table 6.4. The changes of hydrological component values and their effects to runoff.....	71
Table 6.5. Total modeled runoffs as the results of scenarios	72
Table 6.6. Areas of landcover types in two Sub Watersheds.....	73
Table 6.7. areas of soil textures in two Sub Watersheds.....	73

LIST OF FIGURES

Figure 3.1. Location of study area	21
Figure 3.2. Locations of sub watersheds and discharge stations	22
Figure 3.3. Study area located in two districts, Wonosobo and Banjarnegara districts	22
Figure 4.2. Rainfall gauges map	30
Figure 4.3. a flowchart describing model construction.....	35
Figure 4.4. a flowchart describing analyzing runoff dynamics.....	38
Figure 5.2. Thiessen polygon map	40
Figure 5.3. An example of filtering processes	43
Figure 5.4. Location of temperature station	46
Figure 5.5. Distribution of sample points	49
Figure 5.6. Soil texture map.....	50

LIST OF GRAPHS

Graph 2.1. Flood events in the world from 1985 to 2003	6
Graph 3.1. Monthly rainfall from thirteen gauges on the study area	23
Graph 4.1. Correlation between altitude and monthly rainfall on Indo-Australian monsoon	28
Graph 4.2. Correlation between altitude and monthly rainfall on East-Asia monsoon	28
Graph 5.1. EHDs of Paddy Field in Each Soil Texture	56
Graph 5.2. EHDs of Dry Land Cultivation in Each Soil Texture	56
Graph 5.3. Discharge separation of Banjarnegara station.....	58
Graph 5.4. Discharge separation of Clangap station.....	58
Graph 5.5. Modeled runoff of Banjarnegara station	59
Graph 5.6. Modeled runoff of clangap station	59
Graph 5.7. Daily modeled runoff and daily rainfall on the study area during research period	60
Graph 5.8. Average daily interception and rainfall in the study area during research period	60
Graph 5.9. Average daily potential and actual evapotranspirations, and average daily rainfall in the study area during research period	61
Graph 5.10. Average daily infiltration and average daily rainfall in the study area during research period.....	61
Graph 6.1. Monthly modeled and measured runoffs of Integrated Serayu Hulu Sub Watershed.....	66
Graph 6.2. Monthly modeled and measured runoffs of Merawu Sub Watershed. 66	
Graph 6.3. Comparison of modeled and measured runoffs on Integrated Serayu Hulu Sub Watershed	67
Graph 6.4. Comparison of modeled and measured runoffs on Merawu Sub Watershed.....	67
Graph 6.5. Data distribution of interception-total modeled runoff linear relationship.....	69

Graph 6.6. Data distribution of potential evapotranspiration-total modeled runoff linear relationship.....	70
Graph 6.7. Data distribution of infiltration-total modeled runoff linear relationship	70

LIST OF APPENDIX

Appendix 1. Results from field observation and laboratory measurement.....	83
Appendix 2. Bulk density of each soil texture	86
Appendix 3. Analysis of variance for completely randomized design	88
Appendix 4. Pcraster script for runoff dynamic model.....	93
Appendix 5. Calculated EHDs of all combinations, field capacity, and bulk density of all soil textures	100
Appendix 6. Rainfall data	102
Appendix 7. Temperature data.....	108
Appendix 8. an example of measurement table in calculating infiltration	110
Appendix 9. Fieldwork activities and landcover types on the study area.....	111

1. INTRODUCTION

1.1. Background

Flooding is one of the major disasters that often occurred in several regions in the world. It has become a great problem for some countries and even to countries having no solutions yet, flooding has become an annual problem. Flood disrupted economic activity, increased health problem, and degraded environments. Some countries have spent many funds to solve those problems as consequences of flood occurrences. Indonesia as one of those countries considers flooding as a serious problem because it almost occurred every year in the country.

In Indonesia, flood is the disaster having the highest frequency comparing to others such as landslide, tsunami, and earthquake. Indonesian National Board for Disaster Management (2009) showed that floods occurred 198 times, 15 percent of all disasters occurrences, on 2008, and 339 times or 38 percent of all disasters occurrences on 2007. Those two data sets show that floods occurred more often than other disasters and they have caused losses to infrastructures, damage environments and even loss of lives. Related to community, floods have damaged school and market buildings, postponed academic activities, disrupted economic activities, spread diseases, and inundated cultivation areas. On the environment side, they have wiped saplings, and degraded habitat of wildlife. Triutomo (2006) represented that flood was the disaster having highest frequency during the period January 2002 – June 2006. On that time, it occurred 986 times and made 921 people dead, 379 people injured, and 3.167.854 people lost their houses. Those floods occurred in many places, including in Serayu catchment area, one of catchment areas in central Java, Indonesia.

Upper area of Serayu watershed, located mostly on Wonosobo district, affects other district located as the next lower, Banjarnegara, in term of flooding hazard. Suryanto (2010) stated that on May 15, 2010, a flashflood occurred on Susukan, one of sub districts in Banjarnegara and it wiped some settlements located in surrounding Serayu River. At the same time, a flood also inundated other Sub district, Purwareja Klampok, about 10-20 cm. Two factors on the upper area of Serayu Watershed that hypothetically can trigger the occurrences of floods on the lowland areas are natural event and human activities.

Natural factor on the upper area that mainly caused floods on the low land area was an extremely high rainfall intensity or rainfall that occurred in an unusually

long period. Human activities for examples land use changes or degradation of vegetation covers and mis-management of soils have direct influence on rising of water level in the river. The degradation of vegetation covers, mostly caused by human activities, triggers an increase of runoff, causing floods in the low lands. Saeidian, Sulaiman et al. (2009) wrote that the landuse change, mainly from converting ranges to dry farming imposed grazing pressure over natural plants spaces that lead to increase in the Curve Number (CN) and consequently rising runoff volume and peak discharge. The factors, natural and human factors, were interrelated in a certain area and involved in a hydrologic cycle as a system.

The changes of hydrologic cycle on the upper area of Serayu watershed affected the raise of water level on the down river and the changes depend on components of hydrological cycle, rainfall, interception, through fall, evaporation, transpiration, infiltration, and percolation. Some of factors determining value or level of each component in the hydrological cycle are temperature, humidity, landcover, landuse, topography, geomorphology, and soil properties. Those factors can closely represent the character of hydrological cycle in the upper area of Serayu Watershed through constructing a hydrological model by means of hydrology equations, supporting data, and Geographic Information System (GIS). Related to flooding, the constructed hydrological model can represent runoff dynamics on the upper area of Serayu Watershed. The runoff dynamics on the upper area of Serayu watershed can be used as base information in flood analyzing, mitigation, and prediction so an analysis of runoff dynamics through parameterizing a hydrological model in the upper area of Serayu Watershed is required or needed as a support in solving flood problems. The hydrological model furthermore can be used in constructing an early warning system in the Serayu Watershed management.

1.2. Problem Statement

The landcover changes on the upper area directly affect the runoff on the upper area itself and on the lowland area. The more vegetations living on the upper area of a watershed, the more water that will be intercepted and evaporated and the less volume of water flowing in the river as discharge. Some expressions coming from previous researchers mentioned that vegetation cover changes directly affect the runoff. The vegetation intercepts some of the water coming from the rain and then the water is temporarily stored on the vegetation until it evaporates back to the atmosphere (McCuen 1998). On the other hand, David and Gash (2009) explained

that evaporated water from canopy, interception loss, always plays an important role in the water balance system because it can represent a significant proportion of gross rainfall (8-60%) and play as a key position of the overall forest evaporation (25-75%).

The landcover changes on the upper area of Serayu Watershed were mostly affected by human activities. Most people on the upper area of Serayu watershed were interested in cultivation and plantation, and made them as their livelihood. They have converted so many forest areas into dry land cultivation and plantation. Rustanto (2010) concluded that from 1989 to 1999, the upper area of Serayu Watershed was dominated by forest and dry land cultivation and it changed in 2003 and 2009 on which the upper area of Serayu Watershed was dominantly covered by dry land cultivation and plantation. That change led the low land area of Serayu Watershed became a flood prone area, and triggered the occurrences of landslide, erosion, and sedimentation on the low land area. Chehafudin (2007) wrote that the change of land cover in Wonosobo District, from forest to the shrub areas, triggered flood, landslide, erosion, and sedimentation occurrences on the lower areas such as Banjarnegara, Banyumas, and Cilacap Districts. The forest degradation in Wonosobo makes the other districts, Banjarnegara and Banyumas, become flood prone areas in central java. Based on flood prone area maps of central java (Indonesian National Board for Disaster Management 2009), Banjarnegara became one of areas having highest potency of flood occurrence on March 2010 and on the next month, april 2010, it had two statues in potency of flood occurrences, middle and highest potencies.

The landcover changes caused by cultivation and plantation directly influence the hydrological cycle on the upper area of Serayu Watershed and furthermore affect the runoff on the low land area. Based on that statement, it is important to figure and analyze the characteristic of hydrological cycle's components, such as interception, evapotranspiration, infiltration, and rainfall, and effects of landcover changes to runoff dynamics on the upper area of Serayu Watershed in order to solve problems caused by flood on the low land area. Those, figuring and analyzing, can be done through parameterizing a hydrological model.

1.3. Objectives

The general objective of the research is to analyze runoff dynamic through parameterizing a hydrological model in upper area of Serayu Watershed. The specific objectives are:

1. To identify the correlation between each hydrological component and runoff
2. To evaluate the sensitivity of hydrological components in resulting runoff
3. To analyze the runoff response to possible landcover changes

1.4. Research Questions

There are seven research questions need to be addressed to achieve the research objectives, which are described in Table 1.1.

Table 1.1. Research objectives and questions

No	Research objectives	Research questions
1.	To identify the correlation between each hydrological component and modeled runoff	<ul style="list-style-type: none">- What are the correlations between hydrological components and modeled runoff?- Which correlation that is the strongest?
2.	To evaluate the sensitivity of hydrological components in resulting runoff	<ul style="list-style-type: none">- What are the sensitivities of hydrological component changes to the modeled runoff?- Which component that gives the most influence to the runoff change?
3.	To analyze the response of runoff to possible modified landcovers	<ul style="list-style-type: none">- What will be the runoff response if cultivation, plantation, and shrub changed into forest?- What will be the runoff response if forest, cultivation, and shrub changed into plantation?- What will be the runoff response if forest, plantation, and shrub changed to cultivation?

1.5. Hypotheses

1. All hydrological components have negative correlation with modeled runoff
2. The hydrological component that has the strongest correlation with runoff gives the most influence to the runoff change.
3. Enlarging forest area decreases runoff.

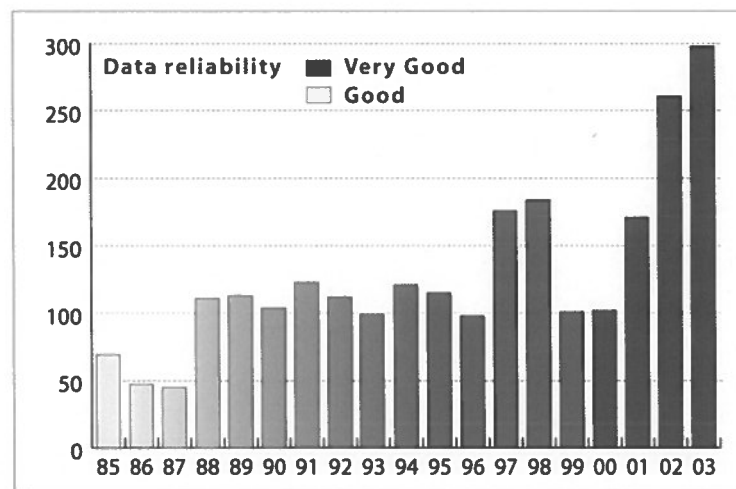
1.6. Benefit of the Research

This research can provide base information related to hydrological processes in upper area of Serayu Watershed, such as fluxes of precipitation, interception, evapotranspiration, infiltration, and runoff which can be used for developing early warning system.

2. LITERATURE REVIEW

Flood is one of the natural hazards that have caused great damages in many countries. It caused many damages, such as lives, infrastructures, and economics. According to the EU Floods directive (2007/60/EC) (European Commission 2007), a Flood is defined as a temporary covering by water of land not normally by water. National Severe Storm Laboratory (NOAA) (2009) mentioned that flooding is an overflowing of water onto land that is normally dry. Potentials that can cause flood events are heavy rains, ocean waves coming to onshore, too fast snow melting, and broken dams or levees.

Floods are the most frequent of all catastrophic natural hazards, costing an average of \$6 billion in losses annually and threatening lives and property in every state (United States Geological Survey 2006). On the other hand, Dartmouth Flood Observatory (2004) stated that the flood events on the world increase in year by year. The graph below (figure 2.1) made by the Dartmouth Flood Observatory shows the increase of flooding events from 1985 to 2003 in the world.



Graph 2.1. Flood events in the world from 1985 to 2003

Dartmouth Flood Observatory (2004) mentioned that there are 11 factors, which can trigger the flood events. They are:

1. Heavy rain
2. Tropical cyclone
3. Extra-tropical cyclone
4. Monsoonal rain

5. Snowmelt
6. Rain and snowmelt
7. Ice jam / break-up
8. Dam/Levy, break or release
9. Brief torrential rain
10. Tidal surge
11. Avalanche related

The degradation of forest or decreasing the vegetation covers on land raises the runoff volume and peak discharge that can trigger the flood events. Vegetation helps in interception, evaporation and transpiration and in reducing the volume of water coming from rainfall and then decreasing the probability of flood occurrences.

2.1. Hydrologic cycle

Many explanations from researchers, engineers and hydrologists describe hydrologic cycle. They explain the cycle by different manners but in general and concept they are same. McCuen (1998) defined a hydrologic cycle as physical processes that control the distribution and movement of water. He described precipitation as the beginning point of hydrologic cycle. He delivered possible processes distributing water from rain when it falls on earth. The processes are entering a water body directly, traveling over the land surface from the point of impact to a watercourse, infiltrating into the ground, intercepted by vegetation, and stored in surface depressions. Some of water in the water body and intercepted water is evaporated back to the atmosphere in which it forms rainfall.

McCuen (1998) defined water loss as water that does not appear as runoff during or immediately following a rainfall event. He stated that water loss is represented by water stored in depressions, water intercepted by vegetation, and water that infiltrates into the soil during early part of a storm.

Other explanation about hydrologic cycle wrote by Witherick, Ross et al. (2001). They defined hydrological cycle as the unending transference of water from the oceans to the land (via the atmosphere), and vice versa (via rivers). They proposed a sequence to represent the processes involved in the hydrological cycle. Water is transferred from the surface to the atmosphere by evaporation from sea, lake and land surfaces, and transpiration from growing vegetation. It is then transferred within the atmosphere, both vertically (by convection) and laterally (by winds) where it cools and condenses. Precipitation then transfers the water back to

the surface where some of it lands directly in the oceans and the rest falls on land, to flow as surface run-off or percolate to supply groundwater. This in turn reemerges by way of springs to augment river flow.

On the other hand, Graham and Butts (2006) wrote the processes involved in the hydrological cycle as follow. First, water evaporates from the oceans, lakes, and rivers, from the soil, and is transpired by plants. Second, the water vapor is transported in the atmosphere, transformed and falls back to the earth as rain and snow. Third, the water infiltrates to the groundwater and discharges to streams and rivers as base flow. Some of water also moves on the land surface as runoff directly to streams and rivers that flow back to the ocean.

De jong and Jetten (2007) stated that the hydrological cycle of a region is majorly controlled by precipitation. They described precipitation as the beginning point in the hydrological cycle and proposed five possible processes occurring after the water of precipitation falls on to the earth. The processes are:

1. The water intercepted by vegetation.
2. The water becomes overland flow over the ground.
3. The water infiltrates into the ground.
4. The water flows through the soil as subsurface flow.
5. The water discharges into streams as surface runoff.

Other statement from them related to hydrological cycle is that some of precipitation water is stored on vegetation or litter then is evaporated back to the atmosphere during and after the rainfall event. They defined water subtracted from rainfall by vegetation and litter as interception and they stated that between 10 and 20% of rainfall is annually intercepted those percentages depends on vegetation type, cover, structure, and potential evaporation.

2.1.1. Precipitation

Precipitation is the deposition of atmospheric moisture at the surface of the Earth, in the form of dew, frost, rain, sleet, hail and snow. The total amount of precipitation at any place varies enormously, from less than 10 mm a year in the 'hyper-arid' deserts (such as the interior of the Sahara) to well over 10,000 mm in some tropical highlands (Witherick, Ross et al. 2001). Witherick, Ross et al. (2001) defined rainfall intensity as the amount of rain that falls in a given time period, usually expressed in millimeters per hour. The intensity represents a condition of how 'heavy' the rain is. Maximum values, which can be as high as 100-150 mm per hour, are usually associated with: tropical environments, where prevailing high

temperatures and rapid evapotranspiration result in large values of absolute humidity. Rainfall intensity is vary in spatial and temporal, and it is very difficult to determine intensity of rainfall exactly for whole study area in a model.

There are many methods to be used in interpolating rainfall intensity, such as Inverse Distance Weighting (IDW), Kriging, and Spline. Each of those methods has strong points and weaknesses. In term of precipitation interpolation, Vieux (2005) wrote that one artifact of the IDW method is the tent pole effect. That is, a local minimum or maximum results at the measured point location. When applied to rain gauge accumulations, this gives the impression that it rained most intensely, where there were measurements, which is clearly nonsensical. Voltz, et. al. in Vieux (2005) stated that kriging demands too much data causing it is often criticized. Since it needs to compute a variogram with reasonable confidence, it requires at least 100 data points for isotropic variation and 300 to 400 data for anisotropic variation. On the other hand, Chen and Farrar (2007) have evaluated capabilities of those methods compared with capability of NEXRAD precipitation data in order to monitor rainfall in Eastern Ontario, Canada. They concluded that the spline interpolation method, yielded the best interpolated rainfall surfaces compared to two other methods, Kriging and IDW. They used a precipitation surfaces produced by NEXRAD as indicator.

Other method used to represent the distribution of rainfall intensity on the specific area is thiessen polygon method. Witherick, Ross et al. (2001) wrote that thiessen polygon is often used to quadrat analysis in the analysis of spatial distribution taking the form of point patterns. They explained how the thiessen polygon is made. First, draw straight lines (perpendicular lines) connecting between each point and its immediate neighbours, and then new drawn lines (construction lines) bisect the straight lines at right angles. The construction lines and their intersections form polygons. This method assumes that each point on which the precipitation is measured dominates the area formed by its polygon. They recommended this method to be used in calculating the average amount of precipitation received over the total area of watershed on the basis of data collected at a small number of rain gauges located at different points in the watershed.

There are many factors affecting spatial distribution of rainfall on the particular area. Isnugraha (1975) stated three factor affecting precipitation on Serayu Watershed, Equatorial double rainy seasons, local influences, and effect of monsoon. The local influence consisted of two sub factors, surface relief and heat occurring on the area. Baruti (2004) found that there were a significant positive

correlation between annual rainfall and altitude. Calculation of annual rainfall from twelve meteorological stations located within and close to Zacandaro sub-watershed as the study area, showed the correlation between precipitation and altitude with correlation coefficient, r^2 , equal to 0.6333. On the other hand, Amboroise, et. al. in Vieux (2005) noted that significant altitudinal variability of rainfall was affected by topographically controlled wind direction. They measured precipitation by involving 14 rain gauges in a 36 ha catchment.

Isnugraha (1975) observed water availability in whole Serayu Watershed and concluded that there was a positive correlation between rainfall intensity and altitude. He analyzed monthly rainfall from 1931 to 1960 by means of 85 rainfall stations within and close to the Serayu Watershed. He respected the monsoon season to find the correlation between monthly rainfall intensity and altitude. He only considered rainfall intensity from January to February for East-Asia monsoon, and from July to September for Indo-Australian monsoon. On the other hand, Baruti (2004) studied the relationship between annual rainfall and elevation and concluded that there was a significant positive correlation between the annual rainfall and the altitude. He observed annual rainfall from 1940 to 2002 on the Zacándaro sub-watershed with an area of approximately 40 km² and involved rainfall data from thirteen stations. The rainfall station density of his research was one station for 3.08 km².

2.1.2. Interception

A part of rainfall or precipitation is caught by leaves or litter and then is evaporated back to the atmosphere during and after the rainfall event (De jong and Jetten 2007). Mulligan (2006) stated that rainfall is intercepted by the vegetation according to the leaf area index (m²/ m²), vegetation cover (fractional), and measured leaf water storage capacity (mm/m²), of the vegetation, the product of which is the canopy storage capacity (CC,mm). De jong and Jetten (2007) considered interception as the amount subtracted from the rainfall by vegetation and litter. On the other hand, Witherick, Ross et al. (2001) assumed that interception is the process by which raindrops are intercepted by plant surfaces (and in particular the leaves of large trees), and thus prevented from falling directly on to the soil surface. Water droplets retained by the leaves will eventually be evaporated or absorbed (interception loss), thus reducing the effectiveness of the rainfall as a whole. Savenjie in Bulcock and Jewitt (2010) define interception as accounts for the

part of the rainfall that is captured before it can take part in the subsequent runoff and sub-surface processes.

Interception forms an important feature of the hydrological cycle because it may vary on annual basis, between 10 and 20 % of the rainfall, depending on vegetation type, cover, structure, and potential evaporation (De jong and Jetten 2007).

To apply interception process into the model, researchers assumed maximum storage capacity of canopy as interception capacity for a particular area and time step. An equation that is available in calculating maximum storage capacity of canopy is Von Hoyningen-Huene equation. The equation converts Leaf Area Index to maximum storage capacity of canopy. De jong and Jetten (2007) applied the equation in estimating spatial patterns of rainfall interception from remotely sensed vegetation indices and spectral mixture analysis. The equation was also used by Kuriakose, Beek et al. (2009) to compute maximum canopy storage in parameterizing a physically based shallow landslide model in a data poor region. On the other hand, Bulcock and Jewitt (2010) calculated S_{max} using the same equation in improving spatial mapping of LAI using hyperspectral remote sensing for hydrological applications with a particular focus on canopy interception.

2.1.3. Evapotranspiration

Yates and Strzepek (1994) considered evapotranspiration as combination of evaporation from bare soils and transpiration from plants. They defined Evaporation as rate of liquid water transformation to vapor from open water, bare soil or vegetation with soil beneath, and transpiration as part of the total evaporation, which enters the atmosphere from the soil through the plants. Witherick, Ross et al. (2001) defined evapotranspiration as the loss of moisture at the Earth's surface by direct evaporation from water bodies and the soil plus transpiration from growing plants. They stated that potential evapotranspiration is the maximum possible that can occur from a soil that is kept continually moist by irrigation and it can be measured directly, using an 'evapotranspirometer', which records percolation; hence, potential evapotranspiration is derived from precipitation minus percolation. On the other hand, Mulligan (2006) calculated evapotranspiration as the sum of soil evaporation, transpiration, and interception loss. Based on those definitions and provided data, the research calculated interception separately from the evapotranspiration.

There are a large number of equations computing evaporation and transpiration as a function of climatological and hydrological data. Because the

availability of the climatological and hydrological data is not homogeneous in all parts of the world, then simpler techniques have to be used to overcome these limitations (Yates and Strzepek 1994).

2.1.4. Infiltration

Witherick, Ross et al. (2001) defined infiltration as the movement of water, derived from rainfall or melting snow, into the soil. The rate of infiltration, called the infiltration capacity, depends on several factors, such as soil porosity, the degree of compaction of the soil surface, the presence of plant roots, and the degree to which soil moisture is already present (the antecedent condition of the soil). On the other hand, McCuen (1998) stated that the soil texture is an important factor in determining the water-holding characteristics of the soil and therefore the infiltration capacity of a soil layer. As the diameters of the soil particles increase, the pore spaces increase in size, which increases the capacity of the soil to pass and store infiltrating water through the soil profile. He also wrote that between storms, especially when the intervals between storms are long, the soils with high percentages of sand pass the water quickly and may not retain sufficient water to fulfill the needs of vegetation. Environmental factors that control infiltration rates are rainfall rates, soil properties (including texture, pore characteristics, organic matter content, and structure), vegetation, land use, depth of soil, and initial moisture (Harden and Scruggs 2003). Jetten, et al. in Harden and Scruggs (2003) stated that based on sample variance of infiltration rates for tropical forest that they found, it was not possible to predict infiltration rate as a simple function of soil properties.

Harden and Scruggs (2003) stated that in mountain environments, slope position might contribute to the spatial variability of infiltration rates. They calculated infiltration rates in three different places, representing the variability of soil, slope position, Geology, litter, topographic position, and forest type. From the experiments, they concluded that in Ecuador, one of their experiment areas, infiltration rates differed significantly between alluvial and upland soils, and in Puerto Rico, another their experiment area, apparent infiltration rates were lower in topographic coves than on slopes. One of their main conclusions also stated that micro site control of infiltration rates, presumably dominated by root and faunal macro pores that exist in association with the forest ecosystem.

A variable that can be applied in the model to represent daily infiltration on the particular area is Soil Moisture storage Capacity. The capacity is determined by multiplying soil bulk density, soil moisture content at field capacity, effective

hydrological depth, and ratio of actual to potential evapotranspiration. Soil bulk density is the weight of oven-dried soil divided by the volume and it reflects the amount of pore space in the soil (Brown 2003). Soil moisture content at field capacity is a condition of soil in on which all 'gravity' water has been drained away and usually over a period of several days (or even weeks) after the cessation of rainfall (Witherick, Ross et al. 2001). Effective hydrological depth is a representation of soil depth in which the moisture storage capacity controls the generation of runoff and it is a function of the plant cover, and influences the depth and density of roots (Baruti 2004).

Soil Moisture Storage Capacity was calculated by Baruti (2004) to find annual runoff on Tancítaro Geopark, located in the central Mexico through RMMF (Revised Morgan-Morgan-Finney) model. On the other hand, Rustanto (2010) also calculated Soil Moisture Storage Capacity to determine soil erosion dynamics in upper Serayu Watershed.

2.1.5. Runoff

Runoff is the amount of water leaving a drainage basin. Expressed simply it is, in effect, the total rainfall falling in a basin minus evaporation from that basin. It therefore comprises overland flow (water flowing over the land surface), through flow (water flowing through the soil) and groundwater flow (water flowing through rock) (Witherick, Ross et al. 2001). McCuen (1998) considered runoff as water which is not stored in depressions, not intercepted by vegetation and not infiltrate into the soil during or immediately following a rainfall.

Travel time need to be considered when the volume of runoff on a watershed is measured on the specific point or station, as an outlet. Travel time is times needed by particle of water to reach the station point from the most distant point on the upper area (McCuen 1998).

2.2. The Effect of Landcover change in Flooding

Zhang, Dawes et al. (1999) stated that vegetation plays an important role in the hydrological cycle through the exchange of energy, water, carbon, and other substances. They mentioned that the vegetation covers play their roles in the hydrological cycle through the interception and evaporation from wet canopies and evapotranspiration.

The plant cover on lands directly affects the hydrological process. Forested catchments intercepts much water and the water may be retained on leaves, flow

down the plant stems to become stem flow, or drop off the leaves to become part of the through fall, or be evaporated from wet canopy surface during the period of storm (Zhang, Dawes et al. 1999). Zhang, Dawes et al. (1999) considered the sum of stem flow and through fall as a net rainfall. They also stated that the difference between gross rainfall and net rainfall is called the interception loss, which is the sum of water stored on canopy surface and evaporation from a wet canopy.

McCuen (1998) defined the evaporation as the process by which the phase of water is changed from a liquid to a vapor. He considered that hydrologists are primarily concerned with evaporation losses from an open water body while water vapor may result from a change of phase from a solid to gas. He also defined transpiration as a process by which water molecules pass to the atmosphere from plant surfaces. In the transpiration process, the water passes through the plant and is evaporated at the surface of the plant. So evapotranspiration is defined as the total water loss from a field in which significant amounts of water are lost through transpiration from plant surfaces and evaporation from underlying soil. This condition shows that amount of vegetations covering an area will reduce runoff on the area through evapotranspiration process. Furthermore, evapotranspiration can decrease the potential of flood occurrences.

Food and Agriculture Organization of the United Nations (2005) stated that considerable quantities of rainfall (up to 35 per cent) are commonly intercepted by the canopies of tropical forests and evaporated back into the atmosphere without contributing to soil water reserves. Much of the water that does soak into the soil is used by the trees themselves and it is assumed that extensive reforestation or afforestation will increase the low flows in the dry season. Based on those statements, they concluded that replacing forest cover with other land uses almost always results in increased runoff and stream flow. Runoff and stream-flow patterns will gradually return to original levels if an area is left to revert back to forest. Converting forest to grasslands, however, will normally result in a permanent increase in total water runoff.

Saeidian, Sulaiman et al. (2009) found that annual runoff will be increased by 19% if the forest lands and Savanna are completely changed to the farming lands. Mendez, Ventura-Ramos et al. (2010) found that soil surface physical conditions were different between low vegetation cover conditions and greater vegetation cover conditions, indicating a positive effect of vegetation on the regulation of surface hydrological processes. Loch (2000) stated that Detachment and transport of sediment by applied overland flow was similarly reduced by vegetative cover, and

results from the overland flow study also indicate that for slopes up to 70 m long with grass cover of 47% or greater, erosion rates will be minimal, even under extreme, rainfall/runoff events.

Rustanto (2010) estimated annual soil loss due to the land use/land cover change, in upper Serayu Watershed for the period 1989 – 2009. He constructed a model representing the increasing trend of soil erosion on the periods 1989 and 2003 on which the domination of landcover types on the upper area of Serayu Watershed changed from forest and dry land cultivation to plantation and dry land cultivation. He compared soil losses in the upper Serayu Watershed in four periods: 1989-1994, 1994-1999, 1999-2003, and 2003-2009. He found that during 1989-1994 periods the total estimated annual soil loss was decreasing while the changes from forest, paddy field and plantation areas to dry land cultivation areas were increasing. This is probably due to the low intensity of annual rainfall during this period. On the other periods, during 1994-1999, the total soil loss was increasing when the land use/land cover change was dominated by the conversion from forest, dry land cultivation, shrub, and paddy field areas to plantation and the increase was also supported by the high intensity of annual rainfall.

On the next period, 1999-2003, Rustanto (2010) discovered that the total estimated soil loss in upper Serayu watershed was decreasing as the shrub and plantation areas increased. The high intensity of annual rainfall on that period also triggered the decreasing of soil loss. On the last observed period, 2003-2009, he concluded that the major land use/land cover changes from paddy field, dry land cultivation, forest, and shrub areas to plantation area, and the increasing of annual rainfall intensity raised the volume of soil loss. The results of the research done by (Rustanto 2010) explains that the total estimated soil loss, carried out by the discharge, on the upper Serayu Watershed, was directly triggered by land use/land cover and rainfall intensity changes.

An additional information and contrary to popular belief, as stated by Food and Agriculture Organization of the United Nations (2005), forests have only a limited influence on major downstream flooding, especially large-scale events. On a local scale, forests and forest soils are capable of reducing runoff, generally as the result of enhanced infiltration and storage capacities. But this holds true only for small-scale rainfall events, which are not responsible for severe flooding in downstream areas. During a major rainfall event, especially after prolonged periods of preceding rainfall, the forest soil becomes saturated and water no longer enters

into the soil but instead flows directly along the soil surface, thus increasing surface runoff.

On the other hand, Hamilton and Pearce in Food and Agriculture Organization of the United Nations (2005), also mentioned that even at the local level, the regulating effect depends mostly on soil depth, structure and degree of previous saturation. Thin soils produce 'flashy' flows. Massive programs of forestation that have often been proclaimed as 'the answer' to preventing floods simply will not do the job, although there may be many other benefits from reforestation.

2.3. Remote sensing in modeling

Remote sensing techniques help to explore earth surface for managing natural resources. De jong and Jetten (2007) stated that earth observation or remote sensing is basically the only tool that provides us with regional overviews of changing vegetation and crop properties at the Earth's surface. Remote sensing is defined as the acquisition of information about an object without being in physical contact with it. Information is acquired by detecting and measuring changes that the object imposes on the surrounding field, be it an electromagnetic, acoustic, or potential (Elachi and Zyl 2006). It provides digital information representing the condition of earth surface and it helps in evaluating and monitoring changes of the earth surface. Jones (2008) stated that Land cover and other digital biophysical data play important roles in environmental assessments relative to a large number of environmental themes and issues. He wrote that in general, landscape-based environmental assessments fall into one or a combination of five categories:

- 1. Status, change, and trends**
- 2. Relationships between pressures or drivers of landscape conditions, changes, or trends and base biophysical conditions**
- 3. Vulnerability and risk analysis**
- 4. Forecasting; and**
- 5. Alternative future landscape analyses**

Since parameterizing a hydrological model is one of efforts in environmental assessments, those categories are involved in model processing and improvement. Status, changes, trends and relationship between landscape and base biophysical conditions can be used as input data, vulnerability and risk analysis, and forecasting

can be considered as results of the model, and alternative future landscape analyses is an improvement in modeling.

Stancalie and Craciunescu (2005) used satellite imageries from different sensors to analyze flood risk in the Crisul Alb-Crisul Negru - Koros transboundary basin, crossing the Romanian – Hungarian border. They presented the capabilities offered by various remote sensing data and GIS techniques to manage flooding and the related risk. They also concluded that although satellite sensors cannot measure the hydrological parameters directly, optical and microwave satellite data can supply information and adequate parameters to contribute to the improvements of hydrological modeling and warning.

The MODIS (Moderate Resolution Imaging Spectroradiometer) 250 m NDVI (Normalized Difference Vegetation Index) product can be used to derive the needed vegetation phenology (Knight, Lunetta et al. 2006). This satellite image is downloadable and accessed easily. Many studies used this image to construct their researches. Knight, Lunetta et al. (2006) used the image to characterize regional scale land cover in North Carolina and Virginia, USA. in order to monitor vegetation changes, Schiffman, Basson et al. (2008) observed capabilities of MODIS in estimating Leaf Area Index (LAI). They compared in-situ data with three spectral vegetation indices derived from Landsat Thematic Mapper imagery: RSR, SR, and NDVI to identify statistical relationships that could be applied to map LAI at higher spatial resolutions to supplement observations available from MODIS. Kuriakose (2006) involved MODIS-derived 16-day composite NDVI data in models, STARWARS+PROBSTAB, to find hydrological effects of vegetation such as interception and bulk through fall. The ability of MODIS satellite images in representing the vegetation phenology can play a role as a parameter in a dynamic hydrological model in region scale, such as in upper area of Serayu watershed.

Knight, Lunetta et al. (2006) investigated the capability of the MODIS 250 m NDVI product (MOD13Q1) to be used in landcover classification through combining and comparing NDVI values represented by MODIS and Landsat ETM+. They demonstrated successful phenology-based Landcover classification using established hyperspectral analysis techniques applied to temporal data. Based on the accuracy of the results, they concluded that classification, using MOD13Q1, is simpler than spectral techniques typically used in large projects, and its temporal classification may provide a viable alternative for regional or national classifications.

2.4. Dynamic Hydrological Model

A hydrological model is one of tools to describe the processes that exist in the hydrologic cycle. A proper hydrological model can represent the complexity of the hydrologic cycle processes through transforming the processes into the mathematical equations. (EPA's Watershed Academy Web 2007) defined two important points in discussing models as follow:

1. Models are a type of tool, and are used in combination with many other assessment techniques.
2. Models are a reflection of our understanding of watershed systems. As with any tool, the answers they give are dependent on how we apply them, and the quality of these answers is no better than the quality of our understanding of the system.

Singh and Frevert (2006) stated the strengths and the deficiencies of the watershed models. They mentioned the strengths of the models, which reflect the increasing role of watershed models in tackling environmental and ecosystems problems. The strengths are as follow:

- The diversity of the models is so large that one can easily find more than one watershed model for addressing any practical problem.
- Many models are quite comprehensive in that they can be applied to a range of problems.
- In many cases model mimic reasonably well the physics of the underlying hydrologic processes in space and time.
- Several of the models attempt to integrate ecosystems and ecology, environmental components, bio systems, geochemistry, atmospheric sciences, and coastal processes with hydrology.

In the other side, they explained the deficiencies of the watershed models as follow:

- Although watershed models have become increasingly more sophisticated, there is a long way to go before they become "household" tools.
- The models are lack of user-friendliness, large data requirements, lack of quantitative measures of their reliability, clear statement of their limitations, and clear guidance as to the conditions for their applicability.
- Some of the models cannot be embedded with social, political, and environmental systems.

Since temperature, humidity, landcover, landuse, and soil properties as factors can represent the conditions of the hydrological cycle components many researchers use the factors as the parameters of hydrological cycle condition. They parameterize the condition by integrating created equations and computer programs through constructing hydrological models. A constructed hydrological model can closely represent the character of hydrological circle on a watershed as stated by Vieux (2005) that the result of modeling can represent the earth hydrologic processes. The models can help other researchers and professions to describe, simulate, and estimate the conditions of hydrologic cycle and the characteristics of its components in the specific areas.

Gitas, Douros et al. (2009) distinguish dynamic model from static model by time variable involved in the model. Dynamic model takes into account element of time as an extra variable and static model does not. Deshmukh and Ghatol (2010) applied multilayer perceptrons neural network and radial basis function neural network to rainfall-runoff static modeling for the upper area of Wardha River in India to predict short term runoff and flood flow. They used seven years (from 2001 to 2007) of rainfall and runoff data to train their neural network models then they compare the methods, multilayer perceptrons and radial basis function neural networks, to determine the most versatile of them in short term flood forecasting. They concluded that radial basis function was more versatile than multilayer perceptrons neural network to forecast runoff for three hours leadtime.

On the other hand, Srinivasan and Lakshmi (2006) used a macroscale hydrological model, one of dynamic hydrological models, to simulate water and energy budgets in the upper Mississippi River basin. They run simulation for the period January 1950 – December 1999 at daily time step and $1/8^\circ$ spatial resolution for the water budget and at hourly time-step and 1° spatial resolution for the energy balance. They used measured soil moisture data from the Illinois State Water Survey and measured stream-gauge observations from U.S. Geological Survey to validate the daily soil moisture and stream flow they simulated through the model. They found that correlation coefficient of monthly measured-modeled stream flow validation was 0.74 and correlation coefficient of monthly measured-modeled soil moisture was from about 0.3 for layer 1 (0-10 cm) to 0.6 for the aggregated layer (0-140 cm). They also identified model characterization of extreme events-drought and floods for the Upper Mississippi River basin in the period 1950-1999.

According to the definition and examples above, there are advantages that can be obtained in using dynamic hydrological model. First, dynamic hydrological

model can represent the characteristics of the components constructing the model along modeled period (depend on time steps involved in the model). Second, a specific time range from the modeled period on which extreme event occurs, such as flood or drought, can be observed more detail, for example identifying the condition of inter correlation components in the model on an extreme event.

3. STUDY AREA

Study area is located in Serayu which is one of the biggest watersheds in Java Island. It is located between $110^{\circ} 4' 12''\text{E}$ and $109^{\circ} 41' 24''\text{E}$ longitudes and between $7^{\circ} 27' 36''\text{S}$ and $7^{\circ} 10' 48''\text{S}$ latitudes (dotted area on figure 3.1.).

With total area 95,173.65 ha, the study area occupies the upper part of the Serayu Watershed which consists of four Sub Watersheds. They are Serayu Hulu, Begaluh, Tulis, and Merawu Sub Watersheds. There are two stations measuring discharges on the study area. First station is located on $109^{\circ} 41' 34.9''\text{E}$ longitudes and $7^{\circ} 23' 19.2''\text{S}$ latitudes, and second station is located on $109^{\circ} 41' 35.2''\text{E}$ longitudes and $7^{\circ} 21' 37.7''\text{S}$ latitudes. First station, Banjarnegara station, located on Banjarnegara bridge, measured discharge coming from Serayu hulu, Begaluh, and Tulis Sub Watersheds. Second station, Clangap station, located on Clangap dam, measured discharge coming from Merawu Sub Watershed. According to locations of discharge stations, the research divided the study area into two Sub Watersheds. Serayu Hulu, Begaluh, and Tulis Sub Watersheds were considered as one Sub Watershed, Integrated Serayu Hulu Sub Watershed, and Merawu Sub Watershed was still considered as one Sub Watershed. The locations of discharge stations and the Sub Watersheds are shown by figure 3.2.

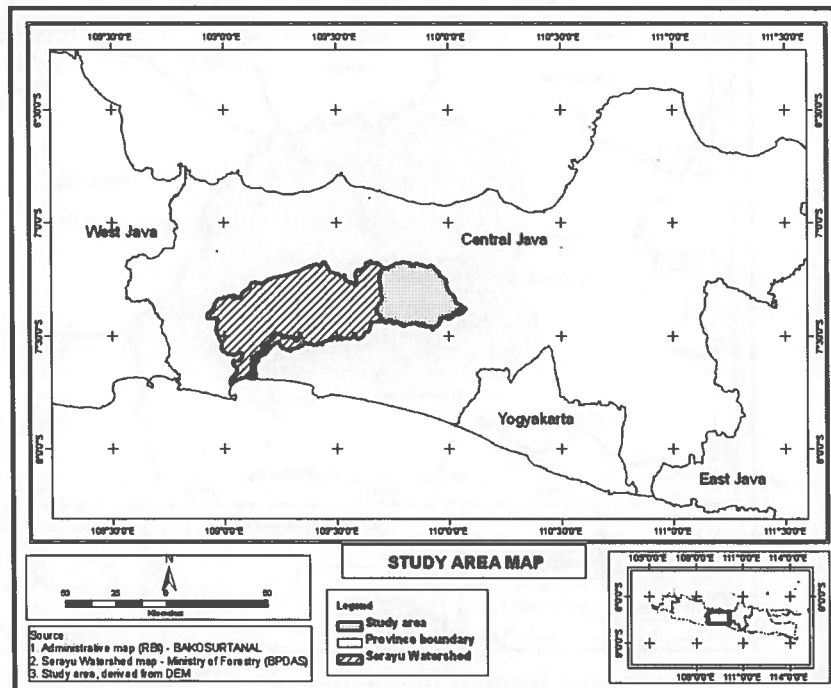


Figure 3.1. Location of study area

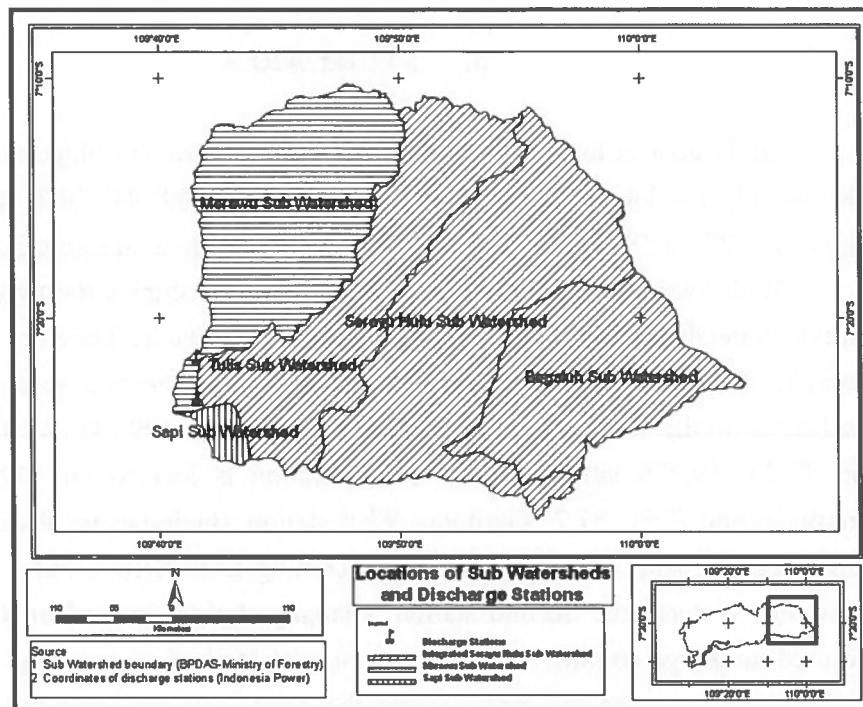


Figure 3.2. Locations of sub watersheds and discharge stations
 Administratively the study area is located in two districts, Banjarnegara and Wonosobo districts (figure 3.3.).

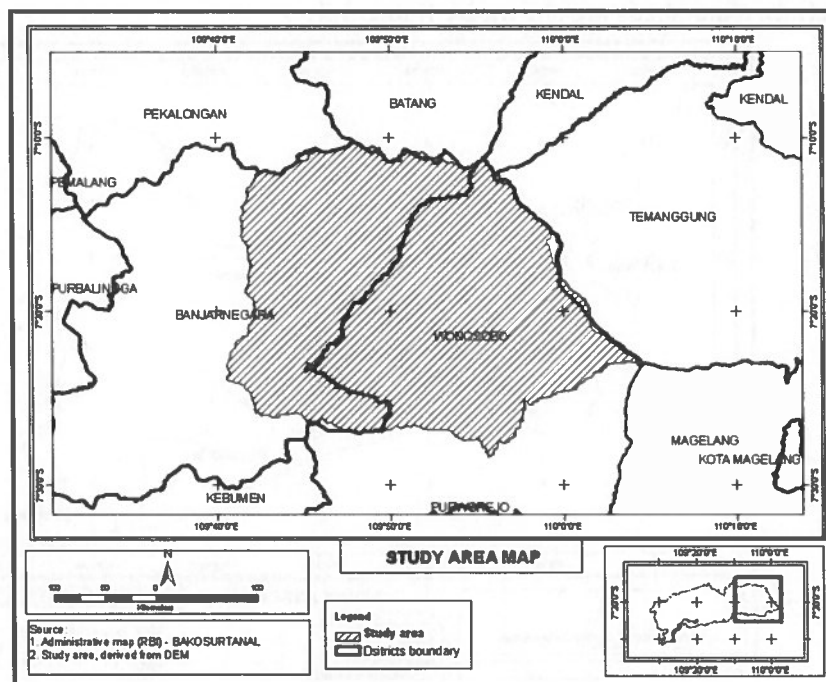
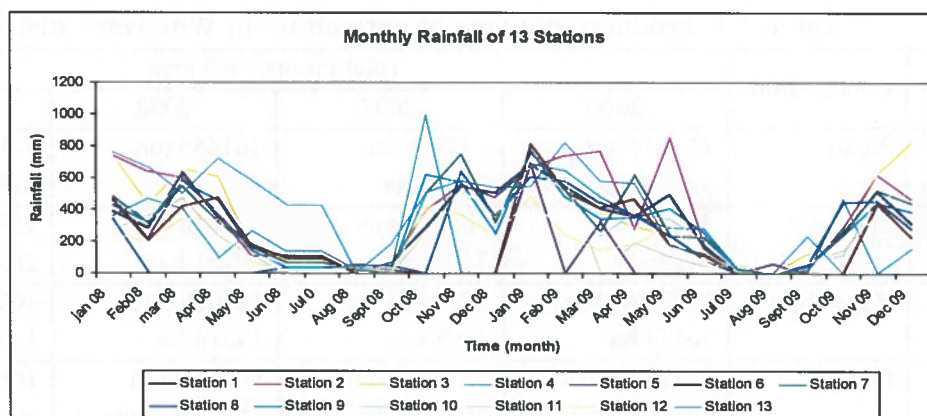


Figure 3.3. Study area located in two districts, Wonosobo and Banjarnegara districts

The elevation of study area varies from 237 to 3037 meters above sea level and the climate is characterized by having an equatorial tropical climate with mean annual rainfall varying from 1700 mm up to 4200 mm per year (Rustanto 2010). The area has two main seasons, rainy season and dry season. Rainy season occurs during November to April, while dry season falls during May to October. About 73 percent of mean annual rainfall falls in the rainy season. Graph 3.1 shows monthly rainfall from January 2008 to December 2009. Rainfall data were collected from thirteen rainfall gauges within the study area.



Graph 3.1. Monthly rainfall from thirteen gauges on the study area

Mean temperature in the area is around 14 up to 27 °C. At higher elevation and particularly in Dieng plateau the temperature can be cooler with annual mean temperature of 14 °C.

According to soil map provided by Indonesian soil and Agro-climate Research Centre soil types in the upper Serayu Watershed are dominated by Regosols, Andosols and Latosols (Cambisol). Regosols and Andosols are mostly located in the volcanic foot slope, volcanic cone, structural depression and plateau area from west to the north. Latosol soil unit dominates in the central part, crossing from South East to the North West in the eroded scarp and mass wasting area.

Mountains relief with relatively steep slope crosses the northern part of study area (from Wanayasa to Kejajar Sub districts). On the Eastern part, there are two high mountains, Sindoro mountain with height of 3136 meters above sea level and Sumbing mountain with height of 3340 meters above sea level. The south part is restricted by mountains relief with relatively moderate slope crossing from Banjarnegara to Sapuran Sub districts. The lowest area, where a reservoir (Mrica) is located, lies in the southwestern part of the study area (Banjarnegara Sub district). The main function of the reservoir is for hydro-power generation. The reservoir has

the capacity of storing water about 47 million cubic meters. The reservoir is also used for recreation and for fishery.

Farmers dominates communities of Wonosobo district. They cultivate paddy, fruits and vegetables, and plant trees. In Wonosobo district, tea, coffee, cacao, coconut, and cloves are planted in addition to the cultivation of potatoes, carica (kind of papaya), cabbage, carrot, and chili. In table 3.1, crop production and cultivation area for the main crops are shown for the period 2006 to 2009 (Wonosobo Local Government).

Table 3.1. Products and area of agriculture in Wonosobo districts

No	Commodities	Total Product and area			
		2006	2007	2008	2009
1	Paddy	151370 ton 32120 ha	137966 ton 29498 ha	161455 ton 30435 ha	118716 ton 22913 ha
2	Secondary crops	259868 ton 36156 ha	266525 ton 34351 ha	279656 ton 39761 ha	159413 ton 26444 ha
3	Vegetables	1872.761 ton 16253 ha	1771.931 ton 14955 ha	1840.566 ton 14514 ha	1607.299 ton 11519 ha
4	Fruits	524.873 ton 6295457 trees	911.274 ton 2645363 trees	899.961 ton 3651955 trees	1667.381 ton 3007101 trees

Source : (Wonosobo Local Government)

The table shows that the agriculture in Wonosobo Districts fluctuated in the period 2006-2009. In addition to field crops the farmers also have livestock such as cow, lamb, goat, buffalo, and chicken.

Agriculture is a vital sector in economy of Banjarnegara District and farm workers dominate the communities. Table 3.2 shows commodities determining the economy of Banjarnegara District in 2004 (Statistic Center Agency of Banjarnegara 2009).

TABLE 3.2. Commodities in Banjarnegara District

No	Commodities	Total Product
1	Cassava	295117.55 ton
2	Paddy	120652.85 ton
3	Maize	68318.65 ton
4	Scallions	85698 ton
5	Cabbage	70286.9 ton
6	Potato	57342.8 ton
7	Coconut	24291.1 ton
8	Tea	1823.94 ton

Source : (Statistic Center Agency of Banjarnegara 2009)

4. MATERIALS, TOOLS, AND METHOD

4.1. Materials

There are two types of materials used in the research, primary and secondary data. Fieldwork measurements and meteorology stations provided the primary data, and literatures and databases supplied secondary data.

4.1.1 Primary Data

1. Daily Rainfall from 13 rainfall gauges within the study area
2. Daily Hydrograph from two discharge stations
3. Daily Temperature from one temperature station outside the study area (about 15 km to south from the study area)
4. Cumulative infiltration from field observation
5. Soil moisture from field observation
6. Soil Bulk Density from field observation

4.1.2. Secondary Data

1. MOD13Q1 (MODIS/Terra Vegetation Indices 16-Day L3 Global 250 m SIN Grid) from June 25, 2008 to August 29, 2009 (28 imageries) downloaded from United States Geological Survey website
2. Digital landcover map of 2009 with resolution 30 m x 30 m (Rustanto 2010)
3. Digital soil texture map with resolution 30 m x 30 m (Rustanto 2010)
4. Monthly Solar radiation from June 2008 to August 2009 with resolution 30 m x 30 m (calculated by using Arcgis 9.2)
5. Digital Elevation Model with resolution 30 m x 30 m (Rustanto 2010)
6. River network map obtained from administrative map at a scale of 1 : 25000 (Indonesian National of Survey and Mapping Coordination)

4.2. Tools

1. NutShell 3.4
2. Arcgis 9.2
3. RSI ENVI 4.3
4. Microsoft Office Excel 2003
5. Microsoft Office Words 2003

6. Double ring infiltrometer with outer cylinder = 15 cm, inner cylinder = 10 cm, and height = 20 cm
7. Core ring with diameter = 5 cm and height = 5 cm
8. Stopwatch
9. Global Positioning System
10. Scales
11. Spade
12. Soil oven

4.3. Method

The research was based on a simple event base hydrological model representing the hydrological processes in the upper part of Serayu Watershed. Runoff Dynamics, as results of the model, were analyzed by observing the hydrological components affecting the runoff dynamics. There are two main part processed in the method, constructing a hydrological model and analyzing runoff dynamic.

4.3.1. Constructing a dynamic hydrological model

The research constructed a dynamic hydrological model, which contains the basic water balance processes, rainfall, interception, evapotranspiration, infiltration, and runoff, and does not take account of base flow aspect. To obtain clear runoff dynamics, the model begins in the driest month of 2008. Based on pre observation to daily rainfall data at 13 rainfall stations on the study area during 2008 and 2009, showing that the driest month of 2008 was on July, and interviews with the farmers mostly stating that in the beginning of july the rainfall will just start, the model was built in daily and starts from July 1, 2008 to August 31, 2009.

According to the lowest pixel size of data used in the research, landcover map, texture map, and Digital Elevation Model (DEM), the research runs all the data in 30 m x 30 m pixel size. NutShell 3.4, a GIS computer program to facilitate the running of PCRaster commands and edit and run PCRaster models, was used to run the model.

Hydrological components, interception, evapotranspiration, and infiltration which affect runoff dynamics, were represented by the model. Imageries and meteorological data were integrated in hydrological equations provided by former reserachers and the equations were applied to the program by using scripts.

4.3.1.1. Rainfall

To determine the minimal number of used rainfall gauges related to measuring spatially variable rainfall in particular observed area, this research used an equation recommended by U.S. Army Corps of Engineers in (Vieux 2005). The equation is:

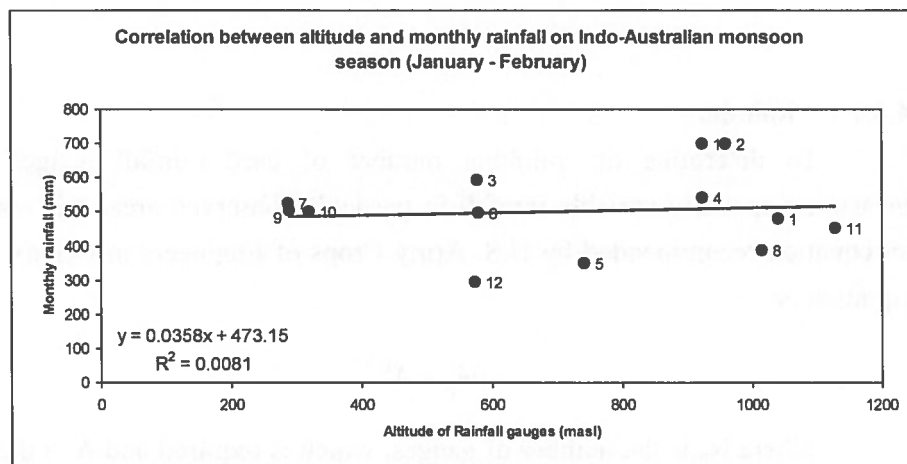
$$N_g = A^{0.33} \quad (4.1)$$

Where N_g is the number of gauges, which is required and A is the watershed area in mi^2 ($2.59 \text{ km}^2 = 1 \text{ mi}^2$).

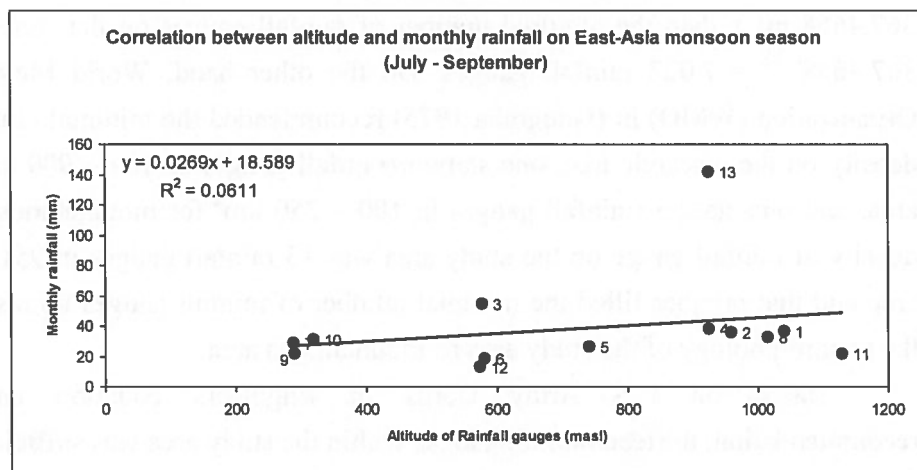
Based on that equation and the extent of the study area ($951.7365 \text{ km}^2 = 367.4658 \text{ mi}^2$), then the required number of rainfall gauges on the study area was $367.4658^{0.33} = 7.022$ rainfall gauges. On the other hand, World Meteorological Organization (WMO) in (Isnugraha 1975) recommended the minimal rainfall gauge density on the research area, one station (rainfall gauge) in $600 - 900 \text{ km}^2$ for flat area, and one station (rainfall gauge) in $100 - 250 \text{ km}^2$ for mountainous area. The density of rainfall gauge on the study area was 13 rainfall gauges in 951.7365 km^2 area and that number filled the minimal number of rainfall gauges up respecting to the geomorphology of the study area as mountainous area.

Based on U.S Army Corps of Engineers equation and WMO recommendation, thirteen rainfall gauges within the study area was sufficient for this research.

Before deciding which method would be used to determine spatial distribution of rainfall intensity in the model, this research did pre observation to rainfall data to identify the relationships between rainfall intensity and altitude. The presence of the relationships was identified by plotting the altitude and the average monthly rainfall of thirteen gauges into scattered graph. Respecting the monsoon seasons that occur on the study area, the monthly rainfall data representing condition on those monsoon seasons were plotted to scattered graph. Monthly rainfall data from January to February were plotted to represent East-Asia monsoon condition, and monthly rainfall data from July to September were used to represent Indo-Australian monsoon. Graph 4.1 and 4.2 show the correlation between monthly rainfall and altitude in two monsoon seasons.



Graph 4.1. Correlation between altitude and monthly rainfall on Indo-Australian monsoon



Graph 4.2. Correlation between altitude and monthly rainfall on East-Asia monsoon

The graphs show that correlation coefficient between monthly rainfall and altitude for Indo-Australian and East-Asia monsoons were positive which means that monthly rainfall increase as the altitude increase. The square of correlation coefficients resulted from the graphs were very low, $R^2 = 0.0081$ for East-Asia monsoon and $R^2 = 0.0611$ for Indo-Australian monsoon. These facts led the research to assume that the correlation between altitude and rainfall intensity during research period was very low.

On the other hand, the research also plotted all monthly rainfall for the period 2008 – 2009 and altitudes of rainfall gauges into scattered graph to identify the square of correlation coefficient between each monthly rainfall and altitude.

Table 4.1 shows the square of correlation coefficient between each monthly rainfall and altitude for the period 2008 – 2009.

Table 4.1. Square of correlation coefficient between each monthly rainfall and altitude for the period 2008 – 2009

Month	Square of Correlation coefficients (R^2)	Correlation coefficient (R)
January	0.05680	-0.2383
February	0.07256	0.2694
March	0.00003	0.0057
April	0.13878	-0.3725
May	0.02078	0.1442
June	0.00265	-0.0515
July	0.06306	0.2511
August	0.05896	-0.2428
September	0.07078	0.2660
October	0.00170	-0.0412
November	0.02588	-0.1609
December	0.01227	-0.1108

Source: Calculation carried in Microsoft Office Excel 2003

Table 4.1 shows that more than half of correlation coefficients between monthly rainfall and altitude in each month were negative (seven of twelve coefficient were negative). Positive coefficients appeared in February, March, May, July, and September, but they were very low, from 0.0057 to 0.2694. Those squares of correlation coefficients were lower than the squares of correlation coefficient calculated by Baruti (2004), 0.6333, showing that relationship between monthly rainfall and altitude during research period was very weak. Based on those facts, the relationship between altitude and rainfall intensity was not involved in the model.

Some factors constrained the research concluding that the relationship between rainfall intensity during research period and altitude was weak or could not be seen. First, the rainfall data used in this research was from January, 2008 to December, 2009, which was very short, comparing to the rainfall data used by Isnugraha (1975) (1931-1960) and Baruti (2004) (1940-2002). Second, the extent of the study area was relatively small compared to the area observed by Isnugraha (1975), the whole Serayu Watershed. Third, the rainfall gauge density involved in this research was so low comparing to the rainfall station density used in Zacándaro sub-watershed research carried by Baruti (2004).

Respecting to the dense and distribution of rainfall gauges on the study area (shown by figure 4.2.), which is inappropriate to be used in interpolation method, and weak correlation between rainfall intensity and altitude on the study area during

research period, the research decided to use thiesen polygon to determine spatial distribution of rainfall intensity in the model.

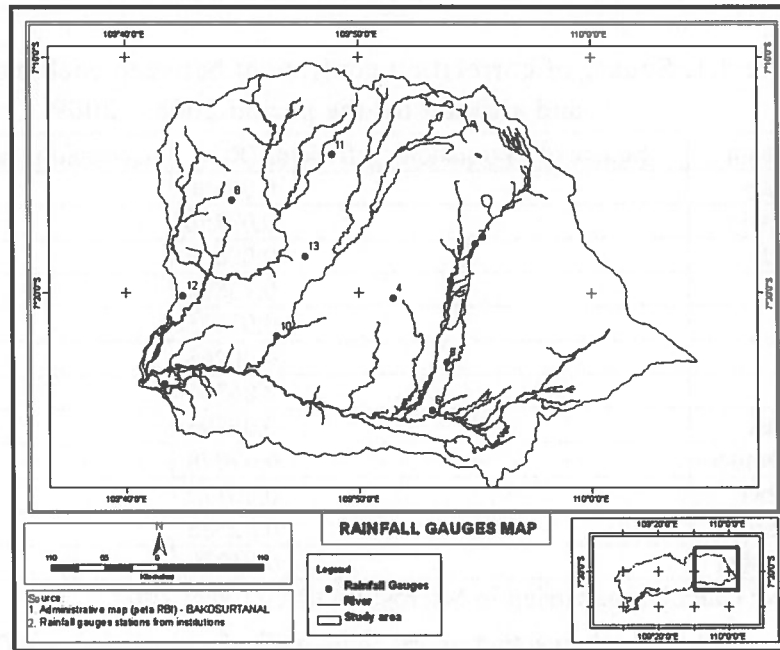


Figure 4.1. Rainfall gauges map

4.3.1.2. Interception

Since vegetation mainly affects interception, the research used 28 MOD13Q1 imageries representing Normalized Difference Vegetation Index (NDVI) on the study area from June 25, 2008 to August 29, 2009. To get reasonable values of NDVI, the imageries was selected and filtered before they were applied into the model. Selection was carried by visualization in which the imageries generally representing bad form were removed from data lists. Imageries filtering was done in two steps. First step was removing anomalous pixel values suspected as clouds and its shadow by applying a threshold value. Second step was eliminating the pixels having NDVI values suddenly dropped or increased and then returned to near the previous NDVI values. This eliminating method has been used by Xiaoxia, Jixian et al. (2008), as Best Index Slope Extraction (BISE), to remove clouds pollution in NDVI imageries. The equations used in the eliminating process are:

$$dNDVI_{t-1,t} = \frac{(NDVI_{t-1} - NDVI_t)}{NDVI_{t-1}} * 100\% \quad (4.2)$$

$$dNDVI_{t+1,t} = \frac{(NDVI_{t+1} - NDVI_t)}{NDVI_{t+1}} * 100\% \quad (4.3)$$

where $NDVI_{t-1}$ and $NDVI_{t+1}$ denote the NDVI values of time $t-1$ and $t+1$ respectively; $dNDVI_{t-1,t}$ and $dNDVI_{t,t+1}$ show the variation rate from $t-1$ to t and from $t+1$ to t respectively. It is assumed that the pixel at time t is affected by clouds if $dNDVI_{t-1,t}$ and $dNDVI_{t,t+1}$ are both surpass 20%, then the t time pixel value is corrected by the average of time $t-1$ and time $t+1$ (Xiaoxia, Jixian et al. 2008).

This research assumed that the pixel at time t is affected by clouds if $dNDVI_{t-1,t}$ and $dNDVI_{t,t+1}$ are both surpass 30%, 10% higher than value used by Xiaoxia, Jixian et al. (2008) because the types of vegetation on the study area possibly could reach that percentage (30%) at least at MODIS time range (16 days). On the other hand, the condition of weather on the study area also supports that change of NDVI value.

To obtain Leaf Area Index (LAI) from NDVI, the research used an equation developed by Campbell and Norman in Kuriakose (2006) representing relation between LAI and NDVI. The equation is:

$$LAI = -2\ln(1-f_c) \quad (4.4)$$

Where, f_c is the fractional vegetation cover.

Fractional vegetation cover was determined by using equation suggested by Walthall et. al. in (Kuriakose 2006). The equation is as follow:

$$f_c = \left[\frac{NDVI_{max} - NDVI_i}{NDVI_{max} - NDVI_{min}} \right] k_c \quad (4.5)$$

Where, $NDVI_{max}$ is the maximum NDVI for each used imagery, $NDVI_{min}$ is the minimum NDVI for each used imagery, $NDVI_i$ is the NDVI of a particular cell, and k_c is the crop factor of the respective landuse. The research used crop factor provided by Allen, Pereira et al. (1998) as FAO Irrigation and Drainage Paper 56.

Next step in determining spatial distribution of interception was calculating maximum storage capacity of canopy as interception capacity. This research computed maximum storage capacity of canopy, S_{max} , from LAI using the equation proposed by Von Hoyningen-Huene in De jong and Jetten (2007), and Bulcock and Jewitt (2010). The equation is:

$$S_{max} = 0.935 + 0.498(LAI) - 0.00575(LAI^2) \quad (4.6)$$

Then interception was calculated as a storage function. The storage S_{max} was filling up with rainfall and emptying with evaporation, and interception could not become more than S_{max} .

4.3.1.3. Evapotranspiration

Available data in the research that can be used in evapotranspiration calculation, consisted of temperature and solar radiation. According to that condition, the research selected Hargreaves equation in Yates and Strzepek (1994) to determine evapotranspiration in the model. The equation is one of temperature-based methods and used as a representative expression for potential evapotranspiration although it gives an expression for the reference crop evapotranspiration (Yates and Strzepek 1994). The equation is:

$$E_{rc} = 0.0022 * R_A * \delta'_T^{0.5} * (T + 17.8) \quad (4.7)$$

Where:

- E_{rc} = reference evapotranspiration (mm/day)
- R_A = mean extra-terrestrial radiation (mm/day)
- δ'_T = temperature difference = mean monthly maximum temperature – mean monthly minimum temperature for the month of interest (°C)
- T = mean air temperature (°C)

The research assumed E_{rc} as potential evapotranspiration.

Mean extra-terrestrial radiation was calculated by using point solar radiation, an extension provided by Arcgis 9.2. This extension requires DEM, points (location to be analyzed), height offset, resolution of the result, latitude of the area, and year (period that is observed) as inputs. The research applied inputs to the extension as follow:

- DEM = DEM file
- Points = 1067316 points on study area (converted from raster with resolution 30 m x 30 m)
- Height offset = 0 m
- Resolution = 30 m x 30 m
- Latitude = -7°
- Year = 2008 and 2009

Temperature was obtained from one temperature station located on 9165983 E longitudes and 369749 S latitudes at 292 masl.

Actual transpiration was determined by multiplying potential evapotranspiration, crop factor, and fractional vegetation cover, and actual evaporation was calculated by multiplying potential evapotranspiration to fractional

vegetation cover minus one. Actual evapotranspiration equaled to actual transpiration plus actual evaporation. Equations used to apply those calculations are:

$$T_a = E_{rc} * f_c * K_c \quad (4.8)$$

$$E_a = E_{rc} * (1 - K_c) \quad (4.9)$$

$$ET_a = T_a + E_a \quad (4.10)$$

Where:

E_t = actual evapotranspiration (mm)

E_{rc} = potential evapotranspiration (Etp) (mm)

f_c = fractional vegetation cover

K_c = Crop factor

4.3.1.4. Infiltration

All available data used in the research which was in daily. According to that condition, infiltration had to have the same unit and a variable that could represent infiltration in daily is soil moisture storage capacity, R_c . Soil moisture storage capacity was calculated by using equation as follow:

$$R_c = MS * BD * EHD * (E_t / E_{T0}) \quad (4.11)$$

Where:

R_c = Soil Moisture Storage Capacity (mm)

MS = soil moisture content at field capacity (%)

BD = Bulk density (mg/m^3)

EHD = Effective Hydrological Depth (mm)

E_t / E_{T0} = Ratio of actual to potential evapotranspiration

(Baruti 2004; Rustanto 2010)

Other researcher, (Basayigit and Dinc 2010), added a power, 0.5, to the ratio of actual to potential evapotranspiration, then the equation became:

$$R_c = 1000MS * BD * EHD * (E_t / E_{T0})^{0.5} \quad (4.12)$$

This research used the second equation, provided by (Basayigit and Dinc 2010).

4.3.1.5. Runoff

This research only concerned in the overland flow or surface runoff, and assumed surface runoff as rainfall, which is not intercepted and transpired by vegetation, not evaporated back to the atmosphere, and not infiltrate into the soil. All “runoff” words in the next sections refer to overland flow or surface runoff.

This research determined runoff value in the model using the equation as follow:

$$\text{Runoff} = \text{rainfall} - (\text{potential evapotranspiration} + \text{interception} + \text{Infiltration}) \quad (4.13)$$

In the model, runoff was applied by using LDD (Local Drain Direction), one of functions in the nutshell that creates a map representing direction of flow of material (in this case water) from each cell to its steepest down slope neighbour. LDD links each cell and creates a line network as flow pattern.

4.3.2. Analyzing runoff dynamics

4.3.2.1. Comparing modeled and measured runoffs

Modeled runoff was produced by the model and measured runoff was obtained from the hydrographs by purposing Fixed time method (Wanielista, Kersten et al. 1997) or Fixed Base Length Method assuming that surface runoff always ends after a fixed time interval. The fixed time interval was determined by equation as follow.

$$\tau = (DA)^n \quad (4.14)$$

Where:

τ = Time from the peak to the end of the runoff hydrograph (days)

DA = Drainage area (miles²)

N = recession constant (0.2)

According to the study area which has relatively large area, travel time of runoff was assumed more than a day so modeled and measured runoffs were compared in monthly unit to reduce bias existence. Modeled runoff was compared to measured runoff by involving Pearson Product Moment Correlation method (McCuen 1998). The method applies the following equation to determine the correlation coefficient between variables.

$$R = \frac{\sum x_i y_i - ((\sum x_i \sum y_i)/n)}{(\sum x_i^2 - ((\sum x_i)^2/n))^{0.5} \cdot (\sum y_i^2 - ((\sum y_i)^2/n))^{0.5}} \quad (4.15)$$

Where:

R = Correlation coefficient

y_i = Value of variable y

x_i = Value of variable x

A correlation coefficient indicates the strength of the correlation and the direction of the relationship between variables. The square of it (R^2) equals to the percentage of the variance in the criterion variable that is explained by variance of the predictor variable. Comparison was also carried by plotting those runoffs into scattered graph. Condition of modeled runoff respected to measured runoff was described descriptively.

4.3.2.2. Identifying the correlation between each hydrological component and modeled runoff

The correlation between each hydrological component, interception, evapotranspiration, or infiltration, and total modeled runoff of two Sub Watersheds was calculated by Pearson Product Moment Correlation method as was done in comparing modeled and measured runoffs. Square of correlation coefficients resulted from the calculation represent the strength of the relationship. The higher the square of correlation coefficient had by a hydrological component, the stronger the relationship between that hydrological component and total modeled runoff.

4.3.2.3. Evaluating the sensitivity of hydrological components to modeled runoff

All hydrological components involved in the model have different affect to the modeled runoff. Although hydrological components were constructed by factors but this research only concerned in hydrological components constructing the model rather than in factors determining the hydrological components themselves.

In order to determine sensitivities of hydrological components to modeled runoff, one of hydrological component values in the model was increased by a half and two times of its initial value, while others retaining in original value, then the percentage off runoff change was obtained by which the sensitivity of each hydrological component is represented. The research applied six simulations into the model to run the process. The simulations were:

1. Interception was multiplied by one and half, and other components were remain
2. Interception was multiplied by two, and other components were remain
3. Potential evapotranspiration was multiplied by one and half, and other components were remain
4. Potential evapotranspiration was multiplied by two, and other components were remain
5. Infiltration was multiplied by one and half, and other components were remain
6. Infiltration was multiplied by two, and other components were remain

4.3.2.4. Analyzing the responses of runoff to possible modified landcover

Landcover types that once dominated on the study area in the periods: 1989, 1994, 1999, 2003, and 2009 are forest, dry land cultivation, and plantation (Rustanto 2010). Based on that fact, the research assumed that those landcover types can be still fluctuating in the future and are appropriate to be used as possible modifying landcovers. According to that statement, the research applied three scenarios into the model to identify the responses of runoff to the landcover change. The scenarios were:

1. Replacing cultivation, shrub, and plantation landcover types by forest
2. Replacing cultivation, shrub, and forest landcover types by plantation
3. Replacing plantation, shrub, and forest landcover types by cultivation

Shrub was applied as one of modified landcovers in the scenarios because that landcover type was assumed easily converted to dry land cultivation, plantation, and forest by communities. Scenarios were carried by modifying coded landcover map in the model, and reconstructing the combinations of landcover and soil texture maps in the model. The results of the scenarios were obtained by rerunning the model. The percentages of modeled runoff changes respected to its original value were considered as the responses of modeled runoff to the landcover change.

In general, analyzing runoff dynamics is represented by flowchart below.

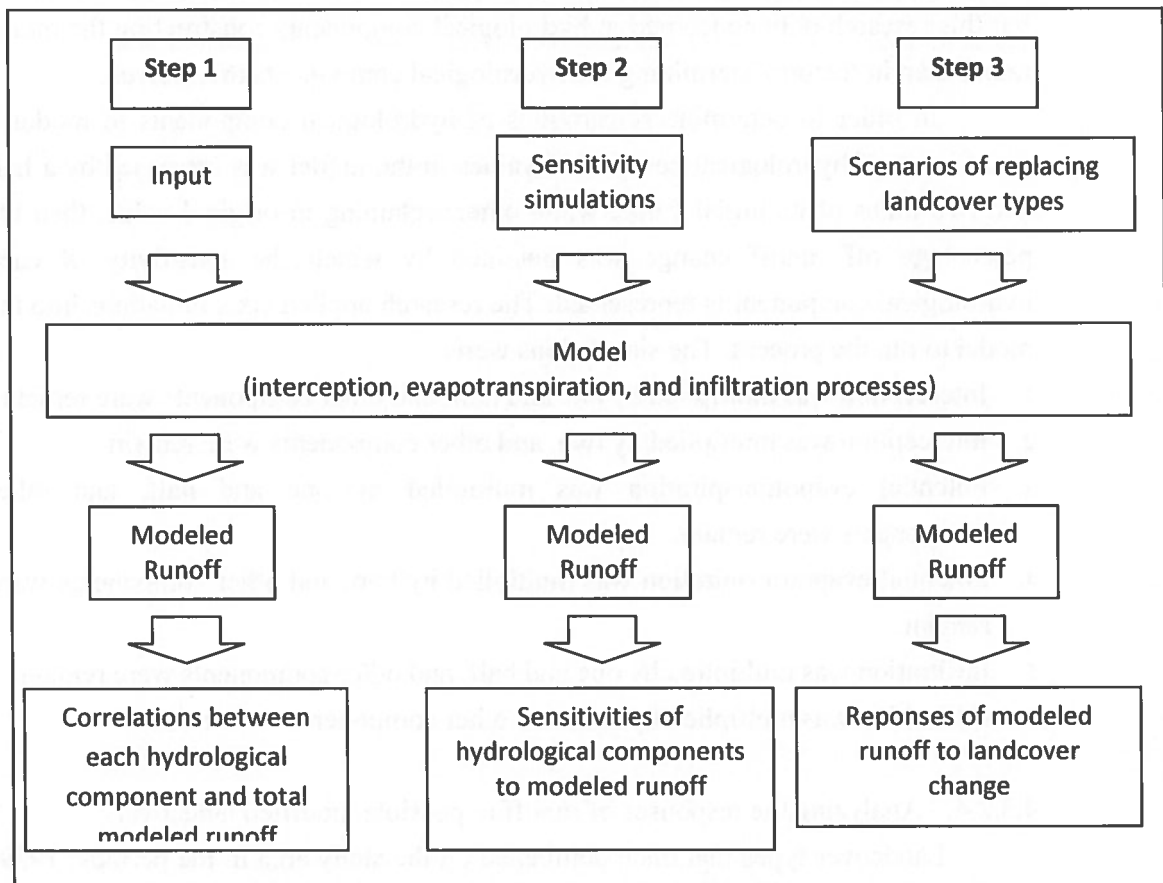


Figure 4.3. A flowchart describing analyzing runoff dynamics

5. DATA PROCESSING

5.1. Constructing a Dynamic Hydrological Model

According to files processed in the Nutshell 3.4 have to be in raster, all data collected from field works, stations, and institutions were spatially transformed to raster. Raster format that is available in Nutshell 3.4 is .map format and that can be formed by converting ascii file by running Nutshell's script as follow.

```
"asc2map --clone clone1.map -DT -NDV mv Ascii1.txt Result.map"
```

Where:

Clone1.map = clone map, a map that must have the location attributes of the maps that want to be used during research

-DT = data type which is assigned to Result.map.

-NDV = no data value, the value in column of ascii file which is converted to a missing value on Result.map.

-mv = missing value on Result.map (converted from -NDV)

Ascii1.txt = ascii file that want to be converted

Result.map = resulted raster map

5.1.1. Rainfall

There are thirteen rainfall stations on the study area providing daily rainfall data, which were applied in the model. Table 5.1 shows the list of the stations with their names and coordinates. Daily rainfall data obtained from July 1, 2008 to August 31, 2009 provided by thirteen rainfall gauges are shown in appendix 6. The daily rainfall data were applied into thiessen polygons, which were formed by Arcgis 9.2, in the model by using following script. Thiessen polygon is shown by figure 5.2.

```
"Percalc rainfall = timeinputscalar(daily rainfall data, thiessen polygons)"
```

Table 5.1. List of rainfall stations on the study area

Sta Nr	Sta Code	Names	Coordinates (meters)		Elevation (m asl)	Sources
			Y	X		
1	24A	Garung	381096	9193619	1041	Public Work Agency of Wonosobo Local Government
2	24F	Wanganaji	380446	9193037	960	Public Work Agency of Wonosobo Local Government
3	26B	Mojotengah	378520	9190191	578	Public Work Agency of Wonosobo Local Government
4	26A	Banjaran	373980	9188817	925	Public Work Agency of Wonosobo Local Government
5	26	Wonosobo	378221	9183781	742	Public Work Agency of Wonosobo Local Government
6	27E	Selomerto	377073	9180022	581	Public Work Agency of Wonosobo Local Government
7	62	Banjarnegara	355853	9182052	289	Water Resource Management Agency of Banjarnegara Local Government
8	-	Karangkoobar	361221	9196420	1016	Geophysics, Meteorology, and Climatology Agency
9	62C	Clangap	355819	9186265	290	Water Resource Management of Banjarnegara Local Government
10	62D	Limbangan	364795	9185793	320	Water Resource Management of Banjarnegara Local Government
11	66	Pejawaran	369140	9200035	1130	Water Resource Management of Banjarnegara Local Government
12	-	Banjarmangu	357343	9188959	575	Geophysics, Meteorology, and Climatology Agency
13	-	Pagentan	367000	9192048	925	Geophysics, Meteorology, and Climatology Agency

Source : Wonosobo and Banjarnegara local Governments, and Geophysics, Meteorology, and Climatology Agency

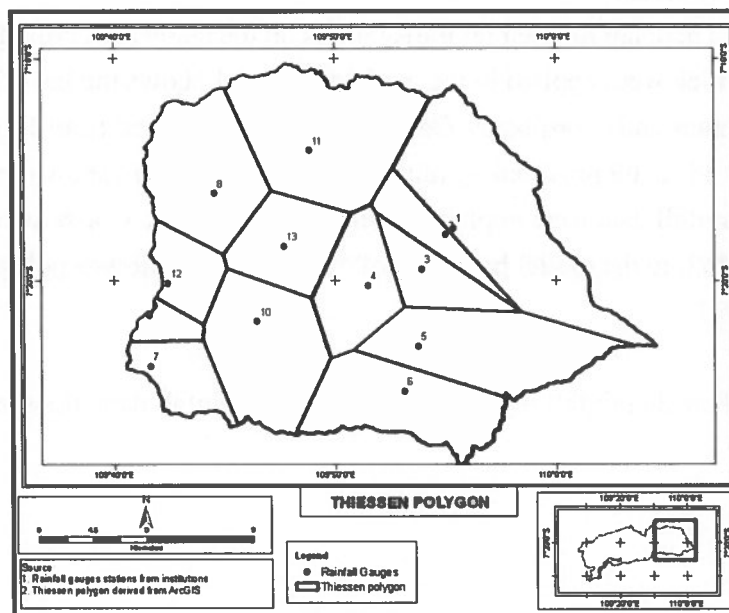


Figure 5.1. Thiessen polygon map

5.1.2. Interception

There were 28 imageries MOD13Q1 selected by visualization and six imageries having bad form of pixel value were removed from the list. Because the model run the input in 30 m x 30 m pixel size then pixel size of selected MOD13Q1 imageries were resized from 250 m x 250 m into 30 m x 30 m by using nearest neighbor method. Table 5.2 shows the list of MOD13Q1 used in the research.

Table 5.2. List of MOD13Q1 imageries used in the research

No	Date of imageries	Imageries code	Note
1	June 25, 2008	MOD13Q1.A2008177.h28v09.005.2008194150725	
2	July 11, 2008	MOD13Q1.A2008193.h28v09.005.2008210193019	
3	July 27, 2008	MOD13Q1.A2008209.h28v09.005.2008237115105	
4	August 12, 2008	MOD13Q1.A2008225.h28v09.005.2008243230656	
5	August 28, 2008	MOD13Q1.A2008241.h28v09.005.2008264020138	Not used
6	September 13, 2008	MOD13Q1.A2008257.h28v09.005.2008275043724	
7	September 29, 2008	MOD13Q1.A2008273.h28v09.005.2008292032021	
8	October 15, 2010	MOD13Q1.A2008289.h28v09.005.2008309004139	Not used
9	October 31, 2010	MOD13Q1.A2008305.h28v09.005.2008326160850	Not used
10	November 16, 2008	MOD13Q1.A2008321.h28v09.005.2008339190619	Not used
11	December 2, 2008	MOD13Q1.A2008337.h28v09.005.2008355230937	Not used
12	December 18, 2008	MOD13Q1.A2008353.h28v09.005.2009012035203	Not used
13	January 1, 2009	MOD13Q1.A2009001.h28v09.005.2009019220141	
14	January 17, 2009	MOD13Q1.A2009017.h28v09.005.2009035183309	
15	February 2, 2009	MOD13Q1.A2009033.h28v09.005.2009059092742	
16	February 18, 2009	MOD13Q1.A2009049.h28v09.005.2009068134854	
17	March 6, 2009	MOD13Q1.A2009065.h28v09.005.2009083143656	
18	March 22, 2009	MOD13Q1.A2009081.h28v09.005.2009100015327	
19	April 7, 2009	MOD13Q1.A2009097.h28v09.005.2009124013147	
20	April 23, 2009	MOD13Q1.A2009113.h28v09.005.2009130175341	
21	May 9, 2009	MOD13Q1.A2009129.h28v09.005.2009149140836	
22	May 25, 2009	MOD13Q1.A2009145.h28v09.005.2009165231614	
23	June 10, 2009	MOD13Q1.A2009161.h28v09.005.2009180181955	
24	June 26, 2009	MOD13Q1.A2009177.h28v09.005.2009199165824	
25	July 12, 2009	MOD13Q1.A2009193.h28v09.005.2009212035338	
26	July 28, 2009	MOD13Q1.A2009209.h28v09.005.2009228031509	
27	August 13, 2009	MOD13Q1.A2009225.h28v09.005.2009248040759	
28	August 29, 2009	MOD13Q1.A2009241.h28v09.005.2009258233458	

Source: United States Geological Survey website

Next step was filtering consisting of two processes, removing and cleaning anomalous values. Removing anomalous low values was carried by using a fixed threshold. The threshold was determined through observation to the selected imageries. Base on the observations, the values of clouds and its shadow were ranging below 0.5 so the threshold was 0.5. Pixel values, which were identified as clouds and its shadows, were replaced by the pixels values of previous imagery. The threshold value was relatively subjective but it made the pixel values of the imageries more reasonable. Script used to apply the threshold in removing process is:

```
“pcrcalc result.map = if(NDVIt.map<0.5, NDVIt-1.map, NDVIt.map)”
```

Where:

result.map = NDVI map with new values

NDVI_t.map = NDVI map which was filtered

NDVI_{t-1}.map = previous NDVI map

The second process was cleaning anomalous values. This process was run by applying Best Index Slope Extraction (Xiaoxia, Jixian et al. 2008) with “barrier” at 30 %. This process was applied into model by using following script.

```
“pcrcalc result.map = if((((NDVIt-1.map-NDVIt.map)/NDVIt-1.map)*100)>30 and  
(((NDVIt.map-NDVIt+1.map)/NDVIt+1.map)*100)<-30, (NDVIt-1.map+NDVIt+1.map)/2, NDVIt.map)”
```

Where:

Result.map = NDVI map with new values

NDVI_t.map = NDVI map which was filtered

NDVI_{t-1}.map = previous NDVI map

NDVI_{t+1}.map = next NDVI map

Figure 5.2 shows an example of filtered imagery.

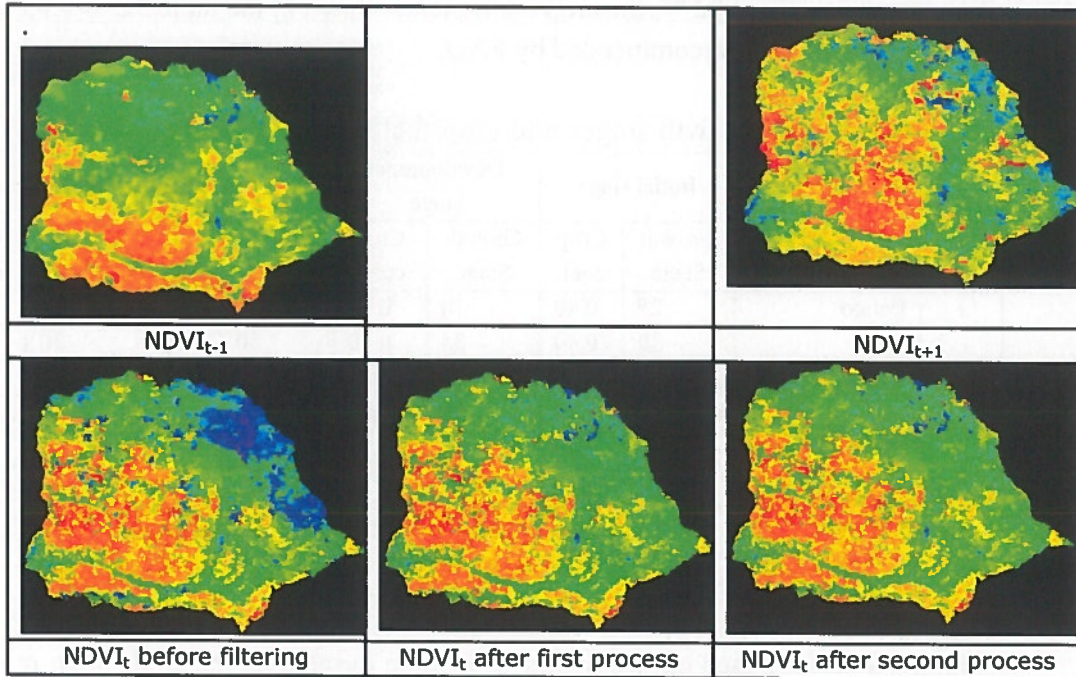


Figure 5.2. An example of filtering processes

Based on field observations, carrot, potato, and cabbage dominated on the dry land cultivation areas. *Paraserianthes falcataria*, *Salacca zalacca*, and *Durio zibethinus* dominated on the plantation areas, and *Pinus merkusii*, *Agathis damara*, and *Altingia excelsa* were the vegetation dominating on the forest areas.

As proposed by FAO, the crop factors of cultivation depended on the types and growth stages of cultivated vegetations. There are four growth stages of crops proposed by FAO and used in this research. The stages are:

1. The initial stage: this is the period from sowing or transplanting until the crop covers about 10% of the ground.
2. The crop development stage: this period starts at the end of the initial stage and lasts until the full ground cover has been reached (ground cover 70-80%); it does not necessarily mean that the crop is at its maximum height.
3. The mid - season stage: this period starts at the end of the crop development stage and lasts until maturity; it includes flowering and grain-setting.
4. The late season stage: this period starts at the end of the mid season stage and lasts until the last day of the harvest; it includes ripening.

The growth stages and crop factors of dry cultivation were the average of carrot, potato, and cabbage growth stages and crop factors. Table 5.3 shows the growth stages and crop factors of each cultivation type, recommended by FAO.

Other recommendation of FAO is that the values of crop factors should be reduced by 0.05 if the area has high relative humidity (RH > 80 %) and low wind speed ($u < 2$ m/s). Respecting to FAO recommendation and condition of relative humidity in the study area, about 82 %, the crop coefficients shown in the table 5.3 is 0.05 lower than crop coefficient recommended by FAO.

Table 5.3. Growth stages and crop factor for dry land cultivation

NO	Crop	Initial stage		Developmnet stage		Mid-seson stage		Late seson stage	
		Growth Stage	Crop coef.	Growth Stage	Crop coef.	Growth Stage	Crop coef.	Growth Stage	Crop coef.
1	Potato	25	0.40	30	0.70	30	1.10	20	0.80
		30	0.40	35	0.70	50	1.10	30	0.80
2	Carrot	20	0.40	30	0.70	30	1	20	0.85
		25	0.40	35	0.70	70	1	20	0.85
3	Cabbage	20	0.40	25	0.70	60	1	15	0.85
		25	0.40	30	0.70	65	1	20	0.85
average		24.17	0.4	30.83	0.7	50.8	1.03	20.83	0.83

Source: Food And Agriculture Organization Of The United Nations

Crop factors of paddy field also refer to FAO crop factors with one additional stage. Based on interviews with some farmers on the study area, rotation of paddy cultivation has a time interval between harvesting and transplanting times, about four weeks, in which paddy field area becomes bare land. The research assumed that on this stage, crop factor of paddy field equals to 0.5.

On the other hand, the research determined fractional vegetation of built up area as fractional vegetation given by the images, so the crop factor for built up area was assumed as one. Crop factor of water body equals to one but later interception scripts in the model made the interception of water body became zero. According to the condition of forest in the study area, which still had good cover of trees, crop factor of forest was assumed as 0,9, 0,1 higher than crop factor of degraded forest recommended by (Kuriakose 2006). Shrub was assumed have the same condition with grassland. Crop factors of Shrub and grass land equal to 0.75 (Kuriakose 2006). Plantation areas had more covers than grassland but less than covers of forest so crop factor of plantation areas was 0.8. For detail, table 5.4 shows the growth stages and the crop factors of each landcover on the study area.

Table 5.4. Growth stage and crop factor of each landcover type

NO	Landcover	Growth stages	Crop Factors
1	Built up area	-	0.3
2	Paddy field	0-60 days after transplant or direct sowing	1.1
		Mid-season (60 – 120 days)	1.3
		Last 30 days before harvested (120 – 150 days)	1
		Interval between harvesting and transplanting (30 days)	0.5
3	Water body	-	1
4	Dry land cultivation	Initial stage (24 days)	0.4
		Development stage (31 days)	0.7
		Mid-season stage (51 days)	1.03
		Late season stage (21 days)	0.83
5	Forest	-	0.9
6	Shrub	-	0.75
7	Plantation	-	0.8
8	Grass land	-	0.75

Source: References and assumptions

The model calculated fraction covers based on times of MOD13Q1 imageries and the model made a linear interpolation to give values of fraction covers in between of two times of imageries. The interpolation was applied by using following script.

“cover = if (day ge daycov1, cov1 + (day - daycov1)/(daycov2-daycov1+0.0001)*(cov2-cov1), cov)”

where:

cover = fraction cover at certain time (between two MOD13Q1 times)

daycov1 = time of previous MOD13Q1

daycov2 = time of next MOD13Q1

cov1 = fraction cover at time of previous MOD13Q1

cov2 = fraction cover at time of next MOD13Q1

Converting fraction cover to Leaf Area Index and Leaf Area Index to maximum storage capacity of canopy was carried by using following scripts.

“LAI = -2*ln(1-fraction cover)”

“Smax = max(0,0.935+(0.498*LAI)-(0.00575*(LAI**2)))”

Maximum storage capacity of canopy of water body and no data equal to zero. Before Intercepted by vegetation, rainfall was reduced by potential evapotranspiration first. Interception never passed maximum canopy storage. Those assumptions were applied into model by using scripts as follow.

“Smax1=if(landcover==waterbody or landcover==no data,0,Smax)”

“Interception = interception + (rainfall-potential evapotranspiration)”

“Interception = (min(Smax1, max(0,interception)))”

5.1.3. Evapotranspiration

Temperature data was obtained from one temperature station that is located 9165983 E longitudes and 369749 S latitudes at 292 masl (shown by figure 5.4).

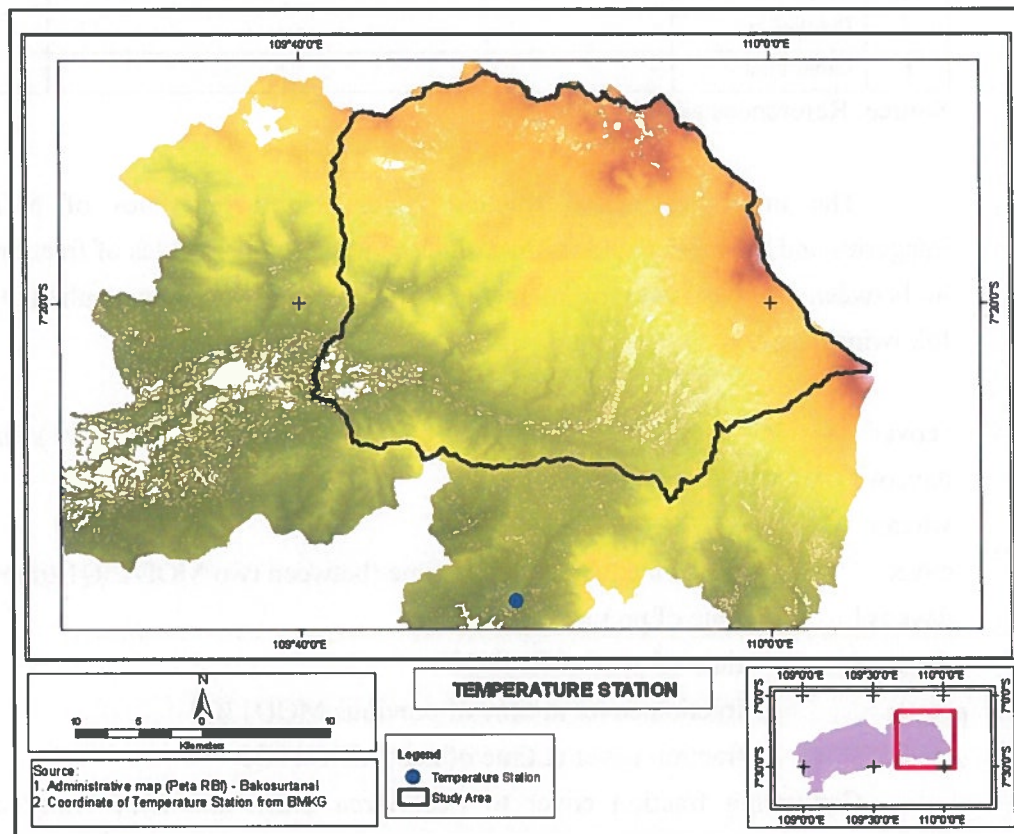


Figure 5.3. Location of temperature station

The script used to apply temperature data into study area is:

“Temperature = timeinputscalar(temperature data, nominal(mask of study area))”

To distribute temperature value on the study area, assumption stating that temperature decreases 0.7 C° when the elevation increase 100 m was applied into model by using following scripts.

“temp1=if(DEM gt 292,-((DEM-292)*0.007))+Temperature, Temperature)”

“temp2=if(DEM lt 292,-((DEM-292)*0.007))+Temperature,temp1)”

“temperature = temp2*mask of study area”

Temperature difference was applied into model by following scripts.

“Temperature difference= timeinputscalar(temperature difference data, nominal(mask of study area))”

Mean extra terrestrial radiations resulted from arcgis 9.2 were in monthly, from July 2008 to August 2009, and the unit of radiation in each point was in Watthour/m². To get daily radiation the result was divided by number of days in each month, then after that, the values were divided by day light hours of each day. The research used mean daylight hours for different latitudes for the 15th of the month, provided by FAO.

FAO calculated mean daylight hours for latitudes 6 and 8, so to get mean day light hours for latitude 7 the research calculated the average of mean daylight hours for latitudes 6 and 8. Mean daylight hours for latitudes of the study area are:

Table 5.5. Mean daylight hours for latitude of the study area

Mean daylight hours (hours)														
year	2008						2009							
month	Jul	Aug	Sept	Oct	Nov	Des	Jan	Feb	Mar	Apr	May	Jun	Jul	Aug
days	1	32	63	93	124	154	185	216	244	275	305	336	366	397
latitudes														
8	11.6	11.7	12	12.2	12.4	12.5	12.4	12.3	12.1	11.8	11.6	11.5	11.6	11.7
6	11.7	11.8	12	12.1	12.3	12.3	12.3	12.2	12	11.9	11.7	11.7	11.7	11.8
7	11.65	11.75	12	12.15	12.35	12.4	12.35	12.25	12.05	11.85	11.65	11.6	11.65	11.75

Source: Food And Agriculture Organization Of The United Nations

As written by FAO there are conversion factors that can be used to convert the unit of solar radiation. The conversion factors used in the research are:

1 Watt/m² = 0.0864 MJ/m² day and 1 MJ/m² day = 0.408 mm/day

So

1 Watt/m² = 0.0864 * 0.408 mm/day = 0.035251 mm/day

The research used that factor to calculate mean extra terrestrial radiation in mm/day. Daily mean extra-terrestrial was directly applied into the model by using script as follow.

“mean extra-terrestrial = mean extra-terrestrial* mask of study area”

The scripts used to calculate potential and actual evapotranspirations in the model are:

“Potential evapotranspiration =0.0022*mean extra-terrestrial*(temperature difference**0.5)*(temperature+17.8)”

“Actual evapotranspiration = actual transpiration + actual evaporation”

“Actual transpiration = potential evapotranspiration*crop factor*fraction cover”

“Actual evaporation = potential evapotranspiration*(1- fraction cover)”

“Crop factor = timeinputscalar(crop factor, landcover)”

“fraction cover had been calculated in interception part”

5.1.4. Infiltration

5.1.4.1. Sample points used to calculate infiltration

There were 73 sample points located in the study area on which initial soil moisture, bulk density, and cumulative infiltration of soil samples were measured. The research used stratified random method and considered landcover and landuse, especially on paddy field and dry cultivation to determine the numbers and distribution of point samples. Table 10 below shows the numbers of sample points of each landcover type.

Table 5.6. Numbers of sample points on each landcover type

NO	Landcover types	Areas (ha)	Percentage	Sample points
1	Built up area	4936.95	5.196428	3
2	Paddy field	5669.10	5.967059	(4) 6
3	Dry land cultivation	20735.91	21.82576	(14) 20
4	Forest	10622.97	11.1813	7
5	Shrub	18340.92	19.30489	13
6	Plantation	34429.41	36.23896	24
7	Grass land	271.35	0.285612	1
8	Total	95006.61	100	73

Source : Calculations carried in Microsoft Office Excel 2003 and Arcgis 9.2

Considering the growth stages in Paddy field and dry land cultivation, the research added sample points to those two landcover types, 2 additional sample points for paddy field and 6 additional sample points for dry land cultivation. The map in figure 5.5 shows the distribution of point samples on landcover map, and the

measurement results of 73 sample points from field observation and laboratory calculation are shown in appendix 1.

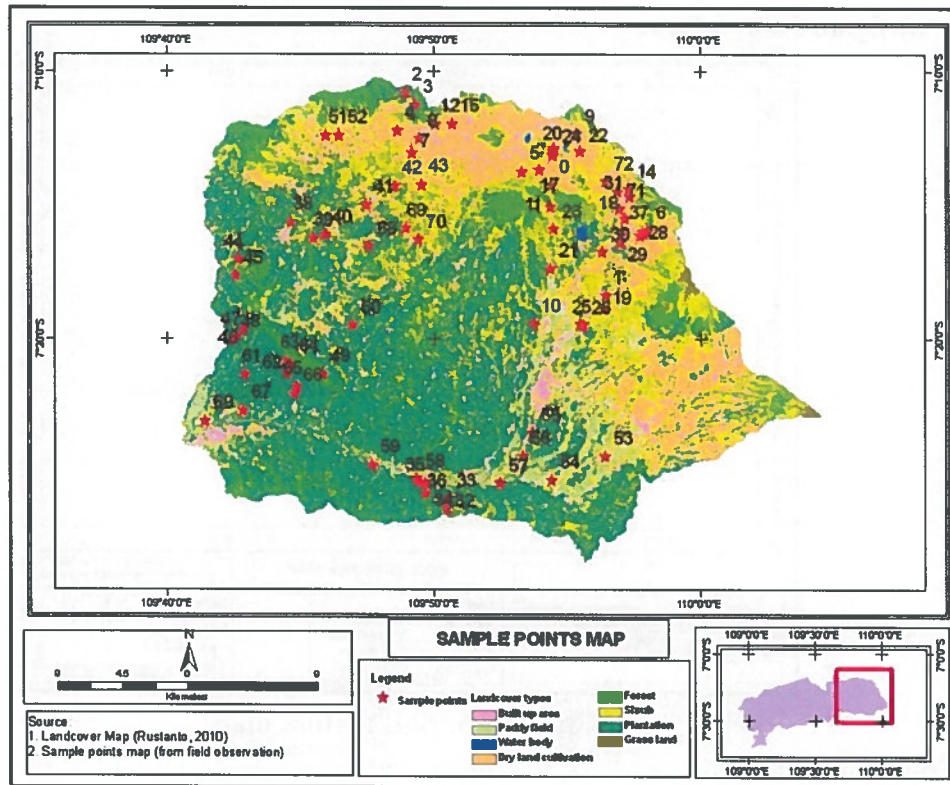


Figure 5.4. Distribution of sample points

5.1.4.2. Soil moisture content at field capacity

This research assumes that each soil texture has the same soil moisture content at field capacity and the research uses values recommended by Morgan in Rustanto (2010). The values are shown in the table 11 as follow.

Table 5.7. Soil moisture content at field capacity on the study area

No	Soil texture	MS (%)
1	Clay	0.45
2	Clay loam	0.4
3	loam	0.2
4	Loamy sand	0.15
5	Sandy loam	0.28
6	Silt loam	0.25
7	Silty clay	0.3

Source: (Rustanto 2010)

Next step of this research is applying soil moisture content at field capacity in to soil texture map of study area (Rustanto 2010). The soil texture map is shown by figure 5.6 as follow.

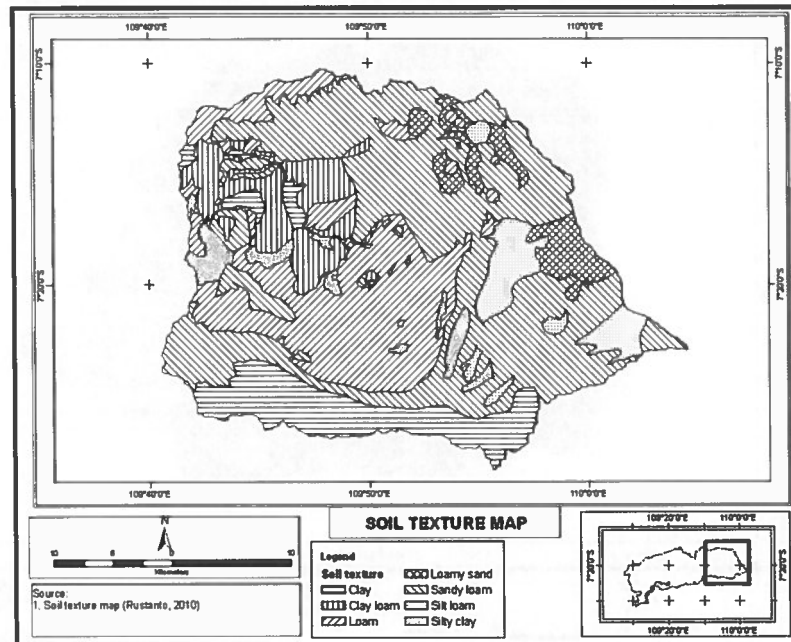


Figure 5.5. Soil texture map

To determine initial soil moisture content, the difference of soil weights at wet and air-dried conditions was measured. Air-dried soil was gathered by putting the soil samples in an open place with temperature between 27°C and 30°C for 24 hours. The process was carried in a laboratory and used an electric pan to blow the samples. Initial soil moisture was calculated by using equation as follow and the results are shown in appendix 1.

$$\text{Initial soil moisture} = \frac{\text{soil weight in wet condition} - \text{soil weight in air dry condition}}{\text{soil weight in wet condition}} \times 100 \% \quad (5.1)$$

5.1.4.3. Bulk density

The research assumed that each soil texture has same bulk density. This assumption was verified by Fixed-effect model, an analysis of variance for completely randomized design (Sudjana 1991). Seven type of soil texture, Clay, Clay loam, Loam, Loamy sand, Sandy loam, Silt loam, and Silt clay were involved in the analysis of variance. Processes of analysis of variance for completely randomized design are explained in appendix 3. The result of the processes

determine that bulk density was affected by soil texture, $F_{\text{test}} = 1.306823 > F_{\text{table}} = 1.23$ with confidence level at 70% and that supported the assumption.

The research took 73 undisturbed soil samples from 5 cm depth to determine the bulk density. The soil samples were taken by using core ring with diameter = 5 cm and height = 5 cm. Bulk density were obtained from field observation and calculated by equation as follow.

$$BD = \frac{M}{V} \quad (5.2)$$

Where,

ρ = Bulk density (mg/m^3)

M = mass of oven dried soil (mg)

V = volume of soil (m^3)

Mass of oven-dried soil was gathered by weighting the soil samples after they were dried in an oven with constant temperature 115 °C for 24 hours. Volume of soil was calculated by measuring the volume of core ring, $(3.142857 \cdot (2.5)^2) \cdot 5 = 98.2143 \text{ cm}^3$. This research assumes that each soil texture has the same bulk density, so the 73 sample points were overlaid on to soil texture map to determine number of sample points on each soil texture. Bulk Density of each soil texture was assumed as the average of bulk densities of sample points that were overlaid with each soil texture polygons. Appendix 2 shows the results of the process.

5.1.4.4. Cumulative infiltration

The research assumed that cumulative infiltration was different in each landcover type. The assumption was also verified by using Fixed-effect model, as done in the bulk density section. Landcover types involved in the analysis of variance were:

1. Paddy field in the growth stage 3
2. Paddy field in the growth stage 4
3. Dry land cultivation in the growth stage 1
4. Dry land cultivation in the growth stage 2
5. Dry land cultivation in the growth stage 3
6. Dry land cultivation in the growth stage 4
7. Shrub
8. Plantation
9. Forest

Processes of analysis of variance are explained in appendix 3. Result of the processes explain that cumulative infiltration was affected by landcover type or

cumulative infiltration was different in each landcover type, with $F_{test} = 10.36943 > F_{table} = 2.10$ and confidence level at 95%.

Cumulative infiltration was calculated by using Horton equations as suggested by Beaver in (Wanielista, Kersten et al. 1997). The equation is:

$$F = \int_0^t f(t) dt = f_c t + \frac{(f_0 - f_c)}{K} (1 - e^{-Kt}) \quad (5.3)$$

That equation is determined by integrating area under the curve built by the equation as follow:

$$K = - \left[\frac{\text{Ln} \left[\frac{(f(t) - f_c)}{(f_0 - f_c)} \right]}{t} \right] \quad (5.4)$$

where:

F = cumulative infiltration volume (mm)

f(t) = infiltration rate (mm/minute)

f_c = constant infiltration (mm/minute)

f_0 = initial infiltration rate (mm/minute)

K = recession constant (minute⁻¹)

t = time-units compatible with K

Recession constant was determined by applying infiltration rate equation into all measured time intervals then the K value producing the closest infiltration rates to the measured infiltration rate was used to build the equation of total infiltration volume or cumulative infiltration. Appendix 8 shows an example of determining recession constant and cumulative infiltration, an example of infiltration measurement on sample number four.

5.1.4.5. Calculating daily infiltration

Basayigit (2010) stated that EHD represents the depth of soil in which the moisture storage capacity controls the generation of runoff and it is a function of the plant cover, and influences the depth and density of roots. Base on that statement, this research assumes that EHD equals to cumulative infiltration when time unit, t, reaches the constant infiltration rate (f_c) by considering porosity of each soil texture and initial moisture content of each soil samples.

Porosity of soil texture obtained from Rawls and Brakensiek in Wanielista et. al. (1997) is shown in the table 5.8.

Table 5.8. Porosity of soil texture on the study area

No	Soil texture	Porosity (%)
1	Clay	0.475
2	Clay loam	0.464
3	Loam	0.463
4	Loamy sand	0.437
5	Sandy loam	0.453
6	Silt loam	0.501
7	Silty clay	0.479

Source: (Wanielista, Kersten et al. 1997)

The research determined the EHD by respecting cumulative infiltration, growth stages, initial soil moisture and soil porosity. An equation used to determine Effective Hydrological Depth is:

$$EHD = \frac{\text{Porosity} \times \text{cumulative infiltration}}{(\text{Porosity} - \text{initial soil moisture})} \quad (5.5)$$

There are four steps carried in the research to determine EHD in each landcover type combined with soil texture (for paddy field and dry land cultivation, the EHD also considered the growth stages of them). First, landcover map was combined with soil texture map, which resulted 45 combinations. Second, EHD of each sample point was calculated by using the equation above. Third, EHDs of sample points, which have same combination, were averaged and the average was assumed as EHD of that combination. Fourth, EHDs of the rest combinations were calculated by respecting to the calculated EHDs and porosity. Table 5.9 shows an example of calculating EHD (calculating EHD of Shrub area).

Table 5.9. Calculating EHD of shrub area

Sample Number	Landcover	soil texture	SM (%)	BD (gram/cm3)	cumulative infiltration	Porosity (%)	SM - Porosity	EHD
69	Shrub	Clay loam	28.32	1.056	133.017	46.4	18.083	341.312
70	Shrub	Loam	36.66	1.127	104.874	46.3	9.641	503.657
6	Shrub	Sandy loam	22.47	0.789	95.526	45.3	22.828	189.563
21	Shrub	Sandy loam	21.58	0.886	97.272	45.3	23.719	185.772
23	Shrub	Sandy loam	23.44	0.915	52.132	45.3	21.861	108.027
42	Shrub	Sandy loam	20.81	0.846	61.230	45.3	24.491	113.257
43	Shrub	Sandy loam	17.21	0.926	146.686	45.3	28.086	236.593
51	Shrub	Sandy loam	20.05	0.755	313.795	45.3	25.255	562.863
52	Shrub	Sandy loam	17.41	1.353	142.691	45.3	27.892	231.747
54	Shrub	Sandy loam	15.03	0.983	55.745	45.3	30.272	83.419
1	Shrub	Silt loam	26.05	0.844	234.327	50.1	24.055	488.045
26	Shrub	Silt loam	17.20	1.277	396.031	50.1	32.897	603.130
55	Shrub	Silty clay	22.14	1.218	6.000	47.9	25.757	11.158

Source: Calculations carried in Microsoft Office Excel 2003

Table 5.10 shows EHDs of Shrub area in each soil texture.

Table 5.10. Effective Hydrological Depths of shrub area

NO	Landcover	Soil texture	EHD	Explanation
1	Shrub	Clay loam	341.31	From table 5.9
2	Shrub	Loam	503.66	From table 5.9
3	Shrub	Sandy loam	213.90	From table 5.9 (average)
4	Shrub	Silt loam	545.59	From table 5.9 (average)
5	Shrub	Silt clay	11.16	From table 5.9
6	Shrub	Clay	323.75	From calculation below
7	Shrub	Loamy sand	297.85	From calculation below

Source: from table 5.9 and calculation

EHDs of the last two combinations, shrub-clay and shrub-loamy sand, were calculated with respect to calculated EHDs and porosity by using equation as follow.

$$A_{(a,b1)} = \frac{\text{Porosity of a texture} * \text{Calculated EHD of b1 texture}}{\text{Porosity of b1 texture}} \quad (5.6)$$

$$\text{EHD of a texture} = \frac{\sum_{i=1}^N A_{(a,b_i)}}{N} \quad (5.7)$$

Where,

bi = soil texture which its EHD is known

N = number of soil textures which their EHDs are known

For an example above, the combination of shrub-clay was calculated as follow:

Shrub-clay combination:

$$\begin{aligned} A_{(a,b1)} &= (47.5 * 341.31) / 46.4 && \text{(Respected to clay loam texture)} \\ A_{(a,b2)} &= (47.5 * 503.66) / 46.3 && \text{(Respected to loam texture)} \\ A_{(a,b3)} &= (47.5 * 213.90) / 45.3 && \text{(Respected to sandy loam texture)} \\ A_{(a,b4)} &= (47.5 * 545.59) / 50.1 && \text{(Respected to silt loam texture)} \\ A_{(a,b5)} &= (47.5 * 11.16) / 47.9 && \text{(Respected to silty clay texture)} \end{aligned}$$

$$\begin{aligned} \text{EHD of shrub-clay combination} &= \frac{(349.40 + 516.71 + 224.29 + 517.28 + 11.07)}{5} \\ &= 323.75 \end{aligned}$$

That process was applied into all combinations except for built up area, paddy field, water body, and grassland.

Two of three sample points on the built area, sample number 71 and 72, have no infiltration value (the water was not infiltrated). That condition occurred because soil structure in the built up area mostly have been compacted by human activities. Besides, surface of built up area was dominantly covered by concrete, asphalt, and building. According to those facts, this research assumes that EHD of built up area equals to 5 mm.

Based on field observations and interviews with farmers, paddy field were inundated from transplanting time until next 90 days (three month). On the other hand, water bodies in the study area were identified as lake and large pond, which are inundated all the time. According to those conditions, the research assumes that EHD of paddy field in the first 90 days, and water body equal to 2 mm.

This research used 110 mm for EHD of Grass land as recommended by Morgan and Duzant in Rustanto (2010). On the other hand, the research assumes that terraces can increase the water storage of the area so EHD for the dry land cultivation was added by 0.01 because almost all dry cultivation areas on the study area are terraced. Appendix 5 shows calculated EHDs of all combinations (landcover types and soil textures), Bulk density, and field capacity of all soil textures.

Scripts used to calculate daily infiltration in the model are:

“A = timeinputscalar(Table1, map of soil texture and landcover combinations)*mask of study area”

“Rc = A*R”

“Infiltration = min(RC, ER)”

Where:

Table1 = a table representing MS*BD*EHD for each combination of landcover and soil texture

R = Ratio of actual to potential evapotranspiration

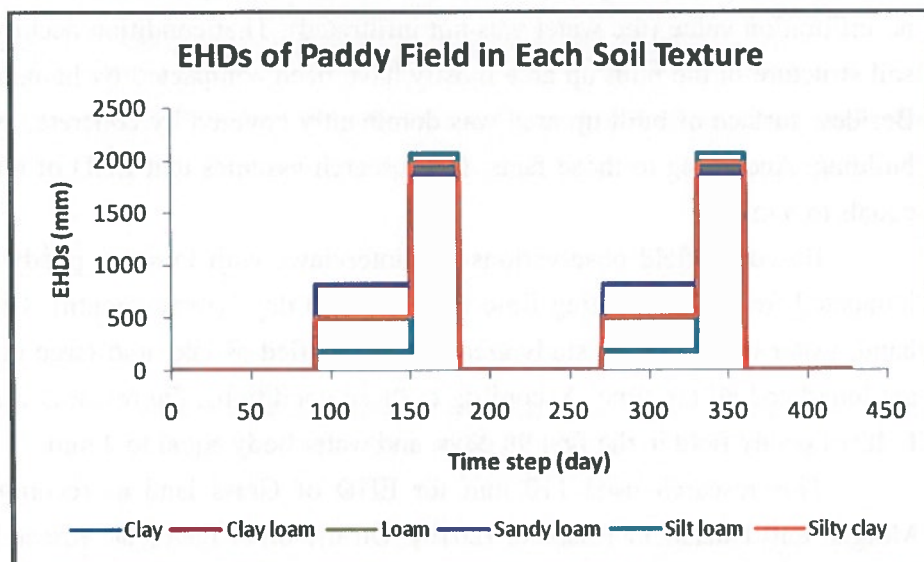
Rc = Soil Moisture Storage Capacity

ER = Effective rainfall (rainfall that has been reduced by potential evapotranspiration and interception)

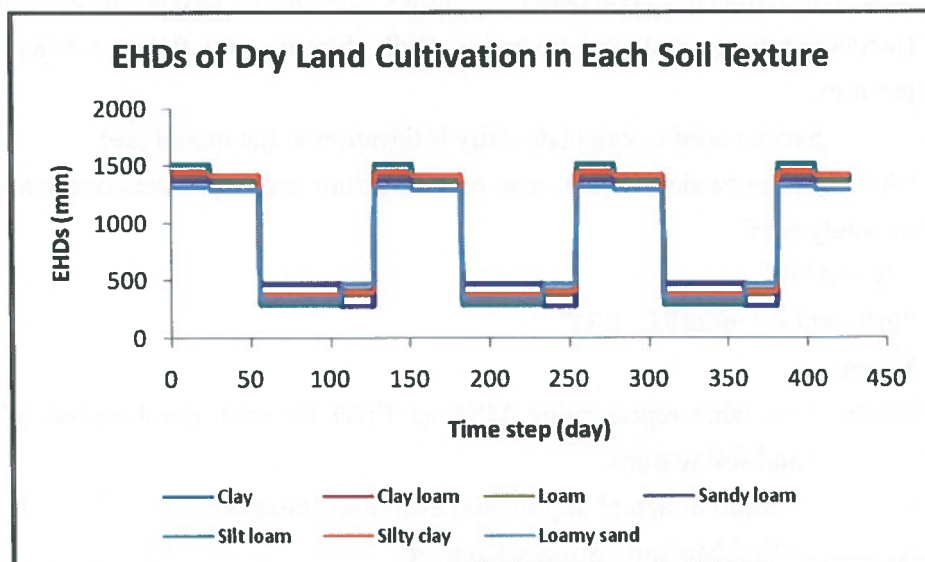
Those scripts show that infiltration never passed soil moisture storage capacity.

There were two EHDs of landcover types, which were affected by their growth stages and soil textures, paddy field and dry land cultivation. When their

growth stages were change, their EHDs also were change. The EHDs of the landcover types in each soil texture are represented by graphs as follow.



Graph 5.1. EHDS of Paddy Field in Each Soil Texture



Graph 5.2. EHDS of Dry Land Cultivation in Each Soil Texture

5.1.5. Runoff

The research only concerned in the over land flow and determined runoff value as rainfall value minus potential evapotranspiration, interception, and infiltration. In the model, runoff was determined by using scripts as follow.

“runoff = (ER-infiltration)”

“runoff2 = 0.001*(runoff)*cellarea()”

“dis=accuflux(LDD, runoff2)”

“table1= timeoutput(map of discharge stations, dis)”

Where:

ER = Effective daily rainfall or rainfall which had been reduced by potential evapotranspiration and interception

Cellarea = area of one cell (900 m² for this research)

LDD = Local Drain Direction (a map representing dirrection of flow of water from each cell to its steepest down slope neighbour and creating a line network as flow pattern)

table1 = a table showing modeled runoff on discharge stations

5.2. Analyzing Runoff Dynamics

5.2.1. Comparing modeled and measured runoffs

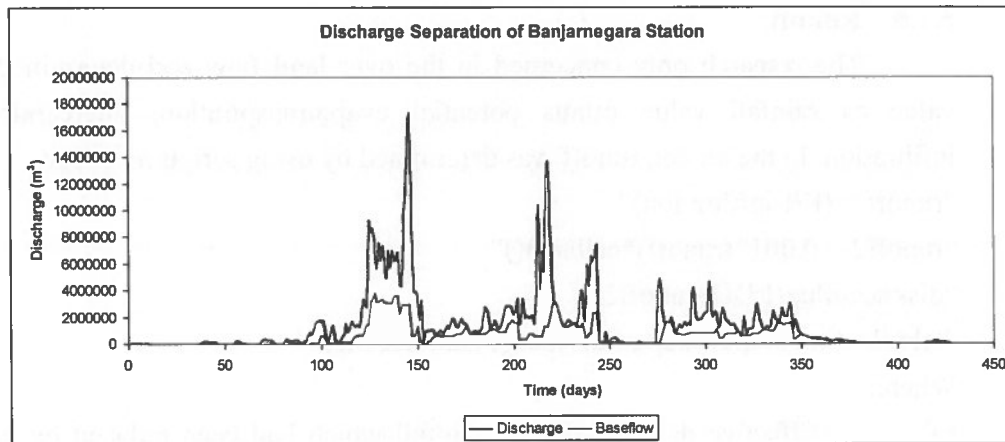
Time from the peak to the end of of the runoff hydrographs on the two stations were calculated by using Fixed time method. The results are shown by the table 5.11.

Table 5.11. Times from the peak to the end for two hydrograph stations

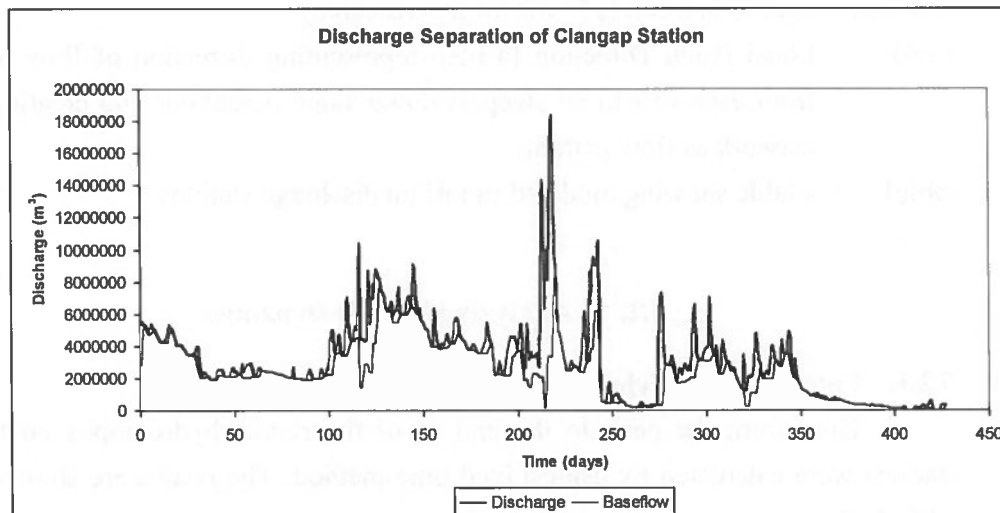
No	Stations	Extent of Sub-watershed (miles ²)	τ (days)
1	Banjarnegara	277.351	3.08 \approx 3
2	Clangap	90.116	2.46 \approx 2

Source: Calculations carried in Microsoft Office Excel 2003

According to the table, this research assumed that when the river flow measured in station 1 (Banjarnegara) continually decreases, after three days from the peak day, the water suplay of river flow is change from surface flow to base flow. The same assumption was applied to station 2 (Clangap), when the flow decreases continually, after two days the water suplay of the flow is change from surface flow to base flow. The surface flows of two stations separated from the dischrages are shown by graphs in graph 5.3 and 5.4.



Graph 5.3. Discharge separation of Banjarnegara station



Graph 5.4. Discharge separation of Clangap station

Total of measured daily runoff from two stations during research period, July 1st, 2008 to August 31st, 2009, is shown by table 5.12.

Table 5.12. Total of Measured Daily Runoffs From Two Stations

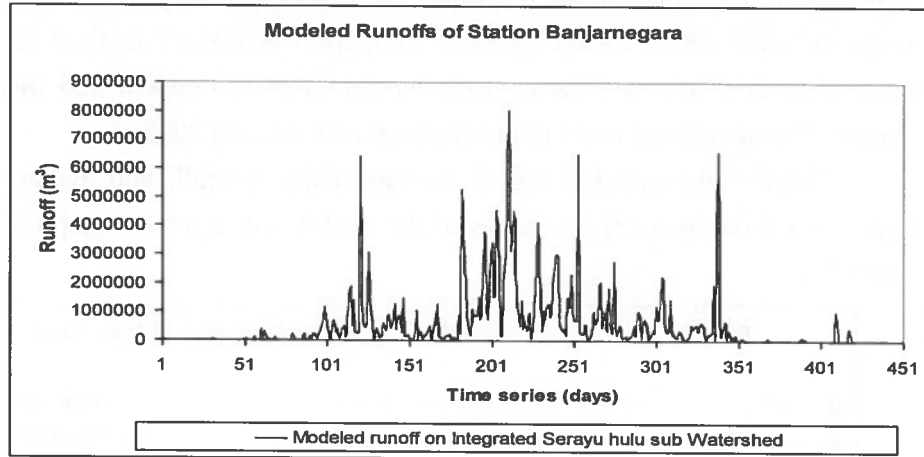
NO	Stations	Discharge (m ³)	Runoff (m ³)	Percentage (%)
1	Banjarnegara	638705410.9	380333747.5	59.55
2	Clangap	1354558084	314490165.9	23.22

Source: Calculations carried in Microsoft Office Excel 2003

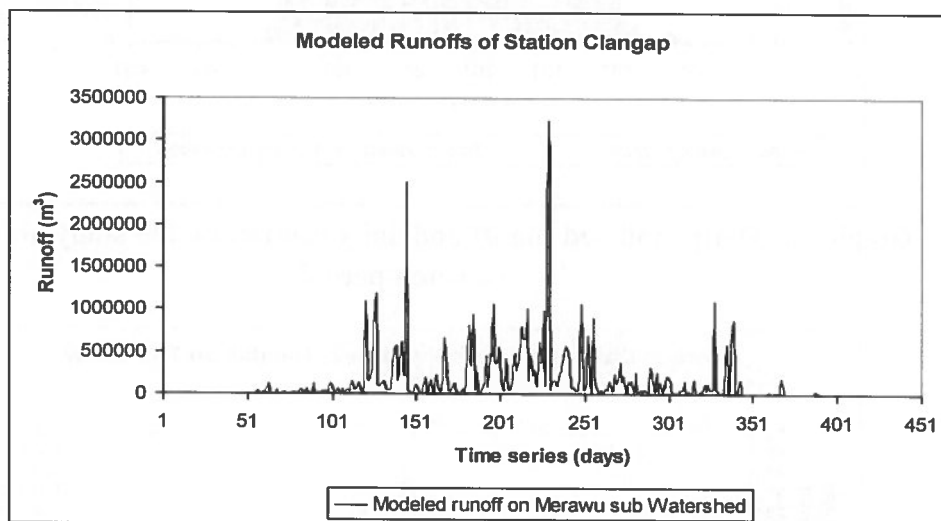
According to the table above, Sub-watershed Merawu had higher discharge than the discharge of Banjarnegara station. By respecting the discharge of two stations, Runoff flowing form Merawu Sub-watershed (23.22 %) was lower than runoff flowing from Integrated Serayu Hulu Sub-watershed (59.56 %). On the other hand, the rasio of runoff to the extent of sub-watershed shows that Merawu Sub-

watershed had higher ratio (3489837.164 m³/day/ miles) than the ratio had by Integrated Serayu Hulu Sub-watershed (1371521 m³/day/ miles²).

Modeled runoffs on the two stations were transformed from the runoff table (.tss format), as result of the model, to graphs as shown by graph 5.5 and 5.6.



Graph 5.5. Modeled runoff of Banjarnegara station



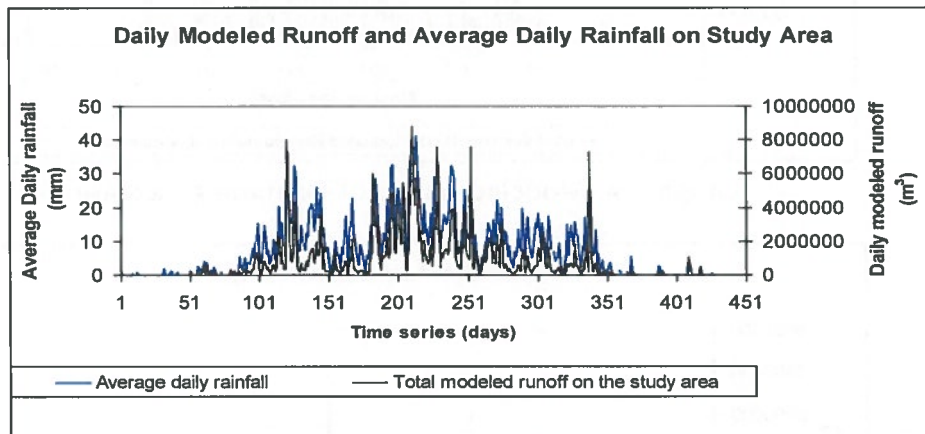
Graph 5.6. Modeled runoff of clangap station

Those measured and modeled runoffs of each station were recalculated to monthly and compared by involving Pearson Product Moment Correlation method and scattered graph in Microsoft office Excel 2003. Comparing modeled and measured runoffs was carried to find how close the modeled runoff to measured runoff.

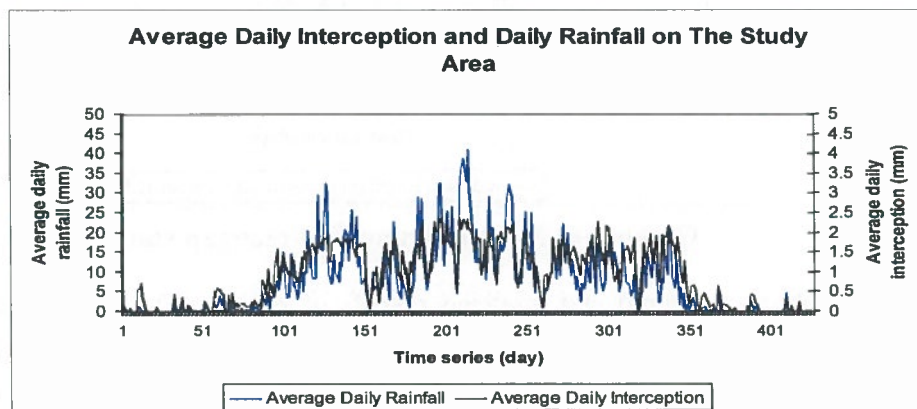
5.2.2. Identifying the correlation between each hydrological component and modeled runoff

Total daily-modeled runoff of two Sub Watersheds and average daily of hydrological components, interception, potential evapotranspiration, and infiltration were included into Pearson Product Moment Correlation method to determine correlation coefficients between each hydrological component and total modeled runoff. The calculating was run in Microsoft office Excel 2003.

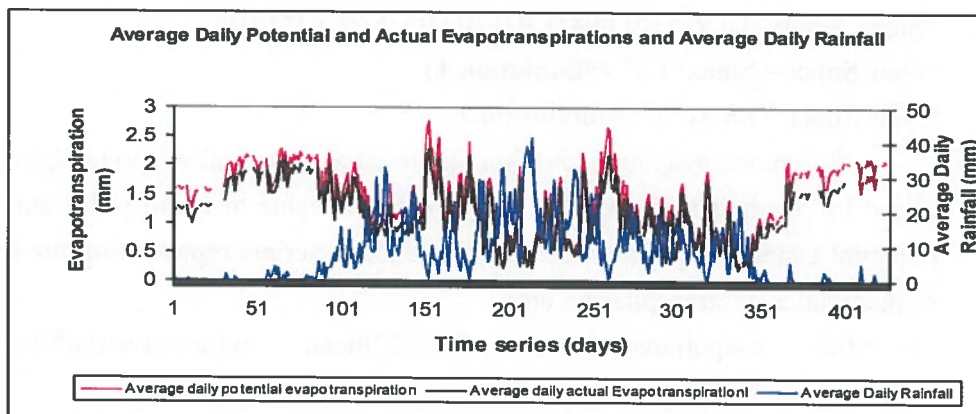
Total daily-modeled runoff, average daily rainfall, and averages daily of hydrological components, as results of the model, are shown by graph 5.7, 5.8, 5.9, and 5.10.



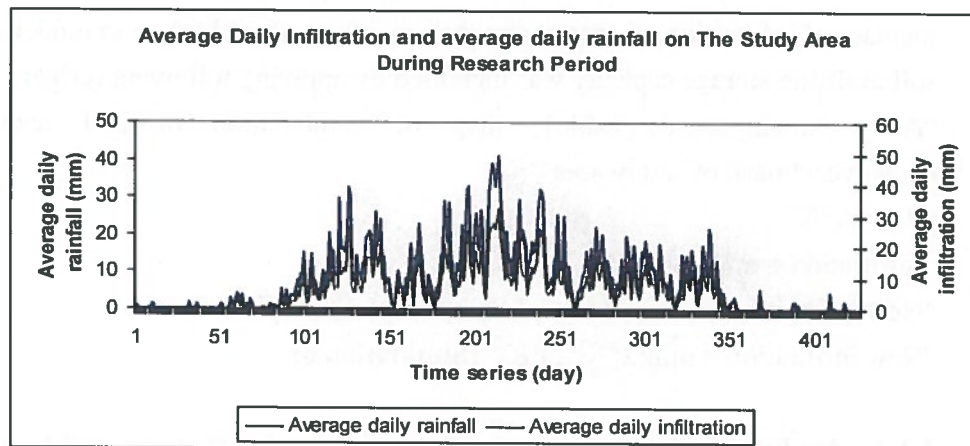
Graph 5.7. Daily modeled runoff and daily rainfall on the study area during research period



Graph 5.8. Average daily interception and rainfall in the study area during research period



Graph 5.9. Average daily potential and actual evapotranspirations, and average daily rainfall in the study area during research period



Graph 5.10. Average daily infiltration and average daily rainfall in the study area during research period

5.2.3. Evaluating the sensitivity of hydrological components to modeled runoff

Six sensitivity simulations were carried in the model by increasing the value of hydrological components. The value of hydrological components were increased by modifying the scripts, and then the model was rerun to generate new runoff. Percentage of total modeled runoff change (from total original runoff to total new runoff) was assumed as the sensitivity of hydrological component to modeled runoff.

Increasing interception in the model was carried by rising maximum storage capacity of canopy to one-half and two times of the original value. That process was carried in the model by applying following scripts.

“ $S_{max} = \max(0, 0.935 + (0.498 * LAI) - (0.00575 * (LAI ** 2)))$ ”

“New $S_{max} = S_{max} * 1.5$ ” (Simulation 1)

“New $S_{max} = S_{max} * 2$ ” (Simulation 2)

Reference evapotranspiration, assumed as potential evapotranspiration, was raised by one-half and two times of its original value to identify the sensitivity of potential evapotranspiration to modeled runoff. Scripts representing the increasing of potential evapotranspiration are:

“Potential evapotranspiration = $0.0022 * \text{mean extra-terrestrial} * (\text{temperature difference} ** 0.5) * (\text{temperature} + 17.8)$ ”

“New potential evapotranspiration = Potential evapotranspiration * 1.5” (Simulation 3)

“New potential evapotranspiration = Potential evapotranspiration * 2” (Simulation 4)

An increase of soil moisture storage capacity (R_c) was considered as an increase of infiltration. To determine the sensitivity of infiltration to modeled runoff, soil moisture storage capacity was increased by applying following scripts.

“ $A = \text{timeinputscalar}(\text{Table1, map of combination of soil texture and landcover}) * \text{mask of study area}$ ”

“ $R_c = A * R$ ”

“Infiltration = $\min(RC, ER)$ ”

“New infiltration = $\min(1.5 * RC, ER)$ ” (Simulation 5)

“New infiltration = $\min(2 * RC, ER)$ ” (Simulation 6)

5.2.4. Analyzing the responses of modeled runoff to possible modified landcover

According to the position of landcover in the model (see the linkages in figure 4.3), replacing landcover type automatically affected values of interception and infiltration. Based on that condition, replacing landcover types was the same as modifying interception and infiltration values. When a landcover type replaced other types, then interception and infiltration values of replacing landcover type were applied to replaced landcover types.

In order to obtain interception value of a certain landcover type, the scripts calculating interception in the model were modified as follows.

“ $S_{max} = \max(0, 0.935 + (0.498 * LAI) - (0.00575 * (LAI ** 2)))$ ”

“ $S_{max1} = \text{if}(\text{landcover} == \text{water body or landcover} == \text{no data}, 0, S_{max})$ ”

“ $S_{max2} = \text{if}(\text{landcover} == \text{a certain landcover type}, S_{max1}, 0)$ ”

“ $S_{max_avg} = \text{maptotal}(S_{max2}) / \text{cell number of a certain landcover type}$ ”

“ $S_{max3} = \text{if}(\text{landcover} == \text{replaced landcover types}, S_{max_avg}, S_{max1})$ ”

“Rainfall = rainfall – potential evapotranspiration”

“Interception = interception + rainfall”

“Interception = (min(Smax3, max(0,interception)))”

Explanation:

1. In the script all landcover types were represented by codes
2. a certain landcover was filled by the code of a landcover type replacing other landcover types.
3. Replaced landcover types were filled by codes of landcover types that were replaced by a certain landcover type

Table 5.13 shows the codes and cell numbers of all landcover types.

Table 5.13. Codes and cell numbers of all landcover types

Code	Landcover types	Cell numbers
1	Built up area	54844
2	paddy field	63009
3	Water body	1856
4	dry cultivation	230220
5	forest	118026
6	shurb	203728
7	plantation	382484
8	grass land	3015

Source: Calculations carried in Arcgis 9.2.

Reconstructing the table representing MS*BD*EHD for each combination of landcover and soil texture, applying the reconstructed table to the map of landcover and soil texture combinations, and reruning the model, were processed to obtain new infiltration distribution in the model. Those processes were carried in the model by modifying the scripts determining infiltration value. Modifying scripts are described as follows.

“A = timeinputscalar(reconstructed Table1, map of soil texture and landcover combinations)*mask of study area”

“Rc = A*R”

“Infiltration = min(RC, ER)”

There were three reconstructed tables applied in the model in accordance with the number of proposed scenarios. Modeled runoffs as the results of scenarios were compared to original runoff to identify the responses of modeled runoff to landcover changes.

6. RESULT AND DISCUSSION

6.1. Characteristics of hydrological components on each landcover type

Total of hydrological components in each landcover type during research period as the result of the model are represented by table 6.1.

Table 6.1. Total of hydrological component in each landcover type

No	Landcover type	Cumulative interception (mm)	Cumulative potential evapotranspiration (mm)	Cumulative actual evapotranspiration (mm)	Cumulative infiltration (mm)	Cumulative runoff (m ³)
1	Built up area	295	734	734 (100 %)	474	1980
2	Paddy field	300	790	819 (104 %)	1257	1074
3	Dry land cultivation	352	632	521 (82 %)	2622	74
4	Forest	421	537	496 (92 %)	2535	416
5	Shrub	427	546	442 (81 %)	2817	138
6	Plantation	432	609	509 (83 %)	2735	178
7	Grass land	483	336	278 (83 %)	2487	960

Source: calculated by the model

Table 6.1 shows that each landcover type resulted specific value of hydrological components. The highest cumulative interception on the study area during research period was on grassland and the lowest was on built up area. That condition was supported by vegetations growth on those two areas, vegetations on built up area was lower than vegetations on grassland. Forest, shrub, and plantation, had relatively same interception with grassland. Their interceptions were in range 421 mm – 483 mm. Those interception values were relatively higher than interception values of three other landcover types, built up area, paddy field, and dry land cultivation. This condition was affected by amount of vegetations covering on those landcover types and by the growth stages had by paddy field and dry land cultivation. Those two landcover types had a growth stage in which the areas was on bare condition or almost had no vegetation. The stage was interval stage between harvesting and transplanting for paddy filed and initial stage for dry land cultivation.

The highest cumulative evapotranspirations on the study area during research period occurred on paddy field and the lowest occurred on Grassland. The difference between potential and actual evapotranspiration is assumed as crop water need (Pidwirny and Jones 2009). The percentage of actual evapotranspiration to potential evapotranspiration was an implication of crop factors used in the model and

represents quantity of water that is actually removed from a surface due to the processes of evaporation and transpiration (Pidwirny and Jones 2009). The research assumed that on the built up area, all the potential evapotranspiration would become actual evapotranspiration (high actual evapotranspiration) respecting the condition of built up area covered by buildings, asphalt, concrete, and other constructions and inflicting crop water need on the built up area became almost zero. This condition is in line with Lin, Velde et al. (2008) stating that mixed effect of construction, water body, street trees and grass parcels that have very high evapotranspiration drive the urban areas to have high actual evapotranspiration.

Forest area had relatively high actual evapotranspiration comparing to its potential evapotranspiration, respecting to the condition of forest that generally was still dense. Actual evapotranspiration of paddy field was higher than its potential evapotranspiration because this research assumed that almost all the crop factors in paddy field growth stages were more than one (table 5.4) representing irrigation involved in paddy field management.

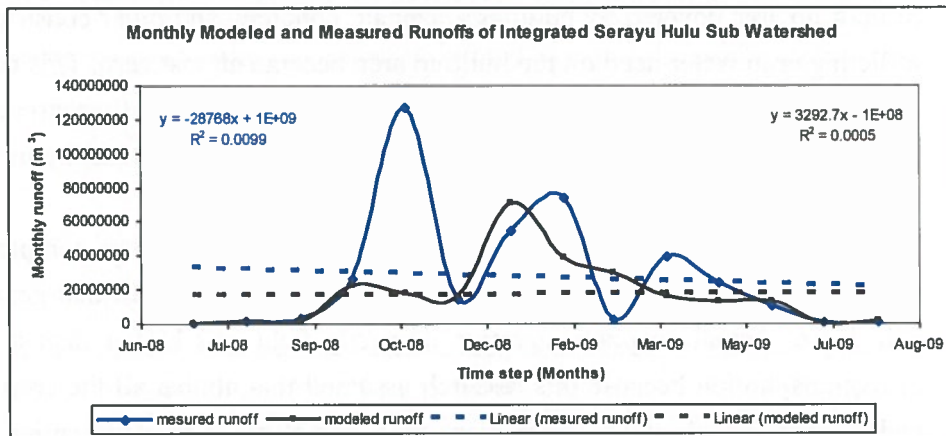
Based on table 6.1, the highest cumulative infiltration on the study area during research period occurred in Shrub area (2864 mm) and the lowest occurred in the built up area (499mm). Dry land cultivation, forest, shrub, plantation, and grassland had relatively high cumulative infiltration. Their cumulative infiltrations were in range 2400 mm – 2900 mm. On the other hand, built up area had the lowest infiltration which was caused by constructions dominantly covered the area, and paddy field also had relatively low infiltration representing the effect of growth stages (stages 1 and 2) in which the area were inundated resulting low infiltration.

Landcover type, which had the highest runoff, was the built up area, with cumulative runoff equaled to 1980 m³. That fact represents the condition of surface on the built up area which was mostly covered by buildings, asphalt, concrete, and other constructions. Constructions covering surface reduce infiltration capability and increase runoff.

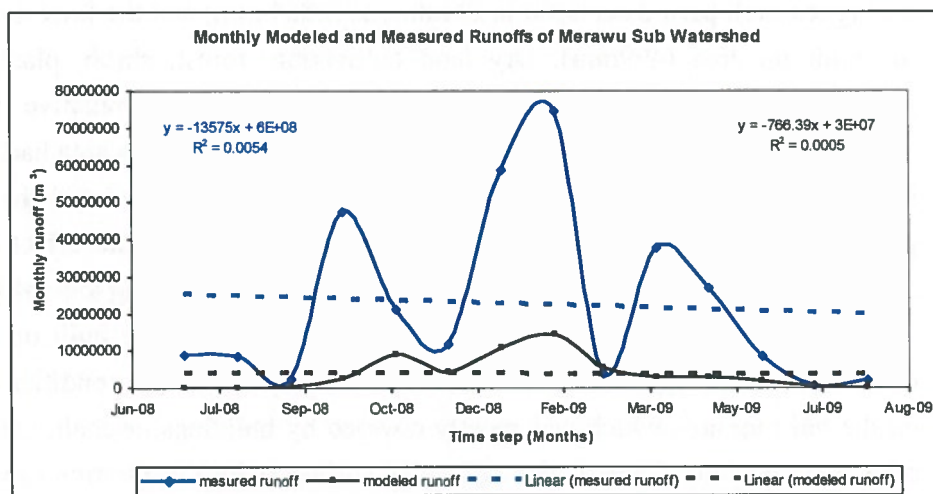
The lowest runoff occurred on dry land cultivation. This condition was caused by high effective hydrological depth (EHD) had by dry land cultivation (appendix 5). Effective hydrological depth of dry land cultivation, especially in initial and crop development growth stages, was very high. That EHD could increase soil moisture storage capacity and reduce runoff. In initial growth stage, farmers cultivated the land and made the water on the land infiltrated easily.

6.2. Comparing Modeled Runoff and Measured Runoff

Monthly Modeled runoffs of two Sub Watersheds, Integrated Serayu Hulu and Merawu, during research period (July 2008 – August 2009) compared to monthly measured runoffs are shown by graph 6.1 and graph 6.2.



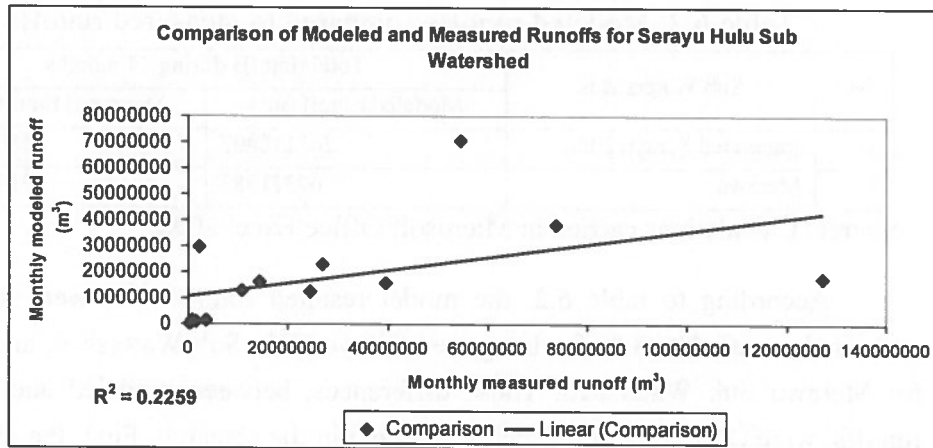
Graph 6.1. Monthly modeled and measured runoffs of Integrated Serayu Hulu Sub Watershed



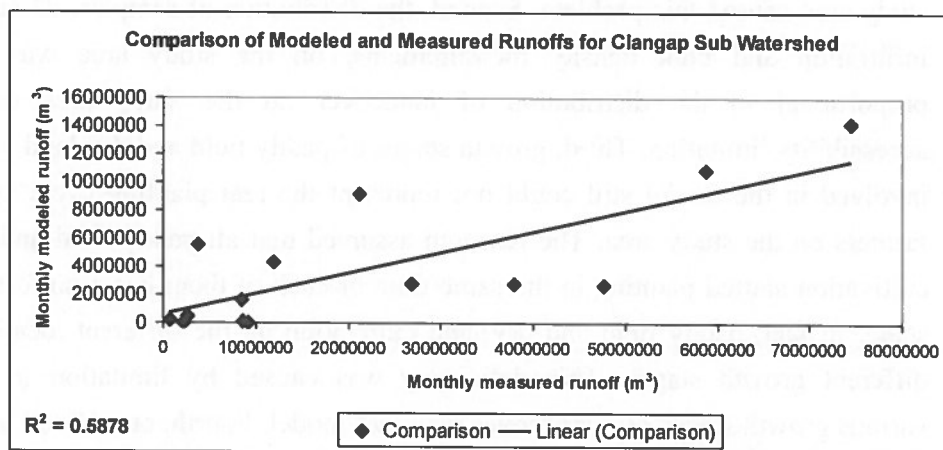
Graph 6.2. Monthly modeled and measured runoffs of Merawu Sub Watershed

According to those graphs, in terms of total runoff, modeled runoff was closer to measured runoff on Integrated Serayu Hulu Sub Watershed than modeled runoff to measured runoff in Merawu Sub Watershed (shown by the position of black fine lines respecting to blue fine lines). On the other hand, in terms of runoff distribution in each month, modeled runoff was closer to measured runoff on Merawu Sub Watershed than modeled runoff to measured runoff in Integrated

Serayu Hulu Sub Watershed (shown by the trends of dashed blue lines and dashed black lines).



Graph 6.3. Comparison of modeled and measured runoffs on Integrated Serayu Hulu Sub Watershed



Graph 6.4. Comparison of modeled and measured runoffs on Merawu Sub Watershed

The correlation coefficients, R^2 s, on the graph 6.3 and 6.4 describe the closeness of modeled runoff to measured runoff with assumption that if correlation coefficient equals to one then modeled runoff is exactly same with measured runoff. The graphs show that in Integrated Serayu Hulu Sub Watershed, 22.59% of the variance in measured runoff could be explained by variance of modeled runoff, and in Merawu Sub Watershed, 58.78 % of the variance in measured runoff could be explained by variance of modeled runoff.

Table 6.2 shows the total model runoffs on two Sub Watersheds during research period (14 months) compared to total measured runoffs from two discharge

stations. This comparison was conducted to determine the position of modeled runoff respected to the measured runoff.

Table 6.2. Modeled runoffs compared to measured runoffs

NO	Sub Watersheds	Total runoffs during 14 months	
		Modeled runoff (m ³)	Measured runoff (m ³)
1	Integrated Serayu Hulu	267118807	380333747
2	Merawu	62371385	314490165

Source: Calculations carried in Microsoft Office Excel 2003

According to table 6.2, the model resulted runoffs that were lower than measured runoff, 70.23 % for Integrated Serayu Hulu Sub Watershed, and 19.83 % for Merawu Sub Watershed. Those differences, between modeled and measured runoffs, were caused by deficiencies involved in the research. First, the distribution of rainfall gauges did not fully cover the distribution of rainfall intensity occurring on the study area. Small number and locations of available rainfall gauges on the study area caused this problem. Second, the distribution of samples, 73 cumulative infiltration and bulk density measurements, on the study area was still not proportional to the distribution of landcover on the study area caused by accessibility limitation. Third, growth stages of paddy field and dry land cultivation involved in the model still could not represent the real planting cycle applied by farmers on the study area. The research assumed that all paddy field and dry land cultivation started planting in the same time or each of them has a uniform growth stage. In fact, paddy field and dry land cultivation on the different locations have different growth stages. This deficiency was caused by limitation in applying various growth stages of a landcover type into model. Fourth, one of soil properties, porosity, involved in the model was obtained from reference, which probably was not appropriate with the condition on the study area.

6.3. Correlation between Each Hydrological Component and Modeled Runoff

Total daily runoff, average daily interception, potential evapotranspiration, and infiltration on the study area had been involved in Pearson Product Moment Correlation method to calculate the correlation between each of hydrological component and total modeled runoff. Calculation was carried in Microsoft Office Excel 2003 and results of calculation are shown by table 6.3.

Table 6.3. Correlation coefficient between hydrological component and modeled runoff

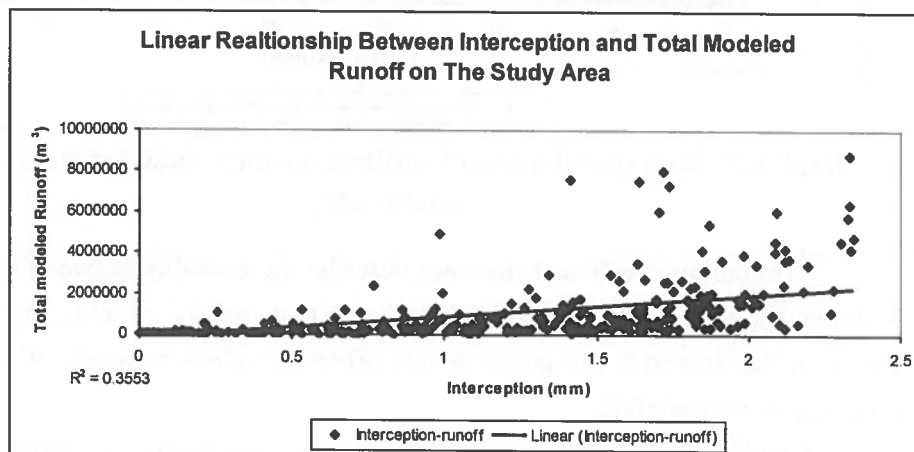
No	Hydrological components	Correlation coefficient between hydrological component and total modeled runoff (R^2)
1	Interception	0.3553
2	Potential Evapotranspiration	0.2585
3	Infiltration	0.6638

Source: Calculations carried in Microsoft Office Excel 2003

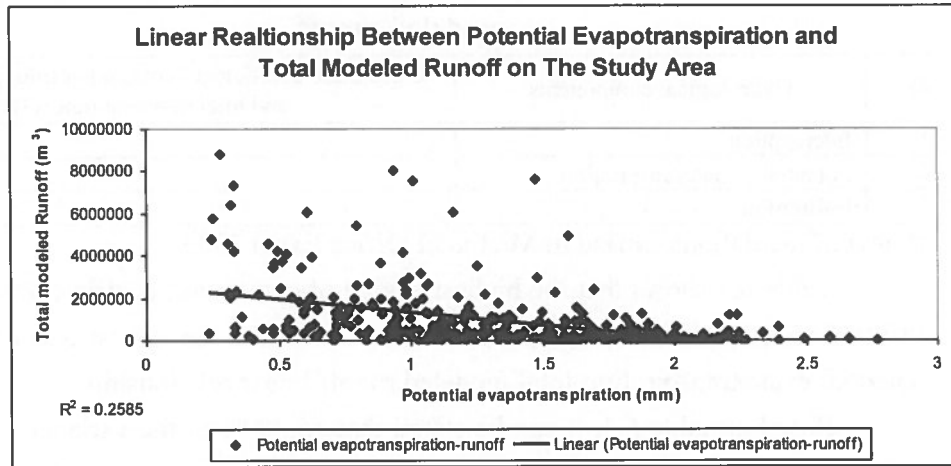
Table 6.3 shows that the highest square of correlation coefficient was had by Infiltration-total modeled runoff linear relationship and the lowest one was had by potential evapotranspiration-total modeled runoff linear relationship.

Based on table 6.3, it can be stated that 66.38 % of the variance in the total modeled runoff could be explained by variance of infiltration, 35.53 % of the variance in the total modeled runoff could be explained by variance of interception, and 25.85 % of the variance in the total modeled runoff could be explained by variance of potential evapotranspiration.

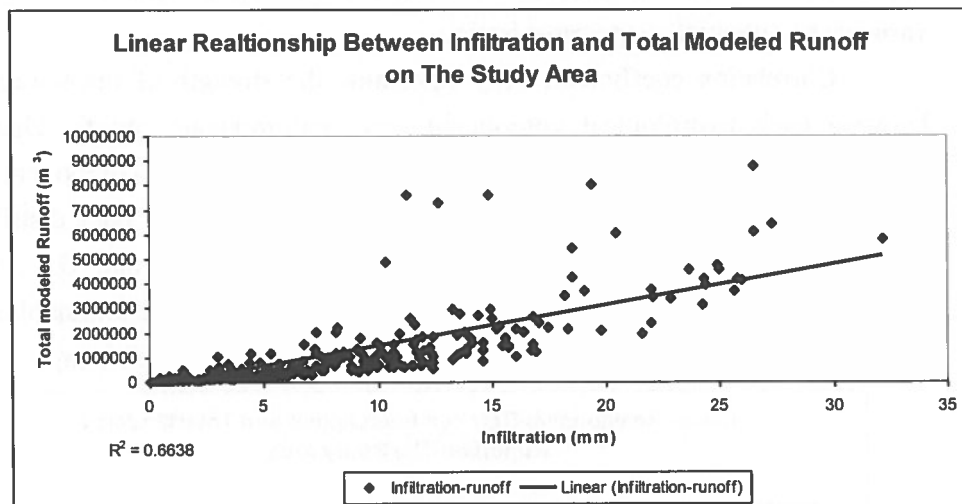
Correlation coefficients only determine the strength of linear relationships between each hydrological component and total modeled runoff. They do not represent the level of causality or effect between hydrological component and total modeled runoff. Correlation coefficient strongly depends on data distribution of variables involved in linear relationship. Graph 6.5, 6.6, and 6.7 show data distribution of interception-total modeled runoff, potential evapotranspiration-total modeled runoff, and infiltration-total modeled runoff linear relationships.



Graph 6.5. Data distribution of interception-total modeled runoff linear relationship



Graph 6.6. Data distribution of potential evapotranspiration-total modeled runoff linear relationship



Graph 6.7. Data distribution of infiltration-total modeled runoff linear relationship

Correlation coefficient does not describe the causality between variables but it shows the responses of variables to factor that mainly affected their values or levels. In this research, the factor mostly affecting values or levels of hydrological components was rainfall.

Graph 6.5 and figure 6.7 show graphs representing positive correlation coefficient in which data of interception-modeled runoff and infiltration-modeled runoff formed an increase trend line with data of total modeled runoff. Those facts represent that all of those variables had the same responses to rainfall. Interception, infiltration, and runoff increased when rainfall increased.

On the other hand, negative correlation coefficient formed by data distribution of potential evapotranspiration-modeled runoff shows that modeled runoff had different response with potential evapotranspiration to rainfall as the main input.

6.4. Sensitivities of Hydrological Components to Modeled Runoff

All sensitivity simulations were processed in the model. Table 6.4 shows the results of the processes representing the changes of hydrological component values and their effects to modeled runoff.

Table 6.4. The changes of hydrological component values and their effects to runoff

No	Hydrological component changes	Original runoff (m ³)		Generated runoff (m ³)		Percentage	
		Integrated Serayu Hulu Sub Watershed	Merawu Sub Watershed	Integrated Serayu Hulu Sub Watershed	Merawu Sub Watershed	Integrated Serayu Hulu Sub Watershed	Merawu Sub Watershed
1	Interception multiplied by one and half	267118807	62371385	257236264	59245374	-3.70	-5.01
2	Interception multiplied by two	267118807	62371385	243845969	55279166	-8.71	-11.37
3	Potential evapotranspiration multiplied by one and half	267118807	62371385	252026111	58299038	-5.65	-6.53
4	Potential evapotranspiration multiplied by two	267118807	62371385	236574503	54089005	-11.43	-13.28
5	Infiltration multiplied by one and half	267118807	62371385	204971070	46758232	-23.27	-25.03
6	Infiltration multiplied by two	267118807	62371385	178892923	39927885	-33.03	-35.98

Source: Calculations carried in Microsoft Office Excel 2003

Based on table 6.4, the most sensitive component to runoff in the model was infiltration. Runoff was raised more than 20 percent when infiltration was increased a half of original value and it raised more than 30 percent when infiltration was increased two times of original value. on the other hand, interception and potential evapotranspiration had low sensitivities respecting to infiltration. Runoff decreased about 3.70 – 5.01 percent when interception was added by a half of original value and reduction increased to 8.71 – 11.37 percent when interception was increased two times of original value. Evapotranspiration had relatively same sensitivity with interception. Runoff decreased 5.65 – 6.53 percent when potential evapotranspiration was increased a half of original value and it decreased 11.43 – 13.28 percent when potential evapotranspiration increased two times.

6.5. Responses of Modeled Runoff to Possible Modified Landcover

Landcover modifications, the scenarios, were applied by reconstructing and rerunning the model. The results of the rerunning model are shown by table 6.5.

Table 6.5. Total modeled runoffs as the results of scenarios

No	Scenarios	Original runoff (m ³)		Generated runoff (m ³)		Percentage	
		Integrated Serayu Hulu Sub Watershed	Merawu Sub Watershed	Integrated Serayu Hulu Sub Watershed	Merawu Sub Watershed	Integrated Serayu Hulu Sub Watershed	Merawu Sub Watershed
1	Replacing cultivation, shrub, and plantation by forest	267118807.9	62371385.52	300245523.2	70012123.19	12.40	12.25
2	Replacing cultivation, shrub, and forest by plantation	267118807.9	62371385.52	311145170.5	47072327.81	16.48	-24.53
3	Replacing plantation, shrub, and forest by cultivation	267118807.9	62371385.52	172390270.3	31237501.19	-35.46	-49.92

Source: calculations carried in Microsoft Office Excel 2003

Results of scenarios shows that all modifying landcover types, forest, plantation, and cultivation, gave different affect to modeled runoff. Cultivation had the most negative influence to runoff comparing to two other landcover types. It greatly reduced runoff, 35.46 % for Integrated Serayu Hulu Sub Watershed, and 49.92 % for Merawu Sub Watershed. Replacing cultivation, shrub, and plantation by forest, increased modeled runoff on those Sub Watersheds, 12.40 % for Integrated Serayu Hulu Sub Watershed, and 12.25 % for Merawu Sub Watershed. On the other hand, replacing cultivation, shrub, and forest by plantation, increased modeled runoff on Integrated Serayu Hulu Sub Watershed about 16.48 %, meanwhile it decreased modeled runoff on Merawu Sub Watershed about 24.53 %.

Replacing landcover types by cultivation decreased modeled runoff on both Sub Watersheds because combination of cultivation with any soil textures had the highest effective hydrological depth compared to combinations of other landcover types with soil textures (appendix 5). Scenario 1 increased runoffs on both Sub Watersheds because forest that has the lowest infiltration and potential evapotranspiration among the modified landcover types (table 6.1) replaced the landcover types which had relatively high infiltration. On the other hand, cultivation, shrub, and plantation had larger areas than forest area (table 6.6) so that condition reduced infiltration capacity and increased runoff on the study area.

Scenario 2, replacing cultivation, shrub, and forest by plantation, decreased modeled runoff on Merawu Sub Watershed because plantation had relatively high interception and infiltration (table 6.1). Even though plantation had high interception and infiltration, modeled runoff on Integrated Serayu Hulu Sub Watershed was increased by scenario 2. This condition was affected by the difference of soil texture distributions on both Sub Watersheds. Combination of plantation and clay loam had

the highest effective hydrological depth in plantation-soil texture combinations (appendix 5) and clay loam in Merawu Sub Watershed had larger area (28.77 %) than clay loam in Integrated Serayu Hulu Watershed (2.22 %), which made the combination, gave more effect in Merawu Sub Watershed than in Integrated Serayu Hulu Sub Watershed. Table 6.7 shows soil texture distribution in both Sub Watersheds.

Another factor, making scenario two increased modeled runoff on Integrated Serayu Hulu Sub Watershed, was the difference of areas that were replaced by plantation. In scenario two, 52.36 % of Integrated Serayu Hulu Sub Watershed area and 55.71 % of Merawu Sub Watershed area were replaced by plantation. The more areas that were replaced the more effect that was given by plantation. Replaced areas on Integrated Serayu Hulu Sub Watershed were lower than replaced areas on Merawu Sub Watershed so plantation, which could greatly raise interception, gave more effects on Merawu Sub Watershed than on Integrated Serayu Hulu Sub Watershed.

Table 6.6. Areas of landcover types in two Sub Watersheds

No	Landcover types	Integrated Serayu Hulu Sub Watershed (pixel number)	%	Merawu Sub Watershed (pixel number)	%
1	Built up area	40809	5.35	9281	3.68
2	Paddy field	49666	6.52	7612	3.02
3	Water body	1482	0.19	208	0.08
4	Dry cultivation	173126	22.71	54428	21.58
5	Forest	74920	9.83	37369	14.82
6	Shrub	151012	19.81	48717	19.31
7	Plantation	268289	35.20	94331	37.40
8	Grass land	2862	0.37	279	0.11

Source: Digital landcover map and calculation carried in Arcgis 9.2

Table 6.7. Areas of soil textures in two Sub Watersheds

No	Soil texture	Integrated Serayu Hulu Sub Watershed (pixel number)	%	Merawu Sub Watershed (pixel number)	%
1	Clay	98607	12.93	14967	5.93
2	Clay loam	16935	2.22	72602	28.77
3	Loam	175643	23.04	61696	24.45
4	Loamy sand	52344	6.86	-	0
5	Sandy loam	347395	45.56	83879	33.24
6	Silt loam	56991	7.47	-	0
7	Silty clay	14561	1.91	19169	7.60

Source: digital texture map and calculation carried in Arcgis 9.2

7. CONCLUSIONS AND RECOMMENDATIONS

7.1. Conclusions

The research attempted to describe the characteristics of hydrological components on each landcover type, figure the correlation between each hydrological component and total modeled runoff, identify the sensitivity of each hydrological component to modeled runoff, and investigate the responses of modeled runoff to landcover changes on the study area. The findings as results of the research that were discussed in the previous section support the following conclusions answering the research objectives and questions.

7.1.1. Characteristics of hydrological components on each landcover type

7.1.1.1. Interception

Condition of interception in each landcover type was affected by amount of vegetation covering on each landcover type and growth stages had by paddy field and dry land cultivation. The highest interceptions occurred on Grassland, plantation, shrub, and forest, and the lowest occurred on built up area.

7.1.1.2. Evapotranspiration

Values of potential and actual evapotranspiration in each landcover type were determined by crop factor and growth stages had by each landcover type. The highest potential and actual evapotranspirations on the study area during research period occurred on paddy field. Meanwhile the lowest occurred on grassland.

7.1.1.3. Infiltration

Factors determining infiltration in each landcover type were, cumulative effective hydrological depth of landcover type, bulk density and soil moisture at field capacity of soil texture, and condition of actual and potential evapotranspirations occurring on each landcover type. Shrub, plantation, dry land cultivation, forest, and grassland had relatively high infiltration. On the other hand paddy field and built up area had low infiltration.

7.1.1.4. Modeled runoff

The highest runoff occurred on built up area and the lowest runoff occurred on dry land cultivation. Surface condition and effective hydrological depth of landcover types determined level of runoff on each landcover type.

7.1.2. Comparing Modeled Runoff and Measured Runoff

1. Modeled runoff on merawu Sub Watershed was closer to measured runoff (correlation coefficient = 0.5878) than modeled runoff on Integrated Serayu Hulu Sub Watershed to measured runoff.
2. Both modeled runoffs on Integrated Serayu Hulu and Merawu Sub Watersheds were lower than measured runoffs on those Sub Watersheds.

7.1.3. Correlation between Each Hydrological Component and Total Modeled Runoff

7.1.3.1. Interception and total modeled runoff

Correlation coefficient of relationship between interception and total modeled runoff was 0.3553. The coefficient was higher than coefficient in relationship between potential evapotranspiration and total modeled runoff, and was lower than coefficient in relationship between infiltration and total modeled runoff.

7.1.3.2. Potential evapotranspiration and total modeled runoff

Correlation coefficient of relationship between potential evapotranspiration and total modeled runoff was 0.2585. The coefficient was the lowest compared to other coefficients, correlation coefficients in relationships between interception and total modeled runoff, and between infiltration and total modeled runoff.

7.1.3.3. Infiltration and total modeled runoff

Correlation coefficient of relationship between infiltration and total modeled runoff was 0.6638. The coefficient was the highest compared to other coefficients, correlation coefficients in relationships between interception and total modeled runoff, and between potential evapotranspiration and total modeled runoff.

According to those facts, not all hydrological components had negative correlation with total modeled runoff, and the hydrological component, which had the strongest correlation with total modeled runoff, was infiltration.

7.1.4. Sensitivities of Hydrological Components to Modeled Runoff

7.1.4.1. Interception to runoff

Modeled runoffs on Integrated Serayu Hulu and Merawu Sub Watersheds decreased 3.70 % and 5.01 % when interception was added by half of its original value. The decreasing reached 8.71 % and 11.37 % when interception was raised two times of its original value.

7.1.4.2. Potential evapotranspiration to runoff

Increasing potential evapotranspiration by half of its original value caused modeled runoffs decreased 5.65 % on Integrated Serayu Hulu Sub Watershed and 6.53 % on Merawu Sub Watershed. The decreasing went down to 11.43 % (Integrated Serayu Hulu Sub Watershed) and to 13.28 % (Merawu Sub Watershed) when the interception was raised two times of its original value.

7.1.4.3. Infiltration to runoff

When infiltration was added by half of its original value, modeled runoffs decreased to 23.27 % on Integrated Serayu Hulu Sub Watershed and to 25.03 % on Merawu Sub Watershed, and the runoffs decreased to 33.03 % on Integrated Serayu Hulu Sub Watershed and to 35.98 % on Merawu Sub Watershed as infiltration increased two times of its original value.

Based on those findings, the hydrological component, which mostly influenced modeled runoff, was infiltration, and compared to findings in identifying correlation between each hydrological component and modeled runoff, can be concluded that the hydrological component having the strongest correlation with runoff gave the most influence to the runoff change.

7.1.5. Responses of Runoff to Possible Modified Landcovers

7.1.5.1. Replacing cultivation, shrub, and plantation by forest

Changing landcover types, cultivation, shrub, and plantation to forest raised runoffs on two Sub Watersheds. The rises were 12.40 % on Integrated Serayu Hulu Sub Watershed, and 12.25 % on Merawu Sub Watershed. That condition was caused by infiltration and potential evapotranspiration of forest which was the lowest among modifying landcover types.

7.1.5.2. Replacing cultivation, shrub, and forest by plantation

Changing cultivation, shrub, and forest to plantation raised runoff on Integrated Serayu Hulu Sub Watershed. On the other hand it reduced runoff on Merawu Sub Watershed. Those changes were affected by the differences of soil texture distribution and amount of areas replaced by plantation on those Sub Watersheds.

7.1.5.3. Replacing forest, shrub, and plantation by cultivation

Changing plantation, shrub, and forest to cultivation greatly reduced runoff on Integrated Serayu Hulu and Merawu Sub Watersheds. Runoff decreased 35.46 % on Integrated Serayu Hulu Sub Watershed and 49.92 % on Merawu Sub Watershed

when cultivation replaced forest, shrub, and plantation. This condition was caused by combination of cultivation with any soil textures having the highest effective hydrological depth compared to combinations of other landcover types with soil textures.

Those facts show that enlarging forest area does not always decrease runoff. Soil properties also have great effect to the runoff dynamic.

7.2. Recommendations

1. To get more accurately result, more dense sampling points are needed to represent infiltration and soil properties more detail on the study area.
2. Comparing hydrological components and factors affecting the components on two Sub Watersheds, Integrated Serayu Hulu and Merawu, in more detail are required to observe the characteristics of those Sub Watersheds and their affects to runoff on the down stream.
3. Reconstructing the model using images that have higher or lower accuracy is required to investigate the effect of data accuracy used in the model to the results comparing to the real condition. This can be used to determine accuracy of precise data that can produce result closest to reality.
4. Installing equipments in well-distributed position to measure the factors affecting hydrological components, such as wind speed, temperature, humidity, solar radiation, and rainfall intensity is needed to obtain the more accurate and representative data.

8. REFERENCES

- Allen, R. G., L. S. Pereira, et al. (1998). Crop evapotranspiration - Guidelines for computing crop water requirements - FAO Irrigation and drainage paper 56. Rome, Food and Agriculture Organization of the United Nations.
- Baruti, J. H. M. (2004). Study of Soil Moisture in Relation to Soil Erosion in The Proposed Tancitaro Geopark, Central Mexico, A Case of the Zacandaro sub-watershed. Department of Earth Systems Analysis Enschede, the International Institute for Geo-information Science and Earth Observation. **Master of Science: 92.**
- Basayigit, L. and U. Dinc (2010). "of Soil Loss in Lake Watershed Using GIS : A Case Study of Egirdir Lake, Turkey." Natural & Environmental Sciences 1(1): 1-11.
- Brown, M. (2003). Soils and Soil Physical Properties. Teaching Organic Farming and Gardening. A. Miles and M. Brown. Santa Cruz, Center for Agroecology & Sustainable Food System, University of California: 1-24.
- Bulcock, H. H. and G. P. W. Jewitt (2010). "Spatial mapping of leaf area index using hyperspectral remote sensing for hydrological applications with a particular focus on canopy interception." Hydrology and Earth System Sciences 14(2): 383-392.
- Chehafudin, M. (2007) Community-Based Management. Study case in Forestry 3
- Chen, D. and A. Farrar (2007). Evaluation of NARAD Precipitation Data for Rainfall Monitoring in Eastern Ontario, Canada. Geomatics Solutions for Disaster Management. J. Li, S. Zlatanova and A. Fabbri. New York, Springer: 451.
- Darhmouth Flood Observatory (2004). World Atlas of Large Flood Events 1985-2002. Floodnumber. Colorado, Darhmouth Flood Observatory. **48 KB.**
- David, J. and J. Gash (2009) Rainfall Interception.
- De jong, S. M. and V. G. Jetten (2007). "'Estimating spatial patterns of rainfall interception from remotely sensed vegetation indices and spectral mixture analysis.'" International Journal of Geographical Information Science 21(5): 529-545.
- Deshmukh, R. P. and A. A. Ghatol (2010). "Short Term Flood Forecasting using Static Neural Networks a Comparative Study." International Journal of Computer Science and Network Security 10(8): 69-74.

- Elachi, C. and J. v. Zyl (2006). Introduction to the Physics and Techniques of Remote Sensing. J. A. Kong. Hoboken, New Jersey, Wiley-Interscience, John Wiley & Sons, Inc. : 559.
- EPA's Watershed Academy Web (2007) Watershed Modeling. 1-35
- European Commision (2007). DIRECTIVE 2007/60/EC OF THE EUROPEAN PARLIAMENT AND OF THE COUNCIL of 23 October 2007 on the assessment and management of flood risks. E. Commision. Strasbourg, European Commision. DIRECTIVE 2007/60/EC: 27-34.**
- Food and Agriculture Organization of the United Nations (2005). RAP Publication 2005/03, Forest Perspective 2. Forest and Floods, Drowning in Fiction or Thriving on Facts?, Center for International Forestry Research and Food and Agriculture Organization of the United Nations.
- Gitas, I. Z., K. Douros, et al. (2009). "Multi-Temporal Soil Erosion Risk Assessment in N. Chalkidiki Using A Modified USLE Raster Model." EARSeL eProceedings 8(1): 40-52.
- Graham, D. N. and M. B. Butts (2006). Flexible Integrated Watershed Modeling with MIKE SHE. Watershed Models. V. P. Singh and D. K. Frevert. Boca Raton, CRC Press-Taylor & Francis Group: 678.
- Harden, C. P. and P. D. Scruggs (2003). "Infiltration on Mountain Slopes: A Comparison of Three Environments." Geomorphology 55(3): 5-24.
- Indonesian National Board for Disaster Management (2009). "Disaster Statistics." Retrieved May 20, 2010, 2010, from http://bnpb.go.id/website/index.php?option=com_content&task=view&id=2100.
- Indonesian National Board for Disaster Management (2009). "Forecasting Flood Prone Areas." Retrieved May 23, 2010, 2010, from <http://bnpb.go.id/>.
- Isnugraha, G. (1975). Availability of Water in Serayu Watershed as Annual Meteorology Function. Faculty of Geography. Yogyakarta, Gadjah Mada University. **Bachelor**: 192.
- Jones, K. B. (2008). Importance of Land Cover and Biophysical Data in Landscape-Based Environmental Assessments. North America Land Cover Summit. J. C. Campbell, K. B. Jones, J. H. Smith and M. T. Koeppel. Washington, DC, Association of American Geographers: 215-250.

- Knight, J. F., R. S. Lunetta, et al. (2006). "Regional Scale Land Cover Characterization Using Modis-Ndvi 250 M Multi-Temporal Imagery: A Phenology-Based Approach." GIScience & Remote Sensing 43(1): 1-23.
- Kuriakose, S. L. (2006). Effect of Vegetation on Debris Flow Initiation - Conceptualisation and Parameterisation of a Dynamic Model for Debris Flow Initiation in Tikovil River Basin, Kerala, India using PCRaster®. Department of Earth Systems Analysis Enschede, the International Institute for Geo-information Science and Earth Observation. **Master of Science:** 121.
- Kuriakose, S. L., L. P. H. v. Beek, et al. (2009). "Parameterizing a physically based shallow landslide model in a data poor region." Earth Surface Processes and Landforms 34(6): 867-881.
- Lin, W., R. v. d. Velde, et al. (2008). Satellite Based Regional-Scale Evapotranspiration in The Hebei Plain, Northeastern China. 2008 Dragon Symposium (Dragon 1 Programme Final Results 2004–2007), Beijing, P. R. China, European Space Agency and National Remote Sensing Center of China.
- Loch, R. J. (2000). "Effects of vegetation cover on runoff and erosion under simulated rain and overland flow on a rehabilitated site on the Meandu Mine, Tarong, Queensland." Australian journal of soil research 38(2): 299-312.
- McCuen (1998). Hydrologic Analysis and Design. New Jersey, Prentice-Hall, Inc. : 833.
- Mendez, R. V., E. Ventura-Ramos, et al. (2010). "Soil erosion and runoff in different vegetation patches from semiarid Central Mexico " Catena 80: 162-169.
- Mulligan, M. (2006). A Simple Distributed Hydrological Model for Tropical Montane Cloud Forests. London, King's College London, University of London: 1-7.
- National Severe Storm Laboratory (NOAA) (2009, July 21, 2009). "Flood Basics." Retrieved May 24, 2010, from http://www.nssl.noaa.gov/primer/flood/fld_basics.html.
- Pidwirny, M. and S. Jones (2009, 05/07/2009). "Introduction to the Hydrosphere " Actual and Potential Evapotranspiration. Retrieved January 10, 2011, from <http://www.physicalgeography.net/fundamentals/8j.html>.
- Rustanto, A. (2010). Soil Erosion Dynamics Due to Land Use / Land Cover Changes, Case Study in Upper Serayu Watershed, Indonesia. Department of

Earth Systems Analysis Enschede, the International Institute for Geo-information Science and Earth Observation. **Master of Science: 73.**

Saeidian, F., W. N. A. B. Sulaiman, et al. (2009). "The Effect of Converting Rangelands to Dry Farming on Flood Events in Kardeh Drainage Basin, Iran." European Journal of Scientific Research 36(4): 662-673.

Schiffman, B., G. Basson, et al. (2008). Estimation of Leaf Area Index (LAI) Through The Acquisition of Ground Truth Data in Yosemite National Park. Annual Conference of American Society for Photogrammetry and Remote Sensing, Portland, Oregon, American Society for Photogrammetry and Remote Sensing.

Singh, V. P. and D. K. Frevert (2006). Introduction of Watershed Models. Watershed Models. V. P. Singh and D. K. Frevert. Boca Raton, CRC Press-Taylor & Francis Group: 678.

Srinivasan, R. and V. Lakshmi (2006). Simulation of Water and Energy Budgets Using a Macroscale Hydrological Model for the Upper Mississippi River Basin. Watershed Models. V. P. Singh and D. K. Frevert. Boca Raton, CRC Press-Taylor & Francis Group: 678.

Stancalie, G. and V. Craciunescu (2005). Contribution of Earth Observation Data Supplied by the New Satellite Sensors to Flood Disaster Assessment and Hazard Reduction. Geo-information for Disaster Management. P. v. Oosterom, S. Zlatanova and E. M. Fendel. New York, Springer-Verlag Berlin Heidelberg: 1457.

Statistic Center Agency of Banjarnegara (2009). "Leading Economic Potential of Banjarnegara District." Map of Local Economy Potency. Retrieved 30 November, 2010, from <http://www.cps-sss.org/web/home/kabupaten/kab/Kabupaten+Banjarnegara>.

Sudjana (1991). Analysis of Varians for completely randomized design. Design and Analysis of Experiments. Bandung, Tarsito: 16-31.

Suryanto (2010, May 15, 2010). "Floods hit Banjarnegara." Retrieved May 21, 2010, from <http://perempuan.kompas.com/read/xml/2010/05/15/13305574/banjarnegara.diterjang.banjir>.

Tampang, E. A. (2010). Determining Rainfall Thresholds for Landslide Initiation, A Case Study in Wadaslintang Watershed, Wonosobo, Central Java Province. Department of Earth Systems Analysis Enschede, the International Institute for Geo-information Science and Earth Observation. **Master of Science: 78.**

- Triutomo, S. (2006). Disaster Management in Indonesia. The 13th Session of The Asia-Pacific Regional Space Agency Forum (APRSAF-13). Jakarta, Asia-Pacific Regional Space Agency Forum: 1-16.
- U.S. Library of Congress (1993). "Indonesia: A Country Study." Retrieved January 3, , 2011, from <http://countrystudies.us/indonesia/29.htm>.
- United States Geological Survey (2006). Flood Hazards-A National Threat. <http://pubs.usgs.gov/fs/2006/3026/2006-3026.pdf>. United States Department of The Interior and United States Geological Survey, United States Geological Survey. **Fact Sheet 2006-3026**: 1-2.
- Vieux, B. E. (2005). Distributed Hydrologic Modeling Using GIS. V. P. Singh, M. Anderson, L. Bengtsson et al. Dordrecht, Springer Science + Business Media, Inc. **48**: 312.
- Wanielista, M., R. Kersten, et al. (1997). Hydrology Water Quantity and Quality Control. Canada, John Wiley and Sons, Inc.
- Wetherick, M., S. Ross, et al. (2001). A Modern Dictionary of Geography. W. Rooke. London, Arnold, a member of the Hodder Headline Group: 304.
- Wonosobo Local Government. "Agriculture." Retrieved November 29, 2010, from <http://www.kabupatenwonosobo.com/index.php?modul=pembangunan&cat=PbAgrikultur&catid=315436303221>.
- Xiaoxia, S., Z. Jixian, et al. (2008). Vegetation Cover Annual Changes Based On Modis/Terra Ndvi In The Three Gorges Reservoir Area. the XXIth ISPRS Congress, Beijing, International Society for Photogrammetry and Remote Sensing.
- Yates, D. and K. Strzepek (1994) Potential Evapotranspiration Methods and their Impact on the Assessment of River Basin Runoff Under Climate Change. 1-28
- Zhang, L., W. R. Dawes, et al. (1999). Predicting The Effect of Vegetation Changes on Catchment Average Water Balance, Cooperative Research Centre for Catchment Hydrology: 1-35.

APPENDIXS

Appendix 1. Results from field observation and laboratory measurement

Sample Numb.	Coordinates		Landcovers	Date	Time	Slope (°)	SM (%)	BD (gram/cm3)	cumulative infiltration (mm)	soil texture
	X	Y								
0	379335	9199898	Dry land cultivation (Potato, 3 month)	30-Sep-10	07,30	50	8.74	0.917	377.13	Sandy loam
1	383116	9192303	Shrub	14-Aug-10	09,30	30	26.05	0.844	234.33	Silt loam
2	369161	9206259	Plantation (Paraserianthes falcataria)	28-Sep-10	17,27	25	26.84	0.915	111.99	Sandy loam
3	369935	9205430	Plantation (Paraserianthes falcataria)	28-Sep-10	16,14	25	23.18	1.018	124.76	Sandy loam
4	368683	9203647	dry land cultivation (carrot, 2 months)	28-Sep-10	15,02	45	30.39	0.820	959.93	Sandy loam
5	377326	9200903	dry land cultivation (potato 9 weeks)	29-Sep-10	17,20	30	22.05	0.841	167.80	Sandy loam
6	385986	9196761	Shrub	15-Aug-10	07,20	30	22.47	0.789	95.53	Sandy loam
7	369675	9202090	Dry land cultivation (harvested/bare)	28-Sep-10	13,00	5	21.10	1.078	1212.89	Sandy loam
8	370215	9203081	Dry land cultivation (carrot, 2.5 month)	28-Sep-10	11,30	10	21.19	1.087	220.62	Sandy loam
9	381024	9203450	Dry land cultivation (harvested/bare)	29-Sep-10	10,19	20	20.74	0.995	875.05	Sandy loam
10	378084	9190350	Plantation (Paraserianthes falcataria)	27-Sep-10	14,00	20	24.63	1.089	403.78	Loam
11	379238	9198394	Plantation (Paraserianthes falcataria)	30-Sep-10	09,00	20	20.88	0.864	33.04	Sandy loam
12	371296	9204102	Dry land cultivation (potato 11 weeks)	28-Sep-10	10,16	10	22.96	1.027	67.23	Sandy loam
13	379515	9202450	Dry land cultivation (harvested/bare)	29-Sep-10	11,00	15	16.10	0.932	937.17	Sandy loam
14	384683	9199652	Dry land cultivation (6 weeks)	15-Aug-10	16,50	15	30.74	1.065	358.51	Sandy loam
15	372402	9204099	dry land cultivation (potato, 5 weeks)	28-Sep-10	08,20	30	14.72	1.027	604.84	Sandy loam
16	383895	9199419	Dry land cultivation (carrot, 11 weeks)	30-Sep-10	16,50	5	23.74	0.890	215.32	Loamy sand
17	37825	9201035	Dry land cultivation (harvested/bare)	29-Sep-10	16,07	5	21.06	0.987	528.43	Sandy loam
18	384414	9197615	Dry land cultivation (cabbage 3 months)	30-Sep-10	16,00	10	18.90	1.023	49.16	Sandy loam
19	382974	9191356	Built up area	14-Aug-10	10,17	15	10.53	1.144	191.72	Silt loam
20	379451	9202241	forest	29-Sep-10	13,55	20	24.67	0.549	235.06	Sandy loam
21	379281	9194116	Shrub	30-Sep-10	13,14	25	21.58	0.886	97.27	Sandy loam
22	381286	9202284	dry land cultivation (potatoe, 10 weeks)	29-Sep-10	09,06	5	21.00	0.784	172.45	Silt loam

Sample Numb.	Coordinates		Landcovers	Date	Time	Slope (°)	SM (%)	BD (gram/cm ³)	cumulative infiltration (mm)	soil texture
	X	Y								
23	379447	9196845	Shrub	30-Sep-10	11,29	45	23.44	0.915	52.13	Sandy loam
24	379486	9202029	Dry land cultivation (potato 2 months)	29-Sep-10	12,30	0	25.91	0.813	673.69	Silt loam
25	381343	9190290	Plantation (<i>Paraserianthes falcataria</i>)	14-Aug-10	14,35	10	12.15	0.813	40.49	Silt loam
26	381524	9190210	Shrub	14-Aug-10	16,20	20	17.20	1.277	396.03	Silt loam
27	385701	9196540	Tea plantation	15-Aug-10	08,14	10	16.04	1.188	112.21	Sandy loam
28	385454	9196451	Tea plantation	15-Aug-10	10,20	15	9.48	1.557	145.97	Sandy loam
29	384036	9195971	Dry land cultivation (cabbage, 10 weeks)	15-Aug-10	09,39	10	21.65	1.046	348.85	Sandy loam
30	382823	9195278	Dry land cultivation (potato, 2 months)	15-Aug-10	12,35	10	14.99	1.100	489.90	Sandy loam
31	384722	9199133	Dry land cultivation (maize 3 months)	15-Aug-10	15,18	5	15.54	1.015	275.58	Sandy loam
32	372132	9177579	Plantation (<i>Paraserianthes falcataria</i>)	14-Aug-10	14,35	10	11.46	0.813	111.54	Clay
33	372223	9178212	Plantation (<i>Paraserianthes falcataria</i>)	11-Oct-10	08,20	45	20.67	0.909	180.92	Clay
34	370634	9178536	Plantation (<i>Paraserianthes falcataria</i>)	11-Oct-10	09,35	20	20.80	1.052	90.48	Clay
35	370636	9179292	Plantation (zalak)	11-Oct-10	11,40	30	26.46	0.851	96.08	Clay
36	370213	9179325	Plantation (zalak)	11-Oct-10	13,50	15	24.30	1.059	67.47	Clay
37	384168	9196751	Dry land cultivation (harvested/bare)	15-Aug-10	11,45	15	11.90	1.067	388.84	Sandy loam
38	361389	9197315	forest	12-Oct-10	08,10	40	21.86	1.136	36.99	Clay loam
39	362930	9196180	Forest (<i>Pinus merkusii</i>)	12-Oct-10	10,15	45	13.09	0.827	128.83	Clay loam
40	363675	9196425	plantation (albasia, jackfruit, and zalak)	12-Oct-10	13,00	45	24.44	1.163	118.70	Clay loam
41	366526	9198488	Dry land cultivation (potato, 2,5 months)	12-Oct-10	15,15	20	20.48	1.219	189.50	Clay loam
42	368469	9199832	Shrub	12-Oct-10	16,15	10	20.81	0.846	61.23	Sandy loam
43	370338	9199960	Shrub	12-Oct-10	17,30	10	17.21	0.926	146.69	Sandy loam
44	357759	9194678	Plantation (<i>Paraserianthes falcataria</i>)	13-Oct-10	07,00	45	21.17	1.081	73.68	Loam
45	357554	9193571	Plantation (<i>Paraserianthes falcataria</i>)	13-Oct-10	09,25	3	11.51	1.086	165.12	Silty clay
46	358112	9189936	Plantation (<i>Paraserianthes falcataria</i>)	13-Oct-10	10,40	20	17.22	1.072	78.28	Silty clay
47	357588	9189367	Forest (<i>Altingia excelsa</i>)	13-Oct-10	12,15	45	21.80	1.178	27.48	Loam
48	357356	9189140	Forest (<i>Altingia excelsa</i>)	13-Oct-10	15,20	30	16.75	1.230	20.87	Loam
49	363535	9186770	forest (<i>Agathis damara</i>)	14-Oct-10	09,10	25	22.39	1.256	94.17	Sandy loam
50	365627	9190177	Plantation (zalak)	14-Oct-10	13,10	35	15.81	0.897	100.36	Clay loam

Sample Numb.	Coordinates		Landcovers	Date	Time	Slope (°)	SM (%)	BD (gram/cm ³)	cumulative infiltration (mm)	soil texture
	X	Y								
51	363739	9203295	Shrub	15-Oct-10	08,20	25	20.05	0.755	313.79	Sandy loam
52	364697	9203292	Shrub	15-Oct-10	09,40	10	17.41	1.353	142.69	Sandy loam
53	383063	9181184	paddy field (5 months)	21-Oct-10	07,00	4	17.62	1.165	116.91	Silt loam
54	379398	9179501	Shrub	21-Oct-10	08,00	4	15.03	0.983	55.75	Sandy loam
55	378046	9182769	Shrub	21-Oct-10	10,55	2	22.14	1.218	6.00	Silty clay
56	377376	9181155	inundated paddy field (1 - 2 months)	21-Oct-10	14,50	0	-	1.024	0.00	Sandy loam
57	375825	9179285	Paddy field (harvested)	21-Oct-10	15,15	20	19.14	1.286	2062.50	Sandy loam
58	370043	9179588	paddy field (harvested)	21-Oct-10	15,55	5	24.81	1.042	73.86	Sandy loam
59	366972	9180524	inundated paddy field (50 - 70 days)	21-Oct-10	16,35	2	-	1.143	0.00	Sandy loam
60	355458	9183542	paddy field (3 months)	21-Oct-10	16,40	3	38.20	1.423	127.29	Sandy loam
61	358183	9186759	plantation (albasia, jackfruit, zalak, and avocado)							
62	361131	9186852	plantation (albasia and kaliandra)	22-Oct-10	06,30	45	20.32	0.800	57.31	Loam
63	360979	9187700	Plantation (Paraserianthes falcataria)	22-Oct-10	07,24	25	29.99	1.156	72.44	Loam
64	361390	9187511	Plantation (Paraserianthes falcataria)	22-Oct-10	09,56	20	24.33	0.873	90.26	Loam
65	361753	9185918	Plantation (Paraserianthes falcataria)	22-Oct-10	11,20	3	19.83	1.044	30.02	Sandy loam
66	361635	9185470	Plantation (zalak)	22-Oct-10	12,30	20	18.52	1.541	9.63	Loam
67	358107	9184248	Forest (<i>Pinus merkusii</i>)	22-Oct-10	14,45	40	20.65	1.664	44.27	Loam
68	366707	9195641	Plantation (zalak)	22-Oct-10	16,30	5	23.94	1.290	230.64	Sandy loam
69	369286	9196898	Shrub	26-Oct-10	08,45	30	30.80	1.015	178.85	Loam
70	370135	9196100	Shrub	26-Oct-10	09,40	20	28.32	1.056	133.02	Clay loam
71	383964	9198273	Built up area	26-Oct-10	10,55	45	36.66	1.127	104.87	Loam
72	383072	9200167	Built up area	28-Oct-10	13,30	20	-	0.975	-	Sandy loam
			Built up area	28-Oct-10	15,00	10	-	0.942	-	Sandy loam

Appendix 2. Bulk density of each soil texture

No	Sample numbers	Soil texture	Bulk Density (gram/cm ³)	Average
1	32	Clay	0.812957	0.936688
2	33	Clay	0.908837	
3	34	Clay	1.052151	
4	35	Clay	0.850751	
5	36	Clay	1.058746	
6	38	Clay loam	1.135603	1.049488
7	39	Clay loam	0.826654	
8	40	Clay loam	1.163251	
9	41	Clay loam	1.218547	
10	50	Clay loam	0.896916	
11	69	Clay loam	1.055956	1.159423
12	10	Loam	1.088931	
13	44	Loam	1.081067	
14	47	Loam	1.17847	
15	48	Loam	1.229708	
16	61	Loam	0.799513	
17	62	Loam	1.155895	
18	63	Loam	0.873072	
19	65	Loam	1.540686	
20	66	Loam	1.664215	
21	68	Loam	1.015371	
22	70	Loam	1.126725	
23	16	Loamy sand	0.890321	0.935886
24	71	Loamy sand	0.975113	
25	72	Loamy sand	0.942225	
26	0	Sandy loam	0.917461	1.032141
27	2	Sandy loam	0.915432	
28	3	Sandy loam	1.018415	
29	4	Sandy loam	0.819805	
30	5	Sandy loam	0.840858	
31	6	Sandy loam	0.78886	
32	7	Sandy loam	1.078277	
33	8	Sandy loam	1.087155	
34	9	Sandy loam	0.994825	
35	11	Sandy loam	0.863687	
36	12	Sandy loam	1.027293	
37	13	Sandy loam	0.932173	
38	14	Sandy loam	1.065341	
39	15	Sandy loam	1.027039	
40	17	Sandy loam	0.987216	
41	18	Sandy loam	1.022727	
42	20	Sandy loam	0.548904	
43	21	Sandy loam	0.886009	
44	23	Sandy loam	0.915179	
45	27	Sandy loam	1.187855	
46	28	Sandy loam	1.557427	
47	29	Sandy loam	1.046182	
48	30	Sandy loam	1.099838	
49	31	Sandy loam	1.014864	

No	Sample numbers	Soil texture	Bulk Density (gram/cm ³)	Average
50	37	Sandy loam	1.067462	0.977075
51	42	Sandy loam	0.846439	
52	43	Sandy loam	0.926086	
53	49	Sandy loam	1.25558	
54	51	Sandy loam	0.754616	
55	52	Sandy loam	1.353237	
56	54	Sandy loam	0.983157	
57	56	Sandy loam	1.164773	
58	57	Sandy loam	1.286272	
59	58	Sandy loam	1.042005	
60	59	Sandy loam	1.142807	
61	60	Sandy loam	1.422991	
62	64	Sandy loam	1.043527	
63	67	Sandy loam	1.28957	
64	1	Silt loam	0.844409	
65	19	Silt loam	1.143754	
66	22	Silt loam	0.783533	
67	24	Silt loam	0.812957	
68	25	Silt loam	0.812957	
69	26	Silt loam	1.277141	
70	53	Silt loam	1.164773	
71	45	Silty clay	1.08614	1.125457
72	46	Silty clay	1.07219	
73	55	Silty clay	1.21804	

Appendix 3. Analysis of variance for completely randomized design

Effect of Landcover Types to Cumulative Infiltration

$$J_i = \sum_{j=1}^{n_i} U_{(ij)}$$

$$J = \sum_{i=1}^k J_i$$

$$\bar{U}_i = J_i/n_i$$

$$\bar{U} = \frac{J}{\sum_{i=1}^k n_i}$$

$$\sum U^2 = \sum_{i=1}^k \sum_{j=1}^{n_i} U_{(ij)}^2$$

$$R_y = \frac{J^2}{\sum_{i=1}^k n_i}$$

$$P_y = \sum_{i=1}^k n_i (\bar{U}_i - \bar{U})^2 = \left[\sum_{i=1}^k (J_i^2/n_i) \right] - R_y$$

$$E_y = \sum_{i=1}^k \sum_{j=1}^{n_i} (Y_{ij} - \bar{U}_i)^2 = \sum U^2 - R_y - P_y$$

- n_i = number of cumulative infiltration samples in landcover type i
- $U_{(ij)}$ = cumulative infiltration sample in landcover type i
- k = number of landcover types
- J_i = sum of cumulative infiltration samples in landcover type i
- J = sum of whole cumulative infiltration samples (in all landcover types)
- \bar{U}_i = mean of cumulative infiltration samples in landcover type i
- \bar{U} = mean of whole cumulative infiltration samples (in all landcover types)
- $\sum U^2$ = sum of whole cumulative infiltration sample squares
- R_y = mean of whole cumulative infiltration sample squares
- P_y = sum of squares
- E_y = mean square error
- R = $R_y/1$

P = variance between landcover types = $P_y/(k-1)$
 E = variance within landcover types = $E_y/\sum (n_i - 1)$
 $F_{test} = P/E$

Cumulative infiltrations samples in each landcover type obtained from field observation

No	Cumulative infiltration in each landcover type (mm)* (k = 9)									
	1	2	3	4	5	6	7	8	9	
1	116.91	2062.50	1212.89	959.93	167.80	377.13	234.33	111.99	235.06	
2	127.29	73.86	875.05	358.51	220.62	67.23	95.53	124.76	36.99	
3			937.17	604.84	172.45	215.32	97.27	403.78	128.83	
4			528.43	673.69	348.85	49.16	52.13	33.04	27.48	
5			388.84	489.90	189.50	275.58	396.03	40.49	20.87	
6							61.23	112.21	94.17	
7							146.69	145.97	230.64	
8							313.79	111.54		
9							142.69	180.92		
10							55.75	90.48		
11							6.00	96.08		
12							133.02	67.47		
13							104.87	118.70		
14								73.68		
15								165.12		
16								78.28		
17								100.36		
18								57.31		
19								72.44		
20								90.26		
21								30.02		
22								9.63		
23								44.27		
24								178.85		
Sum (J_i)	244.20	2136.36	3942.38	3086.87	1099.23	984.42	1839.33	2537.66	774.05	16644.49 (J)
Sample number (n_i)	2.00	2.00	5.00	5.00	5.00	5.00	13.00	24.00	7.00	68 ($\sum n_i$)
Mean (\bar{U}_i)	122.10	1068.18	788.48	617.37	219.85	196.88	141.49	105.74	110.58	244.77 (\bar{U})
$(J_i)^2/n_i$	29817.68	2282009.98	3108471.29	1905754.05	241659.63	193816.65	260240.06	268320.96	85592.99	8375683.28 ($\sum (J_i)^2/n_i$)

*Landcover types:

1. Paddy field in the growth stage 3
2. Paddy field in the growth stage 4
3. Dry land cultivation in the growth stage 1
4. Dry land cultivation in the growth stage 2
5. Dry land cultivation in the growth stage 3
6. Dry land cultivation in the growth stage 4
7. Shrub
8. Plantation
9. Forest

To determine that each landcover type has different effect to cumulative infiltration, this research made a hypothesis, null hypothesis (H_0). The Hypothesis is given as follow:

H_0 : affect of landcover type i (τ_i) = 0 for $i = 1,2,3,4,5,6,7,8,9$ (all landcover types). In other word, all landcover types have the same effect to cumulative infiltration.

From the calculation the research found that $\sum U^2 = 11435075.4$, and from the table above values are obtained as follow:

$$\begin{aligned} R_y &= (16644.49)^2/68 = 4074102.8 \\ P_y &= 8375683.28 - 4074102.8 = 4301580.45 \\ E_y &= 11435075.4 - 4074102.8 - 4301580.45 = 3059392.113 \\ R &= 4074102.8/1 = 4074102.8 \\ P &= 4301580.45/(9-1) = 537697.56 \\ E &= 3059392.113/59 = 51854.104 \\ F_{test} &= 537697.56/51854.104 = 10.36943 \end{aligned}$$

F_{table} , obtained from F distribution table with $v_1 = (k-1) = 8$, $v_2 = \sum (n_i - 1) = 59$, and cumulative probability equals to 0.95, is 2.10 which is lower than F_{test} ($F_{test} > F_{table}$). Based on that condition, null hypothesis H_0 is rejected so each landcover type gave different effect to cumulative infiltration with confidence level at 95%.

Effect of Soil Textures to Bulk density

Equations used in "Effect of Effect of Landcover Types to Cumulative Infiltration" is also applied in this part.

$$\begin{aligned} n_i &= \text{number of bulk density samples in soil texture } i \\ U_{(ij)} &= \text{bulk density sample in soil texture } i \\ k &= \text{number of soil textures} \\ J_i &= \text{sum of bulk density samples in soil texture } i \\ J &= \text{sum of whole bulk density samples (in all soil textures)} \\ \bar{U}_i &= \text{mean of bulk density samples in soil texture } i \\ \bar{U} &= \text{mean of whole bulk density samples (in all soil textures)} \\ \sum U^2 &= \text{sum of whole bulk density sample squares} \\ R_y &= \text{mean of whole bulk density sample squares} \\ P_y &= \text{sum of squares} \\ E_y &= \text{mean square error} \\ R &= R_y/1 \\ P &= \text{variance between soil textures} = P_y/(k-1) \\ E &= \text{variance within soil textures} = E_y/\sum (n_i - 1) \\ F_{test} &= P/E \end{aligned}$$

Bulk density samples in each soil texture obtained from field observation

No	Bulk density in each soil texture (gram/cm ³) (k = 7)							
	Clay	Clay loam	Loam	Loamy sand	Sandy loam	Silt loam	Silt clay	
1	0.812957	1.135603	1.088931	0.890321	0.917461	0.844409	1.08614	
2	0.908837	0.826654	1.081067	0.975113	0.915432	1.143754	1.07219	
3	1.052151	1.163251	1.17847	0.942225	1.018415	0.783533	1.21804	
4	0.850751	1.218547	1.229708		0.819805	0.812957		
5	1.058746	0.896916	0.799513		0.840858	0.812957		
6		1.055956	1.155895		0.78886	1.277141		
7			0.873072		1.078277	1.164773		
8			1.540686		1.087155			
9			1.664215		0.994825			
10			1.015371		0.863687			
11			1.126725		1.027293			
12					0.932173			
13					1.065341			
14					1.027039			
15					0.987216			
16					1.022727			
17					0.548904			
18					0.886009			
19					0.915179			
20					1.187855			
21					1.557427			
22					1.046182			
23					1.099838			
24					1.014864			
25					1.067462			
26					0.846439			
27					0.926086			
28					1.25558			
29					0.754616			
30					1.353237			
31					0.983157			
32					1.164773			
33					1.286272			
34					1.042005			
35					1.142807			
36					1.422991			
37					1.043527			
38					1.28957			
Sum (J _i)	4.683442	6.296926	12.75365	2.807659	39.22135	6.839524	3.37637	75.97892 (J)
Sample number (n _i)	5	6	11	3	38	7	3	73 (Σ n_i)
Mean (\bar{U}_i)	0.936688	1.049488	1.159423	0.935886	1.032141	0.977075	1.125457	1.040807 (U)
(J _i) ² / n _i	4.386925	6.608546	14.78688	2.627649	40.48195	6.682726	3.799958	79.37463 (Σ (J_i)²/ n_i)

To determine that each soil texture has different effect to bulk density, this research made a hypothesis, null hypothesis (H₀). The Hypothesis is given as follow:

H_0 : affect of soil texture i (τ_i) = 0 for $i = 1,2,3,4,5,6,7$ (all soil textures). In other word, all soil textures have the same effect to bulk density.

From the calculation the research found that $\sum U^2 = 81.85969$, and from the table above values are obtained as folow:

$$\begin{aligned}R_y &= (75.97892)^2/73 = 79.0794 \\P_y &= 79.37463 - 79.0794 = 0.295231 \\E_y &= 81.85969 - 79.0794 - 0.295231 = 2.485067 \\R &= 79.0794/1 = 79.0794 \\P &= 0.295231/(7-1) = 0.049205 \\E &= 2.485067/66 = 0.037653 \\F_{test} &= 0.049205/0.037653 = 1.306823\end{aligned}$$

F_{table} , obtained from F distribution table with $v_1 = (k-1) = 6$, $v_2 = \sum (n_i - 1) = 66$, and cumulative probability equals to 0.70, is 1.23 which is lower than F_{test} ($F_{test} > F_{table}$). Based on that condition, null hypothesis H_0 is rejected so each soil texture gave different effect to bulk density with confidence level at 70%.

Appendix 4. Pcraster script for runoff dynamic model

```
#####A RUNOFF DYANIMCS MODEL#####
#####ADHI NURUL HADI#####
#####UGM-ITC#####

#####ANALYZING RUNOFF DYANIMCS MODEL#####

binding

### Input ###
DEM = dem.map;           # digital elevation model
rainfall_tss = ch.tss;   # rainfall data in mm/day
stations = thiessen.map; # thiessen polygon
KC =KC2.tss;             # Corp Factors
maskoum = maskoum2.map;  # mask of Study area
landcover=land.map;     # landcover (2009)
temp = tempe.tss;       # temperature in Celcius
T_differ=Temp_differ.tss; # temperature difference in each month
EHD=inf.tss;            # EHD*BD*FC of each landcover in each soil texture
E = ehd_bd_fc2.map;     # combination of landcover and soil texture maps
LDD=T4.map;             #Local Drain Direction map
dis_st=riv_sta.map;     # discharge station map

### Output ###
Pr = P;                 # daily rainfall (mm)
p_tss = pavg.tss;      # average daily rainfall (mm)
pcum_tss = pcumavg.tss; # average cumulative rainfall (mm)
interception = intc;   # daily interception (mm)
intc_avg=intcavg.tss;  # average daily interception (mm)
ETp = ETp;             # potential evapotranspiration (mm)
etp_tss=Etp.tss;      # Average daily ETp (mm)
intcum_tss = intcum.tss; # average cumulative interception (mm)
ETa=ETa;              # Actual Evapotranspiration (mm)
eta_tss = ETaavg.tss;  # average daily ETa (mm)
etacum_tss = ETacumavg.tss; # average cumulative ETa (mm)
infill=infill;        # daily infiltration (mm)
infil_avg=infilavg.tss; # average daily infiltration (mm)
runoff=run;           # daily runoff (mm)
incum_tss = incum.tss; # average cumulative infiltration (mm)
wtr_tss=wtr.tss;     # daily runoff at two points (m3)

areamap
DEM;

timer
1 427 1;              # runs 427 days from the startday onward

initial

startday = 7; # start day of the simulation, the meteo and raindata start at this day

### Initialize vegetation cover maps ###
cov1 = cov1.map;
cov2 = cov17.map;
cov3 = cov33.map;
cov4 = cov49.map;
```

```
cov5 = cov81.map;
cov6 = cov97.map;
cov7 = cov185.map;
cov8 = cov201.map;
cov9 = cov217.map;
cov10 = cov233.map;
cov11 = cov249.map;
cov12 = cov265.map;
cov13 = cov281.map;
cov14 = cov297.map;
cov15 = cov313.map;
cov16 = cov329.map;
cov17 = cov345.map;
cov18 = cov361.map;
cov19 = cov377.map;
cov20 = cov393.map;
cov21 = cov409.map;
cov22 = cov425.map;
daycov1 = 1;
daycov2 = 17;
daycov3 = 33;
daycov4 = 49;
daycov5 = 81;
daycov6 = 97;
daycov7 = 185;
daycov8 = 201;
daycov9 = 217;
daycov10 = 233;
daycov11 = 249;
daycov12 = 265;
daycov13 = 281;
daycov14 = 297;
daycov15 = 313;
daycov16 = 329;
daycov17 = 345;
daycov18 = 361;
daycov19 = 377;
daycov20 = 393;
daycov21 = 409;
daycov22 = 425;
```

#SR (solar radiation point) provided by arcgis in monthly, SR.map has been divided by day numbers of each month

#have been converted from Wh/m2 to W/m2 (divided by daylight hours)

#converted from W/m2 to mm/day by multiply to 0.035 (FAO converter)

```
Rad1 = SR1.map;
Rad2 = SR2.map;
Rad3 = SR3.map;
Rad4 = SR4.map;
Rad5 = SR5.map;
Rad6 = SR6.map;
Rad7 = SR7.map;
Rad8 = SR8.map;
Rad9 = SR9.map;
Rad10 = SR10.map;
Rad11 = SR11.map;
Rad12 = SR12.map;
Rad13 = SR13.map;
```



```

Rad14 = SR14.map;
dayRad1 = 7;
dayRad2 = 38;
dayRad3 = 69;
dayRad4 = 99;
dayRad5 = 130;
dayRad6 = 160;
dayRad7 = 191;
dayRad8 = 222;
dayRad9 = 250;
dayRad10 = 281;
dayRad11 = 311;
dayRad12 = 342;
dayRad13 = 372;
dayRad14 = 403;

#####
### initialize totals ###
#####

ETp=0;
ETa=0;
ETacum = 0;
ETpcum = 0;
Pcum = 0;
percum = 0;
intcum = 0;
infcum = 0;
Tacum = 0;
Eacum = 0;
R=0*masksoum;
Coverm = 0*masksoum;
interception = 0*masksoum;
Perc = 0*masksoum;
Cfac=0*masksoum;
temperature = 0*masksoum;
ET=0*masksoum;
infil=0*masksoum;
nrCells = maptotal(masksoum);
dt = 1; #timestep 1 day
day = startday; # day is a variable needed for vegetation interpolation, each
                # timestep 1 is added to day

dynamic

#####
### meteo data input ###
#####

P_stat = timeinputscalar(rainfall_tss, stations);
# get the rainfall values at the stations by using thoessen polygons

Pr = P_stat*masksoum;
# restrict to area mask

report p_tss = maptotal(Pr)/nrCells;
# write a graph of the average daily rainfall

```

```

Pcum = Pcum + Pr;
#calculate cumulative P for outut

report pcum_tss = maptotal(Pcum)/nrCells;
# write a graph of the average cumulative rainfall

#####
##### temperature#####
#####
tmp_stat = timeinputscalar(temp, nominal(masksum));

#Under normal atmospheric conditions, temperatures will decrease with elevation
#the mean decrease with increasing elevation is 0.7oC/100 m (3.8oF/1000ft) (Wanielista et. Al.1997)
temp1=if(DEM gt 292,-((DEM-292)*0.007))+tmp_stat,tmp_stat);
temp2=if(DEM lt 292,-((DEM-292)*0.007))+tmp_stat,temp1);

temperature = temp2*masksum*dt;
# restrict to area mask
#report tempt_avg=maptotal(temperature)/nrCells;

Cfac=timeinputscalar(KC, landcover);
Cfac=Cfac*masksum*dt;
#report Cfac_avg=maptotal(Cfac)/nrCells;

#####
##### solar radiation#####
#####
SR = Rad1 *masksum;
SR = if (day ge dayRad1,Rad1,SR);
SR = if (day ge dayRad2,Rad2,SR);
SR = if (day ge dayRad3,Rad3,SR);
SR = if (day ge dayRad4,Rad4,SR);
SR = if (day ge dayRad5,Rad5,SR);
SR = if (day ge dayRad6,Rad6,SR);
SR = if (day ge dayRad7,Rad7,SR);
SR = if (day ge dayRad8,Rad8,SR);
SR = if (day ge dayRad9,Rad9,SR);
SR = if (day ge dayRad10,Rad10,SR);
SR = if (day ge dayRad11,Rad11,SR);
SR = if (day ge dayRad12,Rad12,SR);
SR = if (day ge dayRad13,Rad13,SR);
SR = if (day ge dayRad14,Rad14,SR);

sol_rad = SR*masksum*dt;
#report sol_avg = maptotal(sol_rad)/nrCells;

Tdif_stat = timeinputscalar(T_differ, nominal(masksum));
Tdif=Tdif_stat*masksum;          #Temperature difference

Erc=(0.0022*sol_rad*(Tdif**0.5)*(temperature+17.8)*dt); #Refference crop evapotranspiration by Hargraves

#Ta0=Erc*Cfac*cov2*dt;
#Ea0=Erc*(1-cov2)*dt;
#A=Ta0+Ea0;
#R = (A/Erc)**0.5;

```

```

#####
### vegetation cover interpolation ###
#####

#linear interpolation between two images
cov = cov1*masksum;
cov = if (day ge daycov1, cov1 + (day - daycov1)/(daycov2-daycov1+0.0001)*(cov2-cov1), cov);
cov = if (day ge daycov2, cov2 + (day - daycov2)/(daycov3-daycov2+0.0001)*(cov3-cov2), cov);
cov = if (day gt daycov3, cov3 + (day - daycov3)/(daycov4-daycov3+0.0001)*(cov4-cov3), cov);
cov = if (day gt daycov4, cov4 + (day - daycov4)/(daycov5-daycov4+0.0001)*(cov5-cov4), cov);
cov = if (day gt daycov5, cov5 + (day - daycov5)/(daycov6-daycov5+0.0001)*(cov6-cov5), cov);
cov = if (day gt daycov6, cov6 + (day - daycov6)/(daycov7-daycov6+0.0001)*(cov7-cov6), cov);
cov = if (day gt daycov7, cov7 + (day - daycov7)/(daycov8-daycov7+0.0001)*(cov8-cov7), cov);
cov = if (day gt daycov8, cov8 + (day - daycov8)/(daycov9-daycov8+0.0001)*(cov9-cov8), cov);
cov = if (day gt daycov9, cov9 + (day - daycov9)/(daycov10-daycov9+0.0001)*(cov10-cov9), cov);
cov = if (day gt daycov10, cov10 + (day - daycov10)/(daycov11-daycov10+0.0001)*(cov11-cov10), cov);
cov = if (day gt daycov11, cov11 + (day - daycov11)/(daycov12-daycov11+0.0001)*(cov12-cov11), cov);
cov = if (day gt daycov12, cov12 + (day - daycov12)/(daycov13-daycov12+0.0001)*(cov13-cov12), cov);
cov = if (day gt daycov13, cov13 + (day - daycov13)/(daycov14-daycov13+0.0001)*(cov14-cov13), cov);
cov = if (day gt daycov14, cov14 + (day - daycov14)/(daycov15-daycov14+0.0001)*(cov15-cov14), cov);
cov = if (day gt daycov15, cov15 + (day - daycov15)/(daycov16-daycov15+0.0001)*(cov16-cov15), cov);
cov = if (day gt daycov16, cov16 + (day - daycov16)/(daycov17-daycov16+0.0001)*(cov17-cov16), cov);
cov = if (day gt daycov17, cov17 + (day - daycov17)/(daycov18-daycov17+0.0001)*(cov18-cov17), cov);
cov = if (day gt daycov18, cov18 + (day - daycov18)/(daycov19-daycov18+0.0001)*(cov19-cov18), cov);
cov = if (day gt daycov19, cov19 + (day - daycov19)/(daycov20-daycov19+0.0001)*(cov20-cov19), cov);
cov = if (day gt daycov20, cov20 + (day - daycov20)/(daycov21-daycov20+0.0001)*(cov21-cov20), cov);
cov = if (day gt daycov21, cov21 + (day - daycov21)/(daycov22-daycov21+0.0001)*(cov22-cov21), cov);

cov = min(1, max(0, cov))*masksum;
# make sure Cover is between 0 and 1

cov2 = cov**Cfac;
Ta0=Erc*Cfac*cov2*dt;
Ea0=Erc*(1-cov2)*dt;
A=Ta0+Ea0;
R = (A/Erc)**0.5;
#####
### Interception ###
#####

Coverm = min(cov2, 0.999);
# maximize cover fraction to 0.999, to avoid infinite LAI
LAI = -2*ln(1-Coverm);

Smax = max(0,0.935+(0.498*LAI)-(0.00575*(LAI**2)));
Smax1=if(landcover==3 or landcover==9,0,Smax);
#Smax2=if(landcover==7,Smax,0);
#Smax2_avg = maptotal(Smax1)/382484;
#Smax3=if(landcover==5 or landcover==6 or landcover==4,Smax2_avg,Smax1);

interception = interception + (Pr-Erc)*dt;
# increase or decrease interception

interception = (min(Smax1, max(0,interception)))*masksum*dt;

#interception between 0 and Smax

```

```

report intc_avg = maptotal(interception)/nrCells;

Pr = if (Pr gt 0, Pr - interception, 0);
# calc net rainfall = throughfall when it rains

ETp = max(0, Erc - interception);
# subtract interception from ETp because the energy is used
report etp_tss=maptotal(ETp)/nrCells;

intccum = intccum + interception;

report intccum_tss = maptotal(intccum)/nrCells;
# report cumulative interception
# graph with spatial average cumulative interception (mm)

Pr = Pr-ETp;
# rainfall minus by potential evapotranspiration

#####Actual Evapotranspiration#####

Ta=ETp*Cfac*cov2*dt;
#report TA_avg=maptotal(Ta)/nrCells;
Ea=ETp*(1-cov2)*dt;
#report EA_avg=maptotal(Ea)/nrCells;

ETa=Ta + Ea;

report eta_tss = maptotal(ETa)/nrCells;
# graphs with average and cumulative average ETa of all cells

ETacum = ETacum + ETa;
#report etacum_tss = maptotal(ETacum)/nrCells;

#####
### infiltration ###
#####

ER = if(Pr le 0,0,Pr);
#report ER_avg = maptotal (ER)/nrCells;
# effective rainfall
# EBF = EHD*BD*MS
EBF = timeinputscalar(EHD,E)*masksoum*dt;
RC = EBF*R;
report RC_avg = maptotal (RC)/nrCells;
#RC=MS*BD*EHD*R;

#RC_for_avg = maptotal(RC_for)/230220;
#RC2=iff(landcover==5 or landcover==6 or landcover==7,RC_for_avg,RC);

infil = min(RC, ER);
report infil_avg = maptotal(infil)/nrCells;

#infiltration in mm, is smallest of storage or rainfall

runoff = (ER-infil)*dt;
#runoff in mm
infcum = infcum + infil;

```

```
#report infcum_tss = maptotal(infcum)/nrCells;
```

```
### streamflow ###
```

```
runoffm3 = 0.001*(runoff)*cellarea();
```

```
# convert runoff to m3 per day
```

```
Wtr=accuflux(LDD, runoffm3);
```

```
# accumulate the runoff in mm
```

```
#report wtr_tss = timeoutput(dis_st, Wtr);
```

```
# output in mm/day to compare to measurements
```

```
#####
```

```
### update day number ###
```

```
#####
```

```
day = day + 1;
```

Appendix 5. Calculated EHDs of all combinations, field capacity, and bulk density of all soil textures

no	landcover	stage	soil texture	EHD (mm)	MS	BD	EHD*MS*BD
1	built up area	-	clay	5.00	0.45	0.94	2.11
2			clay loam	5.00	0.40	1.05	2.10
3			loam	5.00	0.20	1.16	1.16
4			loamy sand	5.00	0.15	0.94	0.70
5			sandy loam	5.00	0.28	1.03	1.44
6			silt loam	5.00	0.25	0.98	1.22
7			silty clay	5.00	0.30	1.13	1.69
8	Paddy field	after transplant	clay	2.00	0.45	0.94	0.84
9		(0-90 days)	clay loam	2.00	0.40	1.05	0.84
10			loam	2.00	0.20	1.16	0.46
11			sandy loam	2.00	0.28	1.03	0.58
12			silt loam	2.00	0.25	0.98	0.49
13			silty clay	2.00	0.30	1.13	0.68
14		mid season until harvested	clay	341.28	0.45	0.94	143.85
15		(90-150 days)	clay loam	333.37	0.40	1.05	139.95
16			loam	332.66	0.20	1.16	77.14
17			sandy loam	487.88	0.28	1.03	141.00
18			silt loam	180.34	0.25	0.98	44.05
19			silty clay	344.15	0.30	1.13	116.20
20		after harvested	clay	171.18	0.45	0.94	72.16
21		(150-180 days)	clay loam	167.22	0.40	1.05	70.20
22			loam	166.86	0.20	1.16	38.69
23			sandy loam	163.26	0.28	1.03	47.18
24			silt loam	180.55	0.25	0.98	44.10
25			silty clay	172.63	0.30	1.13	58.28
26	water body	-	clay	2.00	1.00	1.00	2.00
27	dry land cultivation	initial	clay	1437.29	0.45	0.94	615.83
28		(24 days)	clay loam	1404.01	0.40	1.05	599.40
29			loam	1400.98	0.20	1.16	334.87
30			loamy sand	1322.31	0.15	0.94	195.63
31			sandy loam	1370.72	0.28	1.03	406.14
32			silt loam	1515.97	0.25	0.98	380.30
33			silty clay	1449.40	0.30	1.13	499.37
34		crop development	clay	1403.17	0.45	0.94	601.45
35		(31 days)	clay loam	1370.67	0.40	1.05	585.40
36			loam	1367.72	0.20	1.16	327.15
37			loamy sand	1290.91	0.15	0.94	191.22
38			sandy loam	1414.87	0.28	1.03	418.90
39			silt loam	1395.15	0.25	0.98	350.79
40			silty clay	1414.98	0.30	1.13	487.75
41		Mid-season	clay	373.85	0.45	0.94	167.58
42		(51 days)	clay loam	339.24	0.40	1.05	152.41
43			loam	364.41	0.20	1.16	94.50
44			loamy sand	343.94	0.15	0.94	58.28
45			sandy loam	469.94	0.28	1.03	145.81
46			silt loam	296.92	0.25	0.98	82.53

no	landcover	stage	soil texture	EHD (mm)	MS	BD	EHD*MS*BD
47			silty clay	377.00	0.30	1.13	137.29
48		Late season	clay	401.32	0.45	0.94	179.16
49		(21 days)	clay loam	392.03	0.40	1.05	174.57
50			loam	391.19	0.20	1.16	100.71
51			loamy sand	471.37	0.15	0.94	76.17
52			sandy loam	276.85	0.28	1.03	90.01
53			silt loam	423.29	0.25	0.98	113.40
54			silty clay	404.70	0.30	1.13	146.64
55	Forest	-	clay	195.84	0.45	0.94	82.55
56			clay loam	124.70	0.40	1.05	52.35
57			loam	42.32	0.20	1.16	9.81
58			loamy sand	180.17	0.15	0.94	25.29
59			sandy loam	397.15	0.28	1.03	114.78
60			silt loam	206.56	0.25	0.98	50.46
61			silty clay	197.49	0.30	1.13	66.68
62	Shrub		clay	323.75	0.45	0.94	136.46
63			clay loam	341.31	0.40	1.05	143.28
64			loam	503.66	0.20	1.16	116.79
65			loamy sand	297.85	0.15	0.94	41.81
66			sandy loam	213.90	0.28	1.03	61.82
67			silt loam	545.59	0.25	0.98	133.27
68			silty clay	11.16	0.30	1.13	3.77
69	Plantation		clay	196.64	0.45	0.94	82.89
70			clay loam	201.52	0.40	1.05	84.60
71			loam	265.81	0.20	1.16	61.64
72			loamy sand	164.07	0.15	0.94	23.03
73			sandy loam	167.22	0.28	1.03	48.33
74			silt loam	53.46	0.25	0.98	13.06
75			silty clay	169.77	0.30	1.13	57.32
76	Grassland		loam	110.00	0.20	1.16	25.51
77			loamy sand	110.00	0.15	0.94	15.44
78			sandy loam	110.00	0.28	1.03	31.79

Appendix 6. Rainfall data

Month	Date	Days	Station numbers														
			1	2	3	4	5	6	7	8	9	10	11	12	13		
Jul_08	1	1	0	0	18	2	0	0	0	0	0	0	0	0	0	0	0
	2	2	0	0	0	0	0	0	0	0	0	0	0	0	0	0	0
	3	3	0	3	0	1	0	0	0	0	0	0	0	0	0	0	0
	4	4	0	0	0	0	0	0	0	0	0	0	0	0	0	0	0
	5	5	0	0	4	1	0	0	0	0	0	0	0	0	0	0	0
	6	6	0	0	0	0	0	0	0	0	0	0	0	0	0	0	0
	7	7	0	0	0	0	0	0	0	0	0	0	0	0	0	0	0
	8	8	0	0	0	1	0	0	0	0	0	0	0	0	0	0	0
	9	9	0	0	0	0	0	0	0	0	0	0	0	0	0	0	0
	10	10	5	0	0	0	0	0	0	0	0	0	0	0	0	0	0
	11	11	6	0	0	1	0	0	0	0	0	0	0	0	0	0	0
	12	12	2	0	3	2	0	0	0	0	0	0	0	0	0	0	0
	13	13	0	0	0	0	0	0	0	0	0	0	0	0	0	0	0
	14	14	0	0	0	0	0	0	0	0	0	0	0	0	0	0	0
	15	15	0	0	0	0	0	0	0	0	0	0	0	0	0	0	0
	16	16	0	0	0	0	0	0	0	0	0	0	0	0	0	0	0
	17	17	0	0	0	0	0	0	0	0	0	0	0	0	0	0	0
	18	18	0	0	0	0	0	0	0	0	0	0	0	0	0	0	0
	19	19	0	0	0	0	0	0	0	0	0	0	0	0	0	0	0
	20	20	0	0	0	0	0	0	0	0	0	0	0	0	0	0	0
	21	21	0	0	4	0	0	0	0	0	0	0	0	0	0	0	0
	22	22	0	0	0	0	0	0	0	0	0	0	0	0	0	0	0
	23	23	0	0	0	0	0	0	0	0	0	0	0	0	0	0	0
	24	24	0	0	0	0	0	0	0	0	0	0	0	0	0	0	0
	25	25	0	0	0	0	0	0	0	0	0	0	0	0	0	0	0
	26	26	0	0	0	0	0	0	0	0	0	0	0	0	0	0	0
	27	27	0	0	0	0	0	0	0	0	0	0	0	0	0	0	0
	28	28	0	0	0	0	0	0	0	0	0	0	0	0	0	0	0
	29	29	0	0	0	0	0	0	0	0	0	0	0	0	0	0	0
	30	30	0	0	0	0	0	0	0	0	0	0	0	0	0	0	0
	31	31	0	3	0	0	0	0	0	0	0	2	0	0	0	0	0
Aug_08	1	32	0	0	2	18	0	0	0	6	0	0	0	0	0	0	
	2	33	0	0	0	0	0	0	0	0	0	0	0	0	0	0	
	3	34	0	0	1	0	0	0	0	0	0	0	0	0	0	0	
	4	35	0	0	0	0	0	0	0	0	0	0	0	0	0	0	
	5	36	0	0	1	4	0	0	0	1	0	0	0	0	0	0	
	6	37	5	1	0	0	0	0	0	2	0	0	0	0	0	0	
	7	38	0	0	0	0	0	0	0	2	0	0	0	0	0	0	
	8	39	0	0	1	0	0	0	0	0	0	0	0	0	0	0	
	9	40	0	0	0	0	0	0	0	0	0	0	0	0	0	0	
	10	41	0	0	0	0	0	0	0	0	0	3	0	4	0	0	
	11	42	0	0	1	0	0	0	2	2	14	0	0	1	0	0	
	12	43	0	2	2	3	0	0	0	0	0	0	0	0	0	0	
	13	44	0	0	0	0	0	0	0	0	0	0	0	0	0	0	
	14	45	0	0	0	0	0	0	0	1	0	0	0	0	0	0	
	15	46	0	0	0	0	0	0	0	2	0	0	0	0	0	0	
	16	47	0	0	0	0	0	0	0	0	0	0	0	0	0	0	
	17	48	0	0	0	0	0	0	1	0	0	2	0	0	0	0	
	18	49	0	0	0	0	0	0	0	1	0	1	0	0	0	0	
	19	50	0	1	0	0	0	0	0	1	0	1	0	0	0	0	
	20	51	0	0	0	0	7	0	3	1	0	1	0	0	0	0	
	21	52	0	0	0	4	0	0	0	2	0	0	0	0	0	0	
	22	53	0	0	0	0	0	0	5	0	0	0	0	0	0	0	
	23	54	0	0	0	0	0	0	0	0	0	0	0	0	0	0	
	24	55	0	0	0	0	0	0	0	0	0	0	0	0	0	0	
	25	56	0	0	0	0	0	0	0	2	0	0	0	0	3	0	
	26	57	0	0	0	0	10	0	0	12	0	3	0	1	0	0	
	27	58	0	0	0	0	0	0	0	6	6	1	0	8	0	0	
	28	59	0	0	0	0	0	0	5	2	5	4	0	5	0	0	
	29	60	0	0	0	0	10	0	0	9	3	0	0	10	0	0	
	30	61	0	0	0	0	15	0	0	0	0	22	0	0	0	0	
	31	62	0	0	0	0	0	0	7	0	10	10	0	3	0	0	
sept_08	1	63	0	2	31	0	0	0	22	0	0	0	4	0	0		
	2	64	0	0	0	1	0	0	2	0	0	0	0	0	0		
	3	65	0	0	0	1	0	0	0	0	0	0	0	0	0		
	4	66	7	7	0	0	0	0	0	0	0	0	0	0	0		
	5	67	0	0	0	0	0	0	0	0	0	0	0	0	0		
	6	68	8	0	0	0	0	0	0	0	0	0	0	0	16		
	7	69	0	0	16	0	0	0	0	2	0	0	0	0	3		

Month	Date	Days	Station numbers													
			1	2	3	4	5	6	7	8	9	10	11	12	13	
	8	70	0	0	0	0	0	0	0	0	1	0	0	0	0	4
	9	71	0	0	4	0	0	0	0	0	0	0	0	0	1	5
	10	72	0	0	0	0	0	0	0	0	0	0	0	0	0	9
	11	73	0	3	3	0	0	0	0	0	0	0	0	0	0	7
	12	74	0	0	4	0	0	0	0	0	0	2	0	1	5	
	13	75	0	0	0	0	0	0	5	0	0	0	0	0	7	
	14	76	0	0	0	0	0	0	0	0	0	0	0	0	4	
	15	77	0	0	0	0	0	0	0	0	0	0	0	0	9	
	16	78	0	0	0	0	0	0	0	0	0	0	0	0	5	
	17	79	0	0	0	0	0	0	0	0	0	0	0	0	8	
	18	80	0	0	24	0	0	0	0	0	0	0	0	0	7	
	19	81	0	0	0	0	0	0	0	0	0	0	0	0	2	
	20	82	0	0	0	7	0	0	0	0	0	0	0	0	13	
	21	83	0	0	0	0	0	0	0	0	0	0	0	0	17	
	22	84	0	0	0	0	0	0	0	0	0	0	0	1	2	
	23	85	0	4	0	0	0	0	1	0	0	0	0	0	6	
	24	86	0	0	0	0	0	0	0	0	0	0	0	0	21	
	25	87	21	21	0	0	6	0	0	1	0	0	0	0	5	
	26	88	6	6	0	0	0	0	2	0	0	3	0	0	10	
	27	89	0	0	0	0	0	0	0	0	10	0	0	0	11	
	28	90	5	5	0	2	11	0	0	23	0	0	0	0	3	
	29	91	0	0	0	8	0	0	0	0	0	0	0	0	3	
	30	92	18	18	0	4	0	0	0	0	0	0	0	0	2	
Oct 08	1	93	0	5	4	37	0	0	0	0	0	0	0	0	17	
	2	94	4	2	9	21	0	0	0	0	0	1	0	3	19	
	3	95	7	3	3	11	0	0	5	0	32	14	2	0	17	
	4	96	6	4	31	19	0	0	5	0	43	5	10	4	20	
	5	97	0	4	1	47	0	0	1	0	0	0	6	6	23	
	6	98	15	1	46	61	0	0	0	0	0	0	4	0	21	
	7	99	11	2	45	73	0	0	0	0	0	5	7	16	0	
	8	100	22	7	2	21	0	0	0	0	5	65	12	35	0	
	9	101	0	18	0	3	0	0	77	0	83	5	5	0	16	
	10	102	5	0	7	7	0	0	8	0	10	2	0	3	21	
	11	103	6	4	13	14	0	0	0	0	2	0	0	8	19	
	12	104	10	3	0	38	0	0	0	0	0	38	0	16	19	
	13	105	19	5	7	28	0	0	35	0	63	52	0	18	13	
	14	106	4	0	3	17	0	0	58	0	31	5	3	1	14	
	15	107	0	31	3	46	0	0	3	0	0	0	12	0	26	
	16	108	0	23	0	11	0	0	0	0	0	1	2	12	21	
	17	109	0	13	0	26	0	0	0	0	20	4	5	0	19	
	18	110	0	11	7	47	0	0	3	0	12	14	0	23	14	
	19	111	9	0	13	59	0	0	0	0	21	18	14	15	0	
	20	112	2	7	11	0	0	0	29	0	23	10	0	10	19	
	21	113	5	27	2	31	0	0	0	0	0	8	27	19	14	
	22	114	0	22	21	80	0	0	17	0	9	2	7	24	11	
	23	115	61	18	0	26	0	0	4	0	50	31	13	17	22	
	24	116	0	41	24	31	0	0	47	0	34	15	9	20	19	
	25	117	12	6	13	79	0	0	16	0	18	19	24	16	17	
	26	118	10	21	36	13	0	0	16	0	16	3	8	8	21	
	27	119	12	19	8	28	0	0	12	0	0	16	2	11	17	
	28	120	25	17	6	0	0	0	34	0	0	6	6	12	12	
	29	121	8	33	27	63	0	0	6	0	10	128	34	79	16	
	30	122	13	21	27	17	0	0	121	0	115	12	17	13	18	
	31	123	20	24	29	39	0	0	0	0	22	28	26	10	19	
Nov 08	1	124	30	19	18	0	0	0	25	22	47	9	18	18	18	
	2	125	23	11	38	0	0	0	24	31	4	58	21	9	19	
	3	126	37	17	104	0	0	0	67	38	20	66	32	63	17	
	4	127	20	21	59	0	0	0	58	67	105	56	36	17	22	
	5	128	0	13	45	0	0	0	50	25	17	2	8	4	21	
	6	129	3	11	5	0	0	0	0	20	3	24	2	0	20	
	7	130	10	7	0	0	0	0	14	5	0	8	13	35	14	
	8	131	20	4	28	0	0	0	36	15	0	19	23	9	21	
	9	132	14	11	6	0	0	0	5	13	8	10	21	0	15	
	10	133	6	16	6	0	0	0	15	15	7	18	9	12	29	
	11	134	2	17	13	0	0	0	14	9	30	18	5	15	19	
	12	135	13	23	0	0	0	0	9	7	10	64	3	4	15	
	13	136	27	21	13	0	0	0	27	9	5	2	17	0	19	
	14	137	25	31	2	0	0	0	12	4	8	55	33	45	16	
	15	138	7	41	9	0	0	0	76	30	73	22	46	9	29	
	16	139	12	21	0	0	0	0	78	35	29	4	52	14	23	
	17	140	11	27	5	0	0	0	66	24	9	10	13	8	31	
	18	141	47	26	6	0	0	0	10	32	5	10	23	3	19	

Month	Date	Days	Station numbers												
			1	2	3	4	5	6	7	8	9	10	11	12	13
	19	142	51	41	11	0	0	0	6	43	15	37	42	5	12
	20	143	29	37	14	0	0	0	21	60	17	2	17	0	13
	21	144	40	22	0	0	0	0	0	1	0	50	36	17	23
	22	145	29	17	20	0	0	0	65	99	65	1	12	48	14
	23	146	20	27	0	0	0	0	2	2	2	27	19	10	19
	24	147	28	33	91	0	0	0	13	4	40	2	12	2	14
	25	148	10	23	14	0	0	0	19	1	15	12	3	9	17
	26	149	23	14	0	0	0	0	12	5	14	3	5	6	18
	27	150	11	7	0	0	0	0	3	4	7	19	14	7	19
	28	151	0	3	6	0	0	0	19	20	17	0	0	0	25
	29	152	0	0	0	0	0	0	0	0	0	0	0	0	29
	30	153	0	0	0	0	0	0	0	0	0	0	0	0	12
Dec_08	1	154	32	0	0	0	0	0	0	0	0	0	0	0	14
	2	155	53	0	0	0	0	0	0	0	0	0	0	0	19
	3	156	0	0	6	0	0	0	0	31	0	0	9	0	22
	4	157	13	7	45	0	0	0	0	1	0	1	5	0	16
	5	158	20	11	0	0	0	0	0	0	0	0	0	0	27
	6	159	0	17	0	0	0	0	0	2	0	0	2	0	21
	7	160	0	13	0	0	0	0	0	0	0	20	27	18	19
	8	161	16	25	0	0	0	0	34	0	30	4	0	2	13
	9	162	32	8	0	0	0	0	2	18	0	22	6	14	13
	10	163	30	9	0	0	0	0	28	26	45	38	13	36	11
	11	164	3	2	23	0	0	0	40	16	40	0	17	0	21
	12	165	2	6	6	0	0	0	0	5	0	4	0	10	19
	13	166	45	0	0	0	0	0	10	4	28	9	18	20	
	14	167	34	13	21	0	0	0	0	5	20	28	10	18	
	15	168	17	0	69	0	0	0	63	60	29	37	21	4	19
	16	169	10	11	11	0	0	0	21	13	25	14	32	5	18
	17	170	6	18	11	0	0	0	23	18	10	0	7	0	19
	18	171	0	7	9	0	0	0	0	2	0	20	1	2	24
	19	172	0	3	7	0	0	0	0	0	4	1	10	0	21
	20	173	13	5	2	0	0	0	4	0	13	23	10	19	
	21	174	0	0	17	0	0	0	17	4	0	16	5	35	26
	22	175	9	0	0	0	0	0	51	0	0	5	0	0	19
	23	176	3	0	7	0	0	0	4	12	0	0	3	0	18
	24	177	0	0	0	0	0	0	0	0	0	7	1	0	
	25	178	10	31	2	0	0	0	2	0	0	7	2	20	19
	26	179	8	23	6	0	0	0	0	18	0	0	0	0	14
	27	180	18	42	0	0	0	0	0	7	0	13	6	0	13
	28	181	29	47	29	0	0	0	32	20	25	3	17	5	13
	29	182	13	23	14	0	0	0	0	60	10	5	29	2	17
	30	183	93	61	22	0	0	0	3	27	13	3	42	10	16
	31	184	0	97	14	0	0	0	0	8	7	70	31	30	11
Jan_09	1	185	20	23	35	47	0	27	48	58	90	45	7	52	17
	2	186	21	28	10	38	0	19	20	0	55	20	3	15	17
	3	187	21	17	27	6	0	11	15	33	5	1	0	0	17
	4	188	21	0	0	0	0	0	0	8	0	0	0	0	21
	5	189	12	6	0	17	40	0	0	0	0	0	0	0	21
	6	190	16	24	0	27	0	0	0	0	0	56	2	0	17
	7	191	10	33	32	11	0	15	35	14	61	0	0	20	17
	8	192	13	21	15	29	15	4	0	0	10	38	0	27	17
	9	193	15	27	0	48	20	28	21	35	0	14	27	13	20
	10	194	15	34	11	39	0	14	16	10	10	5	15	0	11
	11	195	19	41	2	13	0	21	0	9	6	24	48	34	12
	12	196	27	14	41	17	50	63	16	11	2	30	51	0	21
	13	197	24	1	57	41	50	29	33	66	56	21	22	18	17
	14	198	14	9	34	36	25	11	30	22	20	2	43	3	17
	15	199	5	13	2	0	30	3	0	42	5	0	11	0	18
	16	200	20	18	0	0	45	0	0	4	3	25	61	5	16
	17	201	25	14	21	41	0	91	16	43	10	11	5	21	21
	18	202	29	23	0	0	0	44	50	16	69	5	10	10	23
	19	203	31	13	2	0	30	21	31	5	3	22	3	0	15
	20	204	24	7	10	0	75	2	4	0	0	80	14	56	16
	21	205	29	21	57	3	0	32	82	32	0	0	7	0	19
	22	206	25	19	2	12	0	1	0	0	0	0	2	0	20
	23	207	17	11	0	0	0	0	0	0	2	0	0	2	21
	24	208	23	27	12	0	30	31	0	26	3	7	16	6	19
	25	209	25	18	26	22	50	59	39	20	45	38	23	24	21
	26	210	45	26	29	29	0	51	50	14	30	91	27	35	18
	27	211	25	59	78	31	100	57	74	8	60	10	33	10	16
	28	212	29	37	26	48	90	21	46	14	54	35	36	42	17
	29	213	30	16	70	51	0	52	38	43	47	24	40	21	18

Month	Date	Days	Station numbers												
			1	2	3	4	5	6	7	8	9	10	11	12	13
	30	214	31	41	42	36	45	46	36	30	46	70	45	49	16
	31	215	29	23	73	47	0	59	62	47	82	5	28	18	13
Feb 09	1	216	36	19	7	16	0	24	0	41	9	22	37	20	26
	2	217	12	24	53	32	0	11	47	68	52	0	13	0	13
	3	218	13	31	0	11	0	1	5	0	0	38	21	17	14
	4	219	15	17	26	0	0	32	50	31	21	24	32	1	22
	5	220	8	13	11	0	0	12	14	14	20	23	27	0	13
	6	221	6	33	13	6	0	22	22	15	10	1	32	0	21
	7	222	12	44	0	0	0	0	0	6	1	0	38	0	21
	8	223	29	11	0	42	0	0	0	0	1	6	15	2	24
	9	224	12	0	41	50	0	9	0	52	0	3	29	0	13
	10	225	10	7	3	11	0	0	0	44	0	0	0	0	17
	11	226	11	12	38	28	0	5	0	7	0	50	41	34	12
	12	227	14	21	11	22	0	42	65	50	72	22	60	0	16
	13	228	18	0	26	46	0	73	24	20	10	3	0	2	22
	14	229	10	33	4	39	0	12	0	12	2	0	13	0	197
	15	230	20	51	0	41	0	0	0	0	0	1	2	0	150
	16	231	12	41	2	32	0	0	0	0	0	2	0	0	21
	17	232	13	21	41	31	0	19	0	6	0	14	4	30	15
	18	233	19	13	3	41	0	2	40	0	46	16	9	20	24
	19	234	19	11	9	39	0	16	35	18	19	38	11	0	15
	20	235	25	18	41	36	0	17	16	0	8	16	7	6	25
	21	236	25	39	15	22	0	0	0	8	5	31	28	10	17
	22	237	30	27	4	24	0	11	33	12	30	22	34	21	17
	23	238	35	28	22	25	0	21	25	20	27	45	43	24	14
	24	239	52	37	29	22	0	44	42	26	40	44	32	20	15
	25	240	27	43	12	13	0	56	28	32	42	73	36	22	15
	26	241	42	69	47	18	0	51	31	48	57	17	14	4	13
	27	242	21	43	11	0	0	22	0	35	2	4	16	2	24
	28	243	0	31	7	0	0	11	51	14	8	0	7	5	21
Mar 09	1	244	25	23	0	0	0	0	0	0	0	0	0	23	
	2	245	27	49	0	0	0	0	0	0	4	0	16	17	
	3	246	20	18	0	0	0	4	5	3	36	10	0	12	
	4	247	11	46	14	16	25	35	0	1	38	1	0	24	
	5	248	12	33	6	47	24	9	0	7	2	19	0	29	22
	6	249	21	24	52	58	25	28	1	70	25	16	0	0	15
	7	250	30	23	25	37	0	31	0	0	0	3	0	3	18
	8	251	27	17	25	26	0	8	0	3	0	7	0	4	20
	9	252	35	11	12	17	0	11	1	0	2	1	0	0	31
	10	253	26	19	10	0	110	0	6	61	5	2	0	5	13
	11	254	21	23	23	6	0	0	0	20	4	0	0	0	16
	12	255	15	46	0	0	0	0	0	0	0	1	0	0	15
	13	256	14	33	7	0	0	0	0	66	0	0	0	0	21
	14	257	0	21	40	0	0	0	1	24	7	1	0	0	19
	15	258	0	0	0	0	0	32	0	0	5	0	0	0	20
	16	259	0	0	0	0	0	0	0	0	0	0	0	0	16
	17	260	0	26	0	0	0	0	0	0	0	0	0	0	13
	18	261	15	31	7	0	0	5	0	0	0	0	0	0	18
	19	262	5	41	3	8	25	0	0	0	2	0	0	0	18
	20	263	0	29	13	0	35	0	0	0	0	3	0	16	13
	21	264	25	34	0	37	0	0	17	0	5	4	0	0	21
	22	265	22	41	2	0	0	37	7	0	0	1	0	4	17
	23	266	13	16	14	0	30	42	10	19	0	10	0	10	19
	24	267	0	28	28	11	50	16	26	0	46	2	0	0	13
	25	268	0	17	9	16	0	13	4	1	1	34	0	4	24
	26	269	11	11	6	41	0	21	50	27	27	25	0	11	19
	27	270	0	34	14	36	0	0	37	17	16	6	0	0	21
	28	271	12	29	7	31	0	11	3	35	0	32	0	3	19
	29	272	10	24	31	37	0	41	97	33	108	9	0	38	22
	30	273	0	18	5	49	0	65	5	27	10	12	0	0	16
	31	274	13	4	26	9	0	6	0	33	0	29	0	7	25
Apr 09	1	275	75	2	0	22	0	32	0	0	0	14	4	0	13
	2	276	0	7	15	17	0	71	47	2	2	0	9	0	27
	3	277	0	1	2	29	0	1	0	21	25	8	16	15	17
	4	278	2	0	12	0	0	29	72	17	0	13	11	10	26
	5	279	14	0	7	0	0	21	13	22	60	10	0	17	22
	6	280	0	0	8	11	0	16	20	1	18	1	5	0	19
	7	281	0	0	7	16	0	0	0	33	0	4	18	0	17
	8	282	0	0	0	0	0	1	48	5	25	0	7	6	12
	9	283	0	0	0	6	0	0	0	6	0	0	5	0	13
	10	284	5	4	2	3	0	26	0	0	0	0	12	10	18
	11	285	3	11	0	0	0	0	0	9	0	33	0	0	10

Month	Date	Days	Station numbers												
			1	2	3	4	5	6	7	8	9	10	11	12	13
	12	286	0	7	4	0	0	29	30	1	0	16	0	10	22
	13	287	13	0	4	27	0	38	46	2	23	18	0	0	30
	14	288	11	0	12	13	0	14	51	2	7	0	0	9	15
	15	289	12	8	10	24	0	0	0	4	2	4	7	2	24
	16	290	13	4	36	36	0	0	5	31	70	60	1	34	23
	17	291	0	12	54	0	0	14	55	35	0	0	12	0	28
	18	292	0	16	0	15	0	7	0	0	0	0	11	0	17
	19	293	15	8	27	24	0	12	5	11	0	43	1	0	17
	20	294	16	3	57	21	0	8	40	40	22	21	5	6	16
	21	295	14	7	6	37	0	22	29	1	11	0	0	3	18
	22	296	10	19	0	0	0	6	0	27	0	2	0	10	14
	23	297	0	5	0	8	0	13	21	6	0	2	7	4	13
	24	298	0	39	0	0	0	9	0	13	3	1	18	0	25
	25	299	20	33	6	5	0	21	7	12	1	33	13	11	21
	26	300	16	21	0	12	0	18	10	27	53	8	11	25	19
	27	301	0	11	9	7	0	39	13	11	0	71	19	2	25
	28	302	9	9	7	3	0	17	90	25	28	23	0	5	13
	29	303	45	27	6	0	0	0	20	1	3	0	0	0	13
	30	304	67	23	0	31	0	0	0	1	0	0	0	0	19
May_09	1	305	27	128	37	0	0	0	0	8	0	0	2	0	8
	2	306	48	52	4	0	0	0	0	0	0	0	0	0	9
	3	307	4	67	0	16	0	0	0	0	0	0	9	0	4
	4	308	29	18	0	9	0	0	0	0	0	0	16	0	3
	5	309	55	14	1	27	0	0	0	0	0	27	13	10	17
	6	310	0	19	34	24	0	11	12	27	0	47	0	5	4
	7	311	5	28	3	0	0	31	35	0	25	4	2	0	6
	8	312	12	21	2	0	0	26	0	0	3	7	4	8	7
	9	313	10	23	4	0	0	19	3	0	7	0	7	16	9
	10	314	0	41	6	0	0	16	0	0	0	3	3	7	3
	11	315	6	63	14	0	0	8	0	0	15	4	2	5	5
	12	316	11	23	3	9	0	13	19	31	0	2	0	0	11
	13	317	9	28	2	6	0	0	0	0	0	0	0	0	13
	14	318	0	11	0	0	0	0	0	0	0	0	0	0	0
	15	319	0	17	0	0	0	0	0	0	0	0	0	0	0
	16	320	0	4	0	21	0	0	0	14	0	3	0	4	0
	17	321	17	0	0	23	0	0	0	0	0	1	5	2	9
	18	322	30	14	14	0	0	4	0	0	3	45	15	36	4
	19	323	0	13	21	30	0	2	21	2	68	4	0	0	6
	20	324	17	48	0	12	0	0	30	0	8	37	0	48	11
	21	325	25	21	18	0	0	21	25	0	42	37	2	30	0
	22	326	21	11	9	13	0	12	9	4	68	14	1	15	5
	23	327	30	6	2	11	0	0	28	0	7	3	0	35	0
	24	328	31	26	13	0	0	1	0	73	84	1	0	10	0
	25	329	21	19	3	0	0	0	10	3	0	55	4	22	0
	26	330	19	19	9	0	0	0	25	9	60	26	7	12	12
	27	331	0	8	1	26	0	0	11	0	0	0	0	0	0
	28	332	0	33	0	6	0	0	0	0	17	0	3	0	12
	29	333	12	11	27	17	0	8	4	0	0	10	9	0	7
	30	334	25	46	6	0	0	1	0	12	0	0	0	8	0
	31	335	30	21	7	38	0	7	0	59	2	8	0	25	9
Jun_09	1	336	2	43	2	91	0	8	17	0	39	13	0	0	7
	2	337	14	7	5	13	0	19	13	0	0	4	5	3	41
	3	338	2	3	9	92	0	0	15	0	5	118	0	62	0
	4	339	21	33	11	16	0	21	81	64	12	0	0	9	0
	5	340	12	21	19	0	0	18	0	0	0	29	0	0	7
	6	341	13	17	12	0	0	0	0	0	23	17	3	0	7
	7	342	0	6	2	0	0	11	85	0	48	21	0	0	0
	8	343	23	0	0	23	0	21	11	0	5	3	32	0	6
	9	344	0	3	0	0	0	14	3	0	7	0	0	6	1
	10	345	33	7	3	0	0	0	0	0	0	0	0	0	0
	11	346	0	0	0	13	0	0	0	0	7	0	0	0	4
	12	347	0	11	0	27	0	1	0	0	0	11	4	5	6
	13	348	0	0	5	0	0	0	0	0	0	0	0	0	3
	14	349	0	0	35	0	0	0	0	0	0	0	0	0	0
	15	350	0	18	2	0	0	0	0	0	0	0	0	0	0
	16	351	6	0	0	8	0	0	0	0	0	0	0	0	0
	17	352	15	0	0	0	0	0	0	0	0	0	0	0	5
	18	353	17	9	0	0	0	0	0	0	0	0	0	0	4
	19	354	0	0	16	0	0	0	0	0	0	0	0	0	3
	20	355	0	0	0	0	0	0	0	0	0	0	0	0	0
	21	356	0	0	0	0	0	0	0	0	0	0	0	0	0
	22	357	0	0	0	0	0	0	0	0	0	0	0	0	6

Month	Date	Days	Station numbers													
			1	2	3	4	5	6	7	8	9	10	11	12	13	
	23	358	0	0	0	0	0	0	0	0	4	0	0	0	0	0
	24	359	0	0	0	0	0	0	0	0	6	0	0	0	0	4
	25	360	0	0	0	0	0	0	0	0	9	0	0	0	0	0
	26	361	0	0	0	0	0	0	0	0	4	0	0	0	0	0
	27	362	0	0	0	0	0	0	0	0	0	0	0	0	0	0
	28	363	0	0	0	0	0	0	0	0	0	0	0	0	0	2
	29	364	0	0	0	0	0	0	0	0	0	0	0	0	0	8
	30	365	0	0	0	0	0	0	0	0	0	0	0	0	0	10
Jul_09	1	366	0	0	0	1	0	0	0	0	0	0	0	0	0	0
	2	367	0	0	0	1	0	0	0	0	0	0	0	0	0	0
	3	368	0	0	0	2	0	0	0	0	0	4	32	5	0	0
	4	369	0	0	6	4	0	0	0	0	14	0	0	0	0	0
	5	370	0	0	0	0	0	0	0	0	0	0	0	0	0	0
	6	371	0	0	0	5	0	0	0	0	0	0	0	0	0	0
	7	372	0	0	0	2	0	0	0	0	0	0	0	0	0	0
	8	373	0	0	0	2	0	0	0	0	0	0	0	0	0	0
	9	374	0	0	0	1	0	0	0	0	0	0	0	0	0	0
	10	375	0	0	0	1	0	0	0	0	0	0	0	0	0	0
	11	376	0	0	0	0	0	0	0	0	0	0	0	0	0	0
	12	377	0	5	0	0	0	0	0	0	0	0	0	0	0	0
	13	378	0	3	0	0	0	0	0	0	0	0	0	0	0	0
	14	379	0	0	0	0	0	0	0	0	0	0	0	0	0	0
	15	380	0	0	0	0	0	0	0	0	0	0	0	0	0	0
	16	381	0	0	0	0	0	0	0	0	0	0	0	0	0	0
	17	382	0	0	0	0	0	0	0	0	0	0	0	0	0	0
	18	383	0	0	0	0	0	0	0	0	0	0	0	0	0	0
	19	384	0	0	0	0	0	0	0	0	0	0	0	0	0	0
	20	385	0	0	0	2	0	0	0	0	0	0	0	0	0	0
	21	386	0	0	0	4	0	0	0	0	0	0	0	0	0	0
	22	387	1	0	0	0	0	0	0	0	0	0	0	0	0	0
	23	388	1	0	5	0	0	0	2	0	0	0	14	0	0	0
	24	389	0	0	16	0	0	0	0	0	0	0	9	0	0	0
	25	390	0	0	4	0	0	0	0	0	1	4	0	0	0	0
	26	391	0	0	2	0	0	0	23	0	2	0	0	3	0	0
	27	392	0	0	0	0	0	0	0	0	0	0	0	5	0	0
	28	393	0	0	0	0	0	0	0	0	0	0	0	0	0	0
	29	394	0	0	0	0	0	0	0	0	0	0	0	0	0	0
	30	395	0	0	0	0	0	0	0	0	0	0	0	0	0	0
	31	396	0	0	0	0	0	0	0	0	0	0	0	0	0	0
Aug_09	1	397	0	0	0	0	0	0	0	0	0	0	0	0	0	0
	2	398	0	0	0	0	0	0	0	0	0	0	0	0	0	0
	3	399	0	0	0	0	0	0	0	0	0	0	0	0	0	0
	4	400	0	0	0	0	0	0	0	0	0	0	0	0	0	0
	5	401	0	0	0	0	0	0	0	0	0	0	0	0	0	0
	6	402	0	0	0	0	0	0	0	0	0	0	0	0	0	0
	7	403	0	0	0	0	0	0	0	0	0	0	0	0	0	0
	8	404	0	0	0	0	0	0	0	0	0	0	0	0	0	0
	9	405	0	0	0	0	0	0	0	0	0	0	0	0	0	0
	10	406	0	0	0	0	0	0	0	0	0	0	0	0	0	0
	11	407	0	0	1	0	0	0	0	0	0	0	0	0	0	0
	12	408	0	0	0	0	0	0	0	0	0	0	0	0	0	0
	13	409	1	0	0	0	0	0	0	0	0	0	0	0	0	0
	14	410	1	0	3	0	40	0	0	0	0	0	0	0	0	0
	15	411	0	0	0	0	0	0	0	0	0	0	0	0	0	0
	16	412	0	0	0	0	0	0	3	0	0	0	0	0	0	0
	17	413	0	0	0	0	0	0	0	0	0	0	0	0	5	0
	18	414	0	0	0	0	0	0	0	0	0	0	0	0	0	0
	19	415	0	0	0	0	0	0	0	0	0	0	0	0	0	0
	20	416	0	0	0	0	0	0	0	0	0	0	0	0	0	0
	21	417	0	0	0	0	0	0	0	0	0	0	0	0	0	0
	22	418	0	0	0	0	20	0	0	0	0	0	0	0	0	0
	23	419	0	0	0	0	0	0	0	0	0	0	0	0	0	0
	24	420	0	0	0	0	0	0	0	0	0	0	0	0	0	0
	25	421	0	0	0	0	0	0	0	0	0	0	0	0	0	0
	26	422	0	0	0	0	0	0	0	0	0	0	0	0	0	0
	27	423	0	0	0	0	0	0	0	0	0	0	0	0	0	0
	28	424	0	0	0	0	0	0	0	0	0	0	0	0	0	0
	29	425	0	0	0	0	0	0	0	0	0	0	0	0	0	0
	30	426	0	0	0	0	0	0	0	0	0	0	0	0	0	0
	31	427	0	0	0	0	0	0	0	2	0	0	0	0	0	0

Appendix 7. Temperature data

BADAN METEOROLOGI, KLIMATOLOGI DAN GEOFISIKA												
STASIUN KLIMATOLOGI SEMARANG												
BMKG Jl. Siliwangi 291 Semarang 50145 Tel. 024-7609016 Fax. 024-7612394												
=====												
DAILY TEMPERATURE (° C)												
LOCATION : WADASLINTANG (WONOSOBO).												
=====												
YEAR : 2008												
DATE	JAN	FEB	MAR	APR	MAY	JUN	JUL	AUG	SEP	OCT	NOV	DEC
1	27.9	27.6	24.5	26.5	26.5	25.7	24.6	25.2	26.4	25.1	26.7	27.6
2	25.9	27.6	26.2	26.2	27.5	25.4	25.3	24.7	25.9	25.5	26.1	26.2
3	25.7	27.8	26.0	26.2	27.2	25.6	25.1	24.0	25.3	25.7	24.6	26.7
4	23.4	27.5	25.5	26.4	27.6	25.0	25.0	23.7	25.4	26.3	25.9	26.6
5	26.6	27.5	24.5	27.6	26.9	24.6	24.8	24.5	25.4	25.4	26.7	26.7
6	26.9	27.7	25.7	26.2	26.7	25.1	24.2	24.3	24.3	26.3	26.3	25.9
7	24.6	27.6	26.4	26.4	26.1	24.9	24.6	25.1	25.2	26.7	25.3	25.5
8	27.3	27.1	25.3	26.5	26.4	26.2	24.9	24.2	25.0	25.2	26.0	25.2
9	27.2	25.6	25.1	25.6	25.8	26.0	24.8	25.3	24.9	24.5	26.0	23.7
10	27.4	25.9	26.0	26.6	26.1	25.5	23.6	24.8	26.0	26.2	26.4	23.3
11	26.8	27.8	25.5	26.7	25.7	24.8	24.5	25.7	25.4	25.4	26.3	25.2
12	25.7	27.2	25.8	25.9	25.0	25.2	23.3	26.5	26.6	27.1	26.2	26.9
13	26.4	26.5	26.7	27.3	25.1	25.3	25.0	26.2	25.7	27.3	25.7	26.9
14	24.7	26.4	25.6	28.1	25.8	26.7	25.0	25.5	26.9	26.9	23.9	25.7
15	24.9	26.2	25.4	27.0	25.2	26.1	24.0	25.4	25.6	27.3	24.9	24.7
16	26.8	27.3	26.3	27.4	26.3	26.1	23.9	25.2	25.6	26.8	25.2	26.9
17	27.7	26.1	26.3	26.7	26.1	25.2	24.1	25.7	25.6	26.1	26.8	26.3
18	26.7	27.7	26.4	26.5	26.6	25.0	24.7	23.9	26.3	26.3	26.0	26.2
19	27.1	25.6	26.1	26.7	27.2	24.5	23.9	23.8	25.7	26.1	25.8	24.5
20	27.2	27.7	26.8	26.1	26.3	25.2	23.8	24.2	26.5	27.2	27.7	25.1
21	26.6	26.5	25.2	25.3	26.8	25.2	24.0	25.3	25.7	27.1	28.4	25.5
22	27.5	26.0	25.0	26.8	26.2	25.0	23.3	25.6	25.4	28.0	25.9	25.3
23	28.0	26.5	26.4	27.4	25.8	25.1	24.0	24.6	26.0	28.2	25.7	25.4
24	27.4	27.3	26.6	27.9	25.3	25.7	24.1	24.6	25.9	27.0	26.4	26.1
25	27.4	26.8	27.5	27.8	25.0	26.2	24.5	25.5	26.3	25.5	27.2	25.4
26	26.8	26.0	27.6	28.9	25.6	25.6	24.3	25.8	25.6	24.5	24.7	26.1
27	27.9	26.1	27.6	26.9	26.4	26.4	24.9	25.6	25.9	26.4	25.9	27.5
28	28	25.7	27.2	26.6	25.9	25.8	24.3	25.9	26.2	26.4	27.1	27.1
29	27.1	24.1	26.5	27.1	26.0	24.5	24.6	26.6	25.4	24.2	25.5	27.0
30	26.2		26.0	27.0	25.7	26.0	24.8	26.3	26.6	26.7	26.8	27.1
31	25.4		25.6		25.6		25.5	26.0		26.9		26.5
AVR	26.6	26.7	26.0	26.8	26.1	25.5	24.4	25.2	25.8	26.3	26.1	26.0









	YEAR : 2009											
TGL	JAN	PEB	MRT	APR	MEI	JUN	JUL	AGS	SEP	OKT	NOP	DES
1	26.5	26.7	27.7	27.6	27.7	26.3	26.5	24.0	25.1	25.0	26.8	27.6
2	24.4	25.6	27.4	28.0	27.8	27.7	27.1	23.7	24.6	24.6	26.6	28.0
3	26.9	25.5	27.6	26.2	27.2	27.2	26.8	24.1	25.4	24.8	28.0	27.3
4	26.2	26.4	26.8	26.5	27.5	27.1	26.6	25.6	25.4	25.1	27.5	26.9
5	27.8	26.3	26.7	27.9	27.6	26.7	25.5	25.2	25.9	25.9	27.8	25.4
6	27.3	26.1	26.8	24.8	27.0	27.6	26.6	25.5	25.9	26.1	28.1	26.6
7	27.4	26.9	27.3	24.7	27.4	27.5	25.7	24.6	25.5	26.5	27.6	27.3
8	25.8	28.4	25.0	25.8	26.4	27.4	25.3	24.2	25.4	26.4	27.1	26.8
9	24.6	27.6	27.4	26.3	26.1	26.8	24.6	24.6	25.3	26.7	27.1	26.4
10	25.5	27.5	28.5	27.9	27.1	27.0	25.7	24.9	25.7	27.2	28.1	26.8
11	26.2	25.3	27.9	27.5	27.0	27.6	25.1	25.4	25.5	26.4	26.6	26.9
12	25.5	26.2	28.4	27.1	25.8	27.4	25.4	25.6	25.6	26.4	26.9	27.2
13	24.9	26.9	27.9	27.0	27.4	27.0	24.0	25.0	25.6	25.9	27.7	28.1
14	26.1	27.8	27.4	27.4	27.4	27.2	25.5	25.2	25.4	26.3	27.6	27.8
15	27.3	27.1	28.0	28.0	27.5	26.1	25.7	25.3	26.5	26.9	26.5	27.8
16	27.0	26.1	27.9	27.6	28.2	26.2	25.4	25.3	25.3	26.5	26.2	27.6
17	26.0	26.7	27.8	27.7	28.6	26.8	25.4	26.5	25.7	26.3	25.7	27.5
18	27.1	26.7	27.5	27.5	27.4	26.9	25.4	26.6	25.3	27.6	25.5	27.8
19	26.0	26.4	28.1	26.3	27.5	27.4	25.5	24.7	25.7	27.6	26.5	27.6
20	27.8	27.1	28.8	25.9	26.9	26.8	26.2	26.3	24.3	28.0	25.9	27.8
21	27.6	25.1	27.7	27.6	26.8	26.8	25.4	24.8	24.5	27.5	25.8	26.0
22	26.6	26.6	27.0	26.7	28.2	26.6	25.8	25.4	25.0	26.6	25.3	28
23	27.0	26.5	26.4	28.0	26.7	27.2	25.6	25.6	25.2	26.8	24.3	28.8
24	26.1	25.9	27.8	26.4	26.7	27.0	24.3	25.0	25.8	25.1	26.6	27.3
25	27.3	26.3	28.4	26.8	27.6	25.9	25.5	24.7	26.1	25.9	27.0	26.5
26	27.9	26.7	26.2	26.4	26.6	26.8	26.6	24.8	25.4	25.3	26.3	27.1
27	25.9	26.9	27.6	26.7	27.4	26.4	26.2	24.8	25.4	26.4	25.5	27.5
28	26.9	27.7	26.9	27.9	27.2	27.5	25.6	25.7	24.7	26.6	27.2	26.5
29	26.3	x	26.9	27.7	27.2	27.3	25.2	24.8	25.7	26.6	27.5	27.1
30	25.4	x	26.1	27.4	27.0	26.9	24.1	25.3	25.5	27.2	27.2	25.8
31	24.8	x	26.5		26.2		23.8	25.4		26.0		26.5
AVR	26.4	26.6	27.4	27.0	27.2	27.0	25.6	25.1	25.4	26.3	26.8	27.2

Appendix 8. An example of measurement table in calculating infiltration

Sample number	: 4		Date	: 28/09/2010			
Coordinates	: X (379334)		Time	: 14.35			
	: Y (9203646)		Slope	: 45			
Location	: Batur		Weather	: cloudy			
	: Banjarnegara		Landcover	: dry land cultivation			
Measurement :							
No	t (min)	□ t (min)	□ h (mm)	inf (mm/min)	k	r ²	Fcum (mm)
1	0.5	0.5	25	50	0.00		24.24
2	0.5	1	23	46	0.17	0.96	47.07
3	0.5	1.5	22	44	0.18	0.97	68.67
4	0.5	2	20	40	0.25	0.99	89.17
5	0.5	2.5	21	42	0.15	0.95	108.71
6	0.5	3	19	38	0.21	0.98	127.40
7	0.5	3.5	18	36	0.23	0.99	145.33
8	0.5	4	18	36	0.20	0.98	162.59
9	0.5	4.5	17	34	0.22	0.99	179.27
10	0.5	5	16	32	0.24	0.99	195.43
11	0.5	5.5	15	30	0.28	0.99	211.14
12	1	6.5	30	30	0.24	0.99	241.38
13	1	7.5	29	29	0.23	0.99	270.35
14	1	8.5	29	29	0.20	0.98	298.34
15	1	9.5	27	27	0.24	0.99	325.57
16	1	10.5	27	27	0.22	0.99	352.19
17	1	11.5	27	27	0.20	0.98	378.34
18	1	12.5	27	27	0.19	0.97	404.13
19	1	13.5	26	26	0.21	0.98	429.64
20	1	14.5	26	26	0.20	0.98	454.92
21	1	15.5	26	26	0.18	0.97	480.03
22	1	16.5	26	26	0.17	0.96	505.01
23	2	18.5	51	25.5	0.18	0.97	554.67
24	2	20.5	51	25.5	0.16	0.95	604.07
25	2	22.5	50	25	0.17	0.97	653.31
26	2	24.5	50	25	0.16	0.96	702.46
27	2	26.5	49	24.5	-	-	751.55
28	2	28.5	49	24.5	-	-	800.61
29	2	30.5	49	24.5	-	-	849.64
30	2	32.5	49	24.5	-	-	898.66
31	2	34.5	49	24.5	-	-	947.67
32	2	36.5	49	24.5	-	-	996.68
33	2	38.5	49	24.5	-	-	1045.69

First, recession constant of each time interval was calculated, and then every calculated recession constant was applied to the infiltration rate equation to find the new or calculated infiltration rates of each time intervals. Second, the calculated infiltration rates were compared to measured infiltration rates to get correlation coefficients, r^2 , of each applied recession constant. Third, the recession constant, which has the closest correlation coefficients to 1, (recession constant number four in this example) was applied to cumulative infiltration equation to get a cumulative infiltration value in the time unit on which infiltration rate reached its constant value. In this example, the cumulative infiltration equals to 959.9 mm.

Appendix 9. Fieldwork activities and landcover types on the study area

	
<p>a. Identifying coordinates of a sample point</p>	<p>b. Measuring infiltration in a sample point</p>
	
<p>c. Discharge Station at Banjarnegara bridge</p>	<p>d. Dry land cultivation</p>
	
<p>e. Plantation</p>	<p>f. Paddy field</p>
	
<p>g. Forest</p>	<p>h. Built up area</p>

